ELUCIATING THE BIOLOGICAL FUNCTIONS OF YEATS DOMAIN CONTAINING PROTEINS IN METABOLISM DRIVEN TRANSCRIPTIONAL REGULATION

Jibo Zhang

A dissertation submitted to the faculty at the University of North Carolina at Chapel Hill in partial fulfillment of the requirements for the degree of Doctor of Philosophy in the Curriculum in Biochemistry and Biophysics in the School of Medicine.

Chapel Hill
2021

Approved by:

Brian D. Strahl

Robert K. McGinty

Kerry S. Bloom

Greg Wang

Jill M. Dowen

ABSTRACT

Jibo Zhang: Elucidating the Biological Functions of YEATS Domain Containing Proteins in Metabolism Driven Transcriptional Regulation
(Under the direction of Brian D. Strahl)

DNA is the fundamental basis of our genetic information. Throughout evolution, cells have adapted mechanisms that not only allow compaction of DNA into the nucleus, but also maintain easy access to DNA for precise replication, transcription, and damage repair. DNA is wrapped around histone octamers to form nucleosomes, and then a higher-order structure called chromatin. It was revealed that chromatin has regulatory functions for transcription and other biological processes due to its dynamic quality. In eukaryotic organisms, gene regulation is about the balance between compacted DNA and gaining access for RNA polymerase and other regulatory proteins. As the most basic unit of chromatin, a nucleosome has two copies of canonical histones H2A, H2B, H3 and H4 with a segment of about 147 base pairs of DNA. Canonical histones are only expressed in certain times of the cell cycle and they are incorporated into the newly replicated genome. In contrast, histone variants are expressed throughout the cell cycle and are deposited when canonical histones are removed. Histone variants, such as H2A.Z, affect nucleosome properties with distinct modifiable amino acid sequences. Chromatin function is influenced by histone post-translational modifications (PTMs), which can act in a sequential or combinatorial fashion to influence downstream functions. It has been widely acknowledged that histone PTMs such as histone acetylation, crotonylation, and methylation play crucial roles in various biological processes including gene transcription, DNA repair, gene replication, and apoptosis. Additionally, the precursors of histone acetylation and crotonylation, acetyl-CoA and crotonyl-CoA, are regulated by cellular metabolism. This argues that the transcriptional regulatory

functions from both PTMs are influenced by cellular metabolism. In recent years, YEATS-domain proteins have gained more appreciation due to their ability to bind both acetylation and crotonylation. As acyllysine readers, YEATS domain proteins amplify the impact of histone acylations on transcriptional regulation through communicating with various transcriptional factors. In budding yeast, there are three YEATS domain proteins: Yaf9, Taf14, and Sas5. Each of them is involved in various essential processes and shows binding preference for specific acylations. Previous work has demonstrated that the YEATS domain of Taf14 binding to crotonylated histone lysine down-regulates pro-growth gene expression during the low oxygen consumption phase, suggesting that transcription is regulated by cellular metabolism through the interactions between YEATS domain and acylation. The work in this dissertation focuses on another YEATS domain protein, Yaf9, and discusses the role it plays in connecting gene expression and cellular metabolism.

To my family and friends, who helped me go through all the obstacles and whose support kept me going. This would not be possible without you.

ACKNOWLEDGEMENTS

I put a lot of thought into writing this section because I want to use the people I am thankful for as an example to demonstrate how important it is to be kind to international students. Sometimes the tiniest gesture could be the spark that changes lives. As an international student who came from China, although I wasn't naive about the challenges that a foreigner would have to face, the reality is always crueler than what you would expect. I flew to Florida 10 years ago to fulfill my dream of studying abroad. It's hard to imagine the person I was then. The person who could barely speak in complete sentences would eventually get married, buy a house, and defend his PhD thesis. Throughout my entire journey I received a great amount of support and help.

For a person who needs sponsorship for their legal status, a chance could change their future; a chance to be enrolled into a master's program, a chance to be accepted into a PhD program. I am forever thankful to my advisor Dr. Brian Strahl, who gave me the chance to work in his lab as a graduate student. In hindsight, with the high pressure from classes, I wasn't a promising rotation student to any lab considering the length of my learning curve. Brian took me in with the goal to train me to be a successful scientist. Countless failures and mistakes didn't stop Brian from being my most supportive cheerleader. Even though every meeting with him is overflowing with many brilliant ideas, Brian always trusts me to make my own decisions. To all the interviewers and students, I always say that great mentorship is like a perfect match, and I am one of the few lucky ones. During the five years, I lost three of my close relatives in China. The hardest part was not being able to be there for my family. Even though I didn't explain everything, Brian was always supportive and never once hesitated to let me take time off. This emotional yet incredible journey wouldn't be possible without Brian. His guidance and kindness

not only made the obstacles less challenging, but also encouraged me to realize my full potential as a scientist.

Guidance comes from different angles. I am grateful to my committee members Dr. Robert McGinty, Dr. Jill Dowen, Dr. Kerry Bloom, and Dr. Greg Wang for their brilliant suggestions and stimulating questions. Public speaking is nerve racking to everyone, but especially to international students. My committee members always made me feel comfortable with making mistakes. I was able to express my thoughts freely without any hesitations. They truly cared about the trajectory of the projects and my future career. They are the best team of support any graduate student could ask for. I also want to say thank you to my wonderful lab mates and friends: Dr. Kanishk Jain and Dr. Nathaniel Tate Burkholder. My intense work ethic limits interactions with the lab people. I joined the lab with the intentional thought of not building strong relationships with any coworkers to avoid potential complications, but I unexpectedly became friends with the two of them. Not only have they helped my projects with their effortless knowledge, but also created an extremely positive work environment for everyone. Our lab is lucky to have them, and I am honored to call them my friends. Even though I didn't get many opportunities to mentor, my undergraduate student Aakanksha Gundu is definitely my proudest apprentice. This phenomenal young lady adapted quickly to my high-pressuring teaching style and accomplished all the tasks assigned with her spare time. I have no doubt that she will contribute greatly to the Strahl lab,

The future of my scientific career is immensely brightened by the people I mentioned. However, those who went through a PhD would likely agree that keeping a healthy mental state is arguably more challenging. I can't emphasize enough on how terrifying it is for international students to accomplish the highest degree, in addition to handling all the emotional burdens resulting from living in a different country. When new students ask me about the secret to thrive in PhD studies, I always tell them that the most important thing is to find your tribe. The close friends you surround yourself with will be your ultimate support group that carries you through all the ups and downs. I want to express my deepest gratitude to my best friend Dr. Suruchi Shrestha

and her husband Luis Quintanilla. The three of us started our PhD journey together. We laughed at trauma and celebrated success. With all the major life events taking place during this crazy time, our friendship has evolved into something greater. Three years ago, another wonderful person named Joshua Caleb Hall joined our three people group. He was so wonderful that I decided to spend the rest of my life with him. My husband not only held me through all the terrible moments from both work and life, but he also made me realize that I won't be alone in fighting for a better future. As a foreigner living in the States, nothing is more important than being safe. Caleb had made me feel safe since the moment we met. He is so determined to take care of me and our future family, and I have no doubt that we will build a fantastic future together. The four of us formed an inseparable family. We protected each other from hardships and supported each other on all the life-changing decisions. I am forever thankful for everything they have done for me, and I hope to continue to make them proud.

Last, but not least, I want to say thank you to my parents. It was their sacrifice that gave me the opportunity to come to the States to fight for my dream. Without them, I wouldn't have had such tremendous growth. It has always been our dream to live close by each other and have a close-knit relationship, in order to fulfill that dream we had to make many sacrifices. The greatest of these was having to leave home, move halfway around the world and devote my full attention to my scientific career. Now that my PhD is coming to a close, this dream is finally coming true. Moving forward, mine and my husband's goal is to provide a life for them that is as spectacular as the one they gave to me.

None of the people I mentioned above will ever know the impact they have made on me. Words cannot express how grateful I am for the small acts of kindness that might have seemed minuscule at the time but are the very thing that sparked the changes in my life.

TABLE OF CONTENTS

LIST OF FIGURES

LIST OF TABLES

LIST OF ABBREVIATIONS

°	degree
3D	three dimensional
5-FOA	5-fluoroorotic acid
6-AU	6-azauracil
Å	angstrom
ac	acetyl
ALL	acute lymphocytic leukemia
Bdf1	bromodomain factor 1
Bdf2	bromodomain factor 2
BSA	Bovine serum albumin
C	Celsius
CC	coiled coil
ChIP	chromatin immunoprecipitation
ChIP-seq	chromatin immunoprecipitation sequencing
cr	crotonyl
cryo-EM	cryogenic electron microscopy
CTD	C-terminal domain
DNA	deoxyribonucleic acid
DSB	double strand break
DTT	dithiothreitol
Eaf1	ELL Associated Factor 1
ECL	enhanced chemiluminescence
EDTA	ethylenediaminetetraacetic acid
FACT	facilitates chromatin transcription complex

FBS	fetal bovine serum
G1	Gap 1
G2	Gap 2
GAPDH	glyceraldehyde 3-phosphate dehydrogenase
Gcn5	General control non-depressible 5
GO	Gene Ontology
GST	glutathione S-transferase
H3K4	histone H3 lysine 4
H3K9	histone H3 lysine 9
H3K9ac	histone H3 lysine 9 acetyl
H3K9cr	histone H3 lysine 9 crotonyl
H3K9bu	histone H3 lysine 9 butyral
H3K9pr	histone H3 lysine 9 propionyl
H3K9β-hydro	histone H3 lysine 9 hydroxybutyryl
H4K16	histone H4 lysine 16
H4ac	histone H4 acetyl
HA	hemagglutinin
HAT	histone acetyltransferase
HDAC	histone deacetylase complex
HEPES	4-(2-hydroxyethyl)-1-piperazineethanesulfonic acid
HOC	high oxygen consumption
HR	homologous recombination
HRP	horseradish peroxidase
HU	Hydroxyurea
IPTG	isopropyl β-d-1-thiogalactopyranoside

kDa	kilodalton
LC-MS	liquid chromatography mass spectrometry
LOC	low oxygen consumption
M	mitosis
me	methylation
me1	mono-methylation
mg	miligram
min	minute
mL	mililiter
mM	milimolar
MMS	methyl methanesulfonate
mRNA	messenger ribonucleic acid
MS	mass spectrometry
NC	non-cycling
NFR	nucleosome free region
nM	nanomolar
OD	optical density
ORF	open reading frame
pan H4ac	pan histone H4 acetyl
PCR	polymerase chain reaction
PBS	phosphate-buffered saline
PBS-T	phosphate-buffered saline-tween 20
PC	principal component
PHD	plant homeodomain
Pol II	RNA polymerase II

PTM	post-translational modification
PVDF	polyvinylidene fluoride
rep	replicate
RNA	ribonucleic acid
RNAPII	RNA polymerase II
RNA-seq	RNA sequencing
rpm	rotations per minute
rRNA	ribosomal RNA
RT-qPCR	quantitative reverse transcription polymerase chain reaction
S	DNA synthesis
SAGA	Spt-Ada-Gcn5 acetyltransferase
SC	synthetic complete
SD	synthetic depleted
SDE	significantly differentially expressed
SDS-PAGE	sodium dodecyl sulface-polyacrylamide gel electrophoresis
SEM	standard error of the mean
STAR	spliced transcripts alignment to a reference
ub	ubiquitination
µg	microgram
µl	microliter
µM	micromolar
UV	ultraviolet
qPCR	quantitative polymerase chain reaction
TCA	trichloroacetic acid
TFIIB	Transcription Factor II B
TFIID	Transcription Factor II D

T_m	melting temperature
tp	timepoint
wt	wild-type
YPD	yeast extract, peptone, dextrose
YPG	yeast extract, peptone, glycerol

CHAPTER 1 – INTRODUCTION

The curiosity to discover the origins of life has been the main force that drives scientists to keep asking questions and exploring the marvelous diversity in the natural world. In 1865, the birth of foundational genetic principles was accomplished by Gregor Mendel through his work on plant hybridization (Mendel, 1901). Since then, science has bloomed to allow researchers to gradually enhance our understanding about the truth of life and how life works at a molecular level (De Castro, 2016). As the blueprint of all organisms on earth, deoxyribonucleic acid (DNA) was discovered at the beginning of the 20th century and proven to be the ultimate biological material that was responsible for retaining genomic information from generation to generation. According to Watson and Crick's findings in 1956, the structure of DNA was a spiral of two DNA strands that wound around each other and each strand contains a long chain of monomer nucleotides (Watson and Crick, 1956). Subsequently, in Watson's best-selling book published in 1968, named "The Double Helix", he added that DNA replicated itself by separating into individual strands, each of which became the template for a new double helix. These discoveries prompted more questions, such as how are the instructions in DNA converted into functional products, in the form of proteins? Francis Crick established the concept of the "central dogma" which revealed how a functional protein is the product of ribonucleic acid (RNA) that is transcribed from DNA. In this theory, he stated that portable RNA messages transcribed from DNA travel from the nucleus to the ribosome where they are read to produce specific proteins (Crick, 1958). However, as the nature of science has shown us, no mechanisms or theories are explained in a linear manner without complications. The intricate logic behind life itself has led to numerous discoveries that directly challenged the simplicity and accuracy of the initial central dogma concept (Gayon, 2016). For example, neither Crick nor other scientists of the time considered the impacts proteins have

on DNA expression. There is no doubt that with more advanced techniques and strategies, more details will be unearthed and supplemented into the completion of the “central dogma”.

In order to understand how DNA contributes to life, the first question that needs to be answered is how cells store it. DNA represents a coded or indexed language that conveys all of the genetic information need to go from a single fertilized cell to a complete adult. The length of a DNA, if stretched from end-to-end, in one human cell nucleus is ~6 feet. Cells not only possess mechanisms that allow compaction of DNA into an extremely small space that has the diameter of 10 μm, but they can also maintain easy access to specific locations of DNA for accurate replication, transcription, and damage repair. These complicated processes must be compartmentalized so that one process does not interfere with the other. DNA is wrapped around a histone octamer to form a nucleosome, and then a higher-order structure called chromatin. Both chromatin and nucleosome structures were initially considered as static entities of high intrinsic stability within which DNA was sequestered (Thoma et al., 1979; Richmond et al., 1993). However, just like the “central dogma” theory, chromatin is much more complex and dynamic. It was revealed that chromatin provides regulatory flexibility for transcription and other biological processes due to its dynamic quality (Wolffe and Guschin, 2000). The accessibility of chromatin depends on 1) the degree of physical interaction between nuclear proteins and chromatin-bound DNA; 2) the occupancy and organization of nucleosomes; 3) other transcription factors that occlude access to DNA (Klemm et al., 2019). Chromatin and chromosomal structure have become an extremely rich field for future investigation due to unlimited possibilities.

Nucleosomes and the Histone Code

Eukaryotic gene regulation can be viewed as the balance between compacted DNA in the form of chromatin that does or does not grant access to RNA polymerase and other regulatory proteins. Similar to chromatin, nucleosomes are highly dynamic. Nucleosomes are nucleoprotein complexes that are involved in all genomic processes in eukaryotes (Lai and Pugh, 2017). As the

most basic unit of chromatin, a nucleosome is composed of two copies of histones H2A, H2B, H3 and H4 with a segment of 147 base pairs of DNA that wraps around the core histones (Luger et al., 1997; Kornberg et al., 1999; Richmond and Davey, 2003). Four properties of nucleosomes make their design perfect for genome regulation: 1) they can slide along DNA (Narlikar et al., 2013; Zhou et al., 2016); 2) they can partially or fully disassemble (Rhee et al., 2014); 3) they are easily modified with chemical groups (Strahl and Allis, 2000; Pokholok et al., 2005); 4) the histone components within can be replaced with variant histones (Weber and Henikoff, 2014). Canonical histones mentioned earlier are only expressed in the S phase of the cell cycle (Harris et al., 1991) and they are incorporated into newly replicated genome. In contrast, histone variants are expressed throughout the cell cycle and deposited only when canonical histones are evicted (Malik, Henikoff, 2003). Additionally, histone variants affect nucleosome properties with distinct modifiable amino acid sequences, which subsequently regulate transcription programs (Weber and Henikoff, 2014). Histone H2A variant H2A.Z, one of the most outstanding components of my thesis, will be heavily mentioned in the later paragraphs.

All histones can be modified with chemical groups including acetylation, crotonylation, ubiquitination, and phosphorylation (Rothbart and Strahl, 2014). The locations on histones that can be modified include but are not limited to histone tails and histone folds (Cosgrove et al., 2004). Essential cellular processes such as replication, transcription, and DNA repair are either promoted or inhibited by these histone modifications (Strahl and Allis, 2000). In the early years, it was initially thought that the purpose of the compact chromatin structure was to organize DNA into the nucleus and exist as the obstacle to prevent DNA from unwarranted access. However, at the beginning of the 1960s, Vincent Allfrey revealed how lysine acetylation neutralizes the positive charge of lysines within the histone tails, which disrupts the interaction with negatively charged DNA that is associated with the nucleosome (Allfrey et al., 1964). His findings opened the door for discussions on dynamic functions of all histone modifications. Beginning in the 2000s, it was proposed that chemical groups added onto histones, resulting in modifications that code essential functions. These modifications

could act in a sequential or combinatorial fashion to influence downstream functions, hence the histone code theory (Strahl and Allis, 2000). Information carried by histone codes has to be received by regulatory proteins, which begs the question, who reads the codes? In the late 1990s, bromodomains were shown to interact with histone lysine acetylation in a context-specific fashion, leading to more studies on how various protein motifs and domains receive information to regulate biological events through reading histone codes (Winston and Allis, 1999). My dissertation will focus on the YEATS domain, a newly discovered module that preferably binds to histone acylations.

Histone Lysine Acetylation

It is increasingly evident that histone post-translational modifications (PTMs) play a crucial role in various biological processes including gene transcription, DNA repair, gene replication, and apoptosis (Talbert and Henikoff, 2021; Strahl and Allis, 2000). In general, protein PTMs are chemical modifications that change proteins' properties such as localization pattern, stability, DNA binding strength, and enzymatic activities (Verdin and Ott, 2015). Phosphorylation and acetylation were the first two PTMs to be discovered (Fischer et al., 1959; Phillips, 1963). The former is the most studied PTM due to its role in cell signaling pathways and other cellular processes. Even though the importance of acetylation was hinted at when acetylation pioneer Vincent Allfrey directly linked it to lowering chromatin's ability to inhibit RNA synthesis in 1964 (Allfrey et al., 1964), acetylation was slightly ignored and did not take the spotlight until the beginning of 2000. Soon after the initial discovery, more information about acetylation was revealed including identifying acetylation on not only histone lysines but also non-histone proteins and identifying acetylase and deacetylase enzymes. In the late 1980s, efforts were made by multiple teams to demonstrate that acetylated histones alter the accessibility of chromatin, which subsequently affects gene transcription (Hebbes et al., 1988; Turner et al., 1992).

Researchers slowly realized the potential of acetylation, which led to the blooming of the field. In the late 1990s, a human type A (transcription related) histone acetyltransferase (HAT-A)

was purified and proven to be the homolog of yeast Gcn5 according to the cloning of its encoding gene (Brownell et al., 1996). Meanwhile, the first histone deacetylase (HDAC1), identified as the homolog of yeast Rpd3, was cloned and shown to exhibit HDAC activity (Taunton et al., 1996). These two studies jumpstarted the era of acetylation and how it is coupled to gene transcription. Rapidly thereafter, an enormous amount of information from this PTM were unearthed including the identification of other transcription factors that bind to histone acetylation as well as the discovery other histone acetylases and how these enzymes are found in large, multi-subunit complexes such as is found with the SAGA complex (Marmorstein and Zhou, 2014; Grant et al., 1997). In addition to histones, an increase in acetylation of transcriptional regulatory non-histone proteins were found. Hence, the significance of acetylation progressively expanded. With the previous discoveries of “writers” (HATs) and “erasers” (HDACs), the next puzzle piece was the introduction of “readers” that can recognize histone acetylation. Bromodomains were the first protein domain found to read histone acetyl-Lys (Dhalluin et al., 1999), followed by the recent identification of YEATS domains (Li et al., 2014). Judging by the popularity of protein acetylation, it won’t be surprising to discover more reader motifs in the near future. Meanwhile, all these findings on protein acetylation have prompted the production and testing of inhibitor drugs. As the first FDA-approved HDAC inhibitor, vorinistat was shown to induce *in vitro* tumor cell differentiation (Richon et al., 1998). Additionally, many companies and academic laboratories are working on developing chemical probes that disrupt the interaction between the bromodomain and acetyl-Lys (Filippakopoulos et al., 2010). HAT inhibitors such as EP300 inhibitors are also being developed (Bowers et al., 2010). Medically targeting acetylation related proteins indicates possible clinical applications that go beyond just cancer.

In recent years, one proposal suggested that acetylation reflects and senses the changes of cell environment. This has gained much attention. The precursor of acetylation, acetyl-CoA, was discovered by three Nobel Prize winners; Lipmann, Bloch and Lyne (Bloch and Borek, 1946; Lipmann and Kaplan, 1947; Lipmann, 1954), which essentially started the field of acetylation. In

budding yeast, the generation of acetyl-CoA is highly dependent on the cellular carbohydrate enrichment (Suganuma and Workman, 2018). Abundant glucose induces the production of acetyl-CoA in mitochondria, while fatty acids in peroxisomes are used as resources for acetyl-CoA under starving conditions (Hiltunen et al., 2003). Acetyl-CoA functions as a metabolic signal by inducing histone acetylation at active genes through acetyltransferases (Shen et al., 2015; Peleg et al., 2016). Therefore, the reasoning behind protein acetylation being involved in connecting cell metabolism and gene transcription is a brand-new territory.

Histone Lysine Crotonylation

The number of PTMs recognized to occur on histones was greatly expanded in 2011 using advanced high-sensitivity mass spectrometry (Tan et al., 2011). Most of the newly discovered PTMs are short-chain lysine acylations that can be classified into three categories: the polar acyl group, the acidic acyl group, and the hydrophobic acyl group (Sabari et al., 2017). The initial work published by Tan that identified histone crotonylation amongst other acylations also suggested that crotonylation might be an indicator of gene expression due to the enrichment of crotonylated histones in the promoter and enhancer regions of certain cell lines (Tan et al., 2011). Furthermore, non-histone crotonylation was mostly found in nuclear proteins that are involved in various nuclei-related cellular processes (Wei et al., 2017). In terms of length, crotonyl-lysine (Kcr) is a four-carbon structure with a double bond between the two middle carbons, which results in a rigid planar conformation (Sabari et al., 2017). Crotonyl-CoA is produced during the process of β-oxidation from long chain fatty acids (Sabari et al., 2017). Just like the other short chain acylations, crotonylation is regulated by metabolites (Lu et al., 2018). Research has shown that adding crotonic acid could drastically enhance the levels of histone lysine crotonylation due to the increase of its precursor crotonyl-CoA (Sabari et al., 2015; Wei et al., 2017). These findings laid the groundwork for future studies on how histone acylations receive environmental signals for the purpose of gene regulation. This newly discovered PTM quickly took center-stage and became

heavily studied. Many recent studies have suggested that Kcr is involved in biological processes such as DNA damage repair, spermatogenesis, HIV latency, carcinogenesis, stem cell differentiation, and cardiovascular diseases (Tan et al., 2011; Sabari et al., 2015; Jiang et al., 2018; Lv et al., 2021; Wan et al., 2019; Crespo et al., 2020; Tang et al., 2021). However, all these new findings about Kcr's diverse involvements in diseases couldn't hide the fact that the underlying mechanism is still uncertain.

The level of Kcr is influenced by three factors: 1) intracellular crotonyl-CoA level; 2) the ratio of crotonyl-CoA/acetyl-CoA; and 3) the balance between "writers" and "erasers" (Zhao et al., 2018; Jiang et al., 2021). Even though crotonyl-specific "writer" proteins have yet to be identified, three HAT families (CBP, MYST, and Gcn5-related N-acetyltransferases) have been reported as histone crotonyltransferases (Sabari et al., 2017). As for crotonyl "erasers", two out of the four HDAC groups, HDAC I and HDAC III were demonstrated as the major histone decrotonylases (Seto et al., 2014; Madsen and Olsen, 2012). To fulfill both physiological and pathological functions, Kcr has to be recognized by specific "reader" proteins. Although all three groups of Kac "readers" can recognize Kcr, the question remains whether these common "readers" possess the same downstream impact. Unlike bromodomain-containing proteins that have much higher affinity for Kac, recent work shows YEATS domains and double plant homeodomain finger (DPF) proteins display higher binding preferences for histone Kcr over other acylations (Flynn et al., 2015; Li et al., 2016; Xiong et al., 2016). Each of the two chapters included in this dissertation focus on one "reader" from the YEATS-domain protein family: Taf14 and Yaf9.

YEATS-domain Proteins Recognize Both Acetylation and Crotonylation

In recent years, YEATS-domain proteins have gained more appreciation due to their role in recognizing different degrees of histone acylation (Li et al., 2017; Schulze et al., 2009). Conserved from yeast to human and indispensable for Kcr-mediated transcription, YEATS-domain proteins (Yaf9, ENL, AF9, Taf14, and Sas5) join bromodomain-containing proteins and

double PHD finger domain-containing proteins as the acyllysine readers that can read both histone acetylation and crotonylation (Li et al., 2017; Andrews et al., 2016; Stratton and McKinsey, 2015; Dreveny et al., 2014). As mentioned above, YEATS domains generally show stronger binding preferences for crotonylation than acetylation compared to bromodomains. Structurally, the end-open feature of the YEATS domain aromatic pocket accommodates the longer and more rigid Kcr better than the shorter and more flexible Kac. This explains the binding preference for Kcr and why end-blocked bromodomain can tolerate Kac (Li et al., 2016; Zhang et al., 2016; Flynn et al., 2015). It was demonstrated that the YEATS domains of Taf14 and human AF9 bind to Kcr through a π-π-π stacking mechanism (Andrews et al., 2016; Klein et al., 2018; Li et al., 2016). This confirmation directly links Kcr to various essential biological processes including transcription and nucleosome remodeling. The YEATS domain has been shown to be a potential therapeutic target for acute leukemia (Erb et al., 2017). Its ability to differentiate short chain PTMs and perform both roles of either gene activator or repressor accordingly has prompted interests for further investigation. For example, Kcr-AF9 YEATS is found to regulate gene expression in the inflammatory response (Li et al., 2016), and Kcr-Taf14 YEATS down-regulates pro-growth gene expression during the low oxygen consumption phase (Gowans et al., 2019). Another compelling aspect is that the members of the YEATS domain family have different acyl-binding preferences (Andrews et al., 2016). For instance, as the three YEATS-domain-containing proteins in budding yeast, Yaf9 and Sas5 prefer histone acetylation while Taf14 shows stronger affinity for histone crotonylation (Figure 1.1) (Klein et al., 2018; Zhang et al., 2004; Sutton et al., 2003; Andrews et al., 2016). As acyllysine readers, they convey the impact of histone acylations on transcriptional regulation through recruiting and binding with various transcriptional factors (Schulze et al., 2009). In the case of Kcr, the level change influenced by metabolism adds another layer of complexity to the functions of readers. How cell metabolism regulates transcription though Kcr-YEATS interactions remains elusive.

NuA4 and SWR1-C Complexes

Yaf9 is found in two major catalytic conserved complexes acting on chromatin: 1) the NuA4 acetyltransferase acetylates H4, H2A and its variant H2A.Z. and 2) the SWR1-C chromatin remodeling complex that deposits H2A.Z into chromatin (Kobor et al., 2004; Mizuguchi et al., 2004; Klein et al., 2018; Zhang et al., 2004). The collaboration between NuA4 and SWR1-C can be summarized as SWR1-C uses the energy produced by ATP hydrolysis to alter the nucleosome structure by exchanging H2A for H2A.Z first, then NuA4 acetylates the N-terminal tails of H2A.Z as well as histone H4 (Kobor et al., 2004; Krogan et al., 2004; Mizuguchi et al., 2004; Keogh et al., 2006). Yeast NuA4 is a large acetyltransferase complex that is composed of 13 subunits (Wang et al., 2018). In addition to acetylating histones in a gene-specific fashion, NuA4 also has two independent sub-complex forms: the TINTIN complex composed of Eaf3, Eaf5, and Eaf7; and the piccolo form consisting of Yng2, Eaf6, Esa1, and Epl1 that acetylates global histones (Auger et al., 2008; Boudreault et al., 2003; Rossetto et al., 2014; Cheng and Côté, 2014; Friis et al., 2009). Among the 13 subunits, Eaf1 is the only exclusive member of NuA4 that is essential for the complex integrity and serves as a platform that coordinates all four functional modules: TINTIN, picocolo-NuA4, Tra1, and the Arp4/Act1/Swc4/Yaf9 module (Auger et al., 2008; Mitchell et al., 2008). Tra1 is shown to be a scaffold for the SAGA and SLIK/SALSA complexes while Arp4/Act1/Swc4/Yaf9 module is shared with SWR1-C remodeling complex (Grant et al., 1998; Lu et al., 2009). The module formed by four common subunits has been theorized to play crucial roles in anchoring and regulating the activities of the two chromatin-modifying complexes (Lu, et al., 2009). The NuA4 cryo-EM structure has shown the scaffold protein Eaf1 has a HSA domain from amino acid 347 to 418 that binds to Arp4 and Act1 (Wang et al., 2018). Mutating hydrophobic residues within the Eaf1 HSA domain disrupts interaction with the SWR1-C module, suggesting that NuA4 is recruited onto the SWR1-C module through essential Arp4/Act1-Eaf1 binding (Wang et al., 2018). Within the SWR1-C module, Yaf9 and Swc4 interact with each other though their C-termini (Bittner et al., 2004; Szerlong et al., 2008; Wu et al., 2009). Arp4 is required for Yaf9 and

Swc4 association with SWR1-C and its own recruitment depends on the interaction with Act1 (Szerlong et al., 2008; Wu et al., 2009). Hence the general order is the Eaf1 HSA domain recruits Act1 and Arp4, which binds to the Yaf9-Swc4 dimer. The four members intertwine with each other and are important for the anchoring of NuA4 and SWR1-C complexes.

As the SWR1-C complex deposits H2A.Z, this section will discuss how H2A.Z functions. The H2A.Z variant was initially identified in the early 1980s in mouse L1210 cells (West and Bonner, 1980). Since its discovery, scientists have extensively explored its functions in chromatin and in signaling pathways (Giaimo et al., 2019). H2A.Z has been linked to great number of biological processes. Examples include transcriptional memory, anti-silencing at chromatin boundaries, DNA repair, and both transcriptional activation and repression (Zovkic et al., 2014; Narkaj et al., 2018; Babiarz et al., 2006; Zhou et al., 2010; Nishibuchi et al., 2014; Vardabasso et al., 2015; Gowans et al., 2019). How this histone variant functions in a wide range of activities still awaits to be answered. Like all the other canonical histones, H2A.Z can be modified with PTMs. Research has shown that the transcription regulatory functions of H2A.Z, repressive or promotive, can be enhanced by certain PTMs (Giaimo et al., 2018; Gallant-Behm et al., 2012). For instance, H2A.Z can be acetylated by NuA4 to become H2A.Zac, which is associated with gene activation (Valdés-Mora et al., 2012). Since both acetylation and crotonylation levels are influenced by metabolites, it is reasonable to propose that H2A.Z deposition and its impacts on downstream transcription could be indirectly manipulated by cell metabolism. H2A.Z is frequently found in enhancer regions and transcriptional start sites of both active and inactive genes (Raisner et al., 2005). Most research suggested a positive correlation between H2A.Z deposition and gene expression. However, opposite viewpoints exist, which is supported by the antagonistic relationship found between H2A.Z and RNA polymerase II (RNAPII) (Li et al., 2005).

The main function of the 14-subunit complex SWR1-C appears to be depositing H2A.Z into promoters and transcriptional start sites of genes and at DNA double-stranded breaks (Lu, et al., 2009), hinting at the potential importance of H2A.Z in transcription and DNA repair. The

discovery of SWR1-C is an outstanding step forward to learning more details of the dual role of H2A.Z in gene regulation. The energy demanding process to deposit H2A.Z involves partial unwrapping of the DNA from the nucleosome (Willhoft et al., 2018). As a member of the SWR1-C complex, Swr1 is a catalytic chaperone that delivers the H2A.Z-H2B dimer to nucleosomes by a precise mechanism: one H2A.Z-H2B dimer is deposited to form a heterotypic H2A-H2A.Z nucleosome, then a second H2A.Z-H2B is deposited to form a homotypic H2A.Z-H2A.Z nucleosome (Hong et al., 2014; Willhoft et al., 2018). Even though H2A.Z deposition is performed by SWR1-C, NuA4 is required to stimulate the process (Auger et al., 2008; Keogh et al., 2006). The catalytic subunit of NuA4, Esa1, not only promotes SWR1-C recruitment by acetylating H4 and H2A tails within the nucleosome, but also acetylates newly deposited H2A.Z (Altaf et al., 2010; Ranjan et al., 2013). Acetylated nucleosome H4 and H2A are recognized by a SWR1-C component, Bdf1, via its bromodomain (Altaf et al., 2010). In summary, the possible order of the events is: SWR1-C module Arp4/Act1/Yaf9/Swc4 binds to chromatin which recruits scaffold protein Eaf1 through its HSA domain; subsequently, the interaction between Eaf1 and Arp4-Act1 recruits the rest of the NuA4 complex; Esa1 of NuA4 acetylates H4 and H2A in the nucleosome; the acetyl-reading Bdf1 recognizes acetylated H4 and H2A, and recruits SWR1-C onto the nucleosome; SWR1-C substitutes H2A-H2B for H2A.Z-H2B, depositing H2A.Z into the nucleosome.

Yeast Metabolic Cycle

Yeast has certainly left its mark on the history of biology. In the early 1990s, Edward Buchner used yeast to demonstrate enzymatic activities outside of a living cell, which practically started the field of metabolic pathway study (Bohley and Fröhlich, 1997). Not only was the yeast genome the first eukaryotic genome to be fully sequenced, but the ease with which scientists can manipulate its genes for mutation or deletion also quickly established yeast as a premier model organism to study transcription and protein functions (Goffeau et al., 1996). To yeast workers, the

most common assay to show growth phenotypes is to perform the yeast growth assay on Yeast extract Peptone Dextrose agar plates (YPD). It is a rather easy experiment with decisive interpretation of outcomes. However, the growth phenotypes presented by the assay only answer limited types of questions such as whether a certain mutation prevents or affects the growth of yeast on various agent-added plates. The yeast metabolic cycle (YMC) is a phenomenon that ensures the full usage of energy and efficiency of compartmentalized biological activities (Figure 1.2). Ever since I learned about using a chemostat to observe the YMC, I realized the YMC is a much stronger type of phenotypical evidence that not only shows the impact of gene and protein mutations, but also is a dynamic tool to observe the acute impact that chemicals have on yeast growth. Additionally, the chemostat allows users to collect yeast timepoint samples while the YMC is progressing. This feature substantially increases the possibilities of downstream experiments including Western Blotting, RNA-sequencing, ChIP-qPCR, and chromatin association assay. YMC is a powerful system to connect transcriptional changes and environmental influences (Klevecz et al., 2004; Tu et al., 2005; Tu and McKnight, 2007; Mellor, 2016). The chemostat allows users to observe visual evidence of the YMC by controlling the growth condition to mimic the wild living environment of yeast, which has direct ties with circadian rhythms (Tu and McKnight, 2006). Yeast cells metabolically synchronize together and go though cycles of a high-oxygen consumption (HOC) phase and a low-oxygen consumption (LOC) phase under glucose-limiting media (Tu and McKnight, 2007; Mellor, 2016). These nutrient-limiting conditions enforced by the chemostat can also be altered and observed directly on the control screen. Yeast cells cycle through the HOC phase have a hallmark of a high level of acetyl-CoA which is often related to high-energy production. The energy produced in the HOC phase is to support high-energy demanding processes such as pro-growth activities and ribosome synthesis (Tu et al., 2007). On the other hand, yeast cells oscillate through the LOC phase show a high level of crotonyl-CoA which is a product of β-oxidation and the precursor for histone crotonylation (Hiltunen et al., 2003; Mellor, 2016; Gowans et al., 2019). During this phase, cells utilize previously produced energy

and perform activities such as DNA replication and repair, and cell division (Tu et al., 2007). The HOC and LOC phases can be subdivided into additional subphases based on gene expression and GO ontology profiles (oxidative phase (OX), reductive building (RB) phase, and reductive charging (RC) phase (Tu et al. 2005; Mellor, 2016). Therefore, the chemostat livestreams the breathing cycles of yeast which is represented in the form of the YMC.

Concluding Remarks and Contributions of This Work

It has been highly speculated that the cellular metabolic environment influences transcription so that biological processes can be compartmentalized for better efficiency. However, the connection between cellular metabolism and transcription remains mysterious. Previously, we learned that Taf14 links yeast metabolic state to gene expression through the interaction between its YEATS domain and Kcr. Even though histone acetylation is associated with the HOC phase of the YMC, histone crotonylation occurs in the LOC phase, and, by the action of Taf14, is responsible for the repression of pro-growth genes as cells transition from the HOC into the LOC stages (Gowans et al., 2019). The work inspired us to focus on dissecting the role of another YEATS domain-containing protein, Yaf9, and how it conveys information from metabolites to transcription. My thesis project started with the intention to compare Yaf9's role in metabolic-driven transcription with Taf14's mechanism. However, we gradually realized that Yaf9 not only operates in a completely different style than Taf14, but there is also more information about the YMC that needs to be addressed. With a weaker association for histone crotonylation than that of Taf14, the YEATS domain of Yaf9 shows binding for both Kac and Kcr. Since the cellular level of acetyl-CoA is three folds higher than crotonyl-CoA (Sabari et al., 2015), this became our first clue that Yaf9's role in metabolic-driven transcription regulation is different than the one of H3K9cr-preferring Taf14. Additionally, we know that the two proteins are involved in different machineries, as Yaf9 is shared by only two major complexes (SWR1-C and NuA4) (Lu,

et al., 2009). This makes Yaf9 an easier candidate to study the YEATS domain than Taf14, which is shared by eight complexes.

Figure Legends

Figure 1.1: YEATS Domain Containing Proteins in Yeast

In budding yeast, there are three YEATS-domain containing proteins: Taf14, Sas5, and Yaf9.

Figure 1.2 Yeast Metabolic Cycle (YMC)

Metabolically synchronized yeast cells go through cycles of a high-oxygen consumption (HOC) phase and a low-oxygen consumption (LOC) phase under nutrient-limiting media.

Figures

Figure 1.1: YEATS Domain Containing Proteins in Yeast

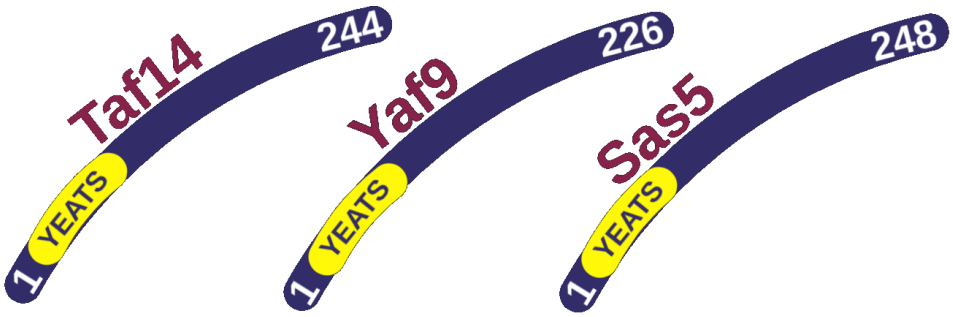

Figure 1.2 Yeast Metabolic Cycle (YMC)

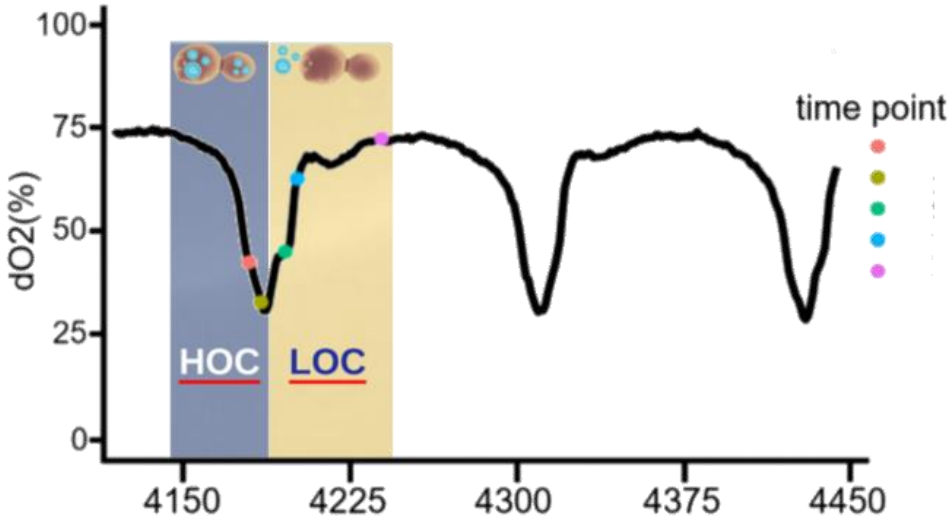

CHAPTER 2 – RECOGNITION OF HISTONE CROTONYLATION BY TAF14 LINKS METABOLIC STATE TO GENE EXPRESSION

Summary

Metabolic signaling to chromatin often underlies how adaptive transcriptional responses are controlled. While intermediary metabolites serve as co-factors for histone-modifying enzymes during metabolic flux, how these resulting modifications contribute to transcriptional responses is poorly understood. Here, we utilize the highly synchronized yeast metabolic cycle (YMC) and find that fatty acid β-oxidation genes are periodically expressed coincident with a β-oxidation byproduct, namely histone crotonylation. Specifically, we found that H3K9 crotonylation peaks when H3K9 acetylation declines and energy resources become limited. During this metabolic state, pro-growth gene expression is dampened; however, mutation of the YEATS domain of Taf14, a prominent H3K9 crotonylation reader, results in de-repression of these genes. Conversely, exogenous addition of crotonic acid results in increased histone crotonylation, constitutive repression of pro-growth genes, and disrupted YMC oscillations. Together, our findings expose an unexpected link between metabolic flux and transcription, and demonstrate that histone crotonylation and Taf14 participate in the repression of energy-demanding gene expression.

Introduction

To ensure efficient growth and survival, cells must sense diverse and dynamic nutrient environments and rapidly reprogram their metabolic output accordingly. One way this can be achieved is through the synchronization of gene expression with the metabolic environment. Chromatin modifications provide an ideal mechanism to link the metabolic status of the cell to

transcriptional output, as these changes are rapid, reversible and are reliant upon metabolic intermediates as cofactors for the modification (Gut and Verdin, 2013). Understanding the relationship between environment, chromatin and gene expression provides insights into general principles of metabolic homeostasis as well as being relevant for a number of disease states where energy metabolism is a major contributing factor, including cancer and diabetes (Gut and Verdin, 2013).

The yeast metabolic cycle (YMC) offers a powerful system for studying the relationships between metabolic flux, chromatin modifications, and transcriptional output (Klevecz et al., 2004; Tu et al., 2005). Similar relationships between energy metabolism and gene expression regulation have been observed during circadian rhythms in mammals (Mellor, 2016; Tu and McKnight, 2006). The YMC occurs in glucose-limited conditions and, therefore, likely simulates low-carbon environments encountered in the wild. A primary characteristic of the YMC is respiration cycles, as yeast rapidly synchronize their metabolic states and oscillate from periods of low oxygen consumption (LOC) to high oxygen consumption (HOC). These phases are accompanied by coordinated changes in gene expression, with over half of all transcripts displaying periodic expression (Kuang et al., 2014), as well as fluctuations in metabolic intermediates (Tu et al., 2007) and histone post-translational modifications (PTMs) (Cai et al., 2011). For example, the HOC phase is characterized by increased histone lysine acetylation and expression of pro-growth genes, including ribosomal subunits and those involved in translation. This temporal regulation coordinates energy production, such as acetyl-CoA, with energy-demanding processes, such as ribosome biogenesis. Disruption of a number of metabolic regulators disturbs YMC profiles and causes a disconnect between metabolism and gene expression. These regulators include chromatin remodelers, transcription factors and TORC1 signaling components (Cai et al., 2011; Gowans et al., 2018; Kuang et al., 2017).

Recent advancements in mass spectrometry have identified a number of novel histone PTMs, greatly expanding the potential complexity of the histone code (Strahl and Allis, 2000; Tan

et al., 2011; Zhao and Garcia, 2015). Many of these are short-chain lysine acylations with differences in the length of carbon chain or degree of saturation. The precursor metabolites of these acylations are often generated in alternate energy metabolism pathways during low glucose conditions (Sabari et al., 2017; Suganuma and Workman, 2018). For example, crotonyl-CoA, the precursor for histone lysine crotonylation is produced via the fatty acid oxidation pathway. In yeast, unlike mammals, this occurs in the peroxisome where fatty acids are taken up and processed through a series of reactions to generate acetyl-CoA and a fatty acid of carbon chain length n-2, which can then itself be processed (Hiltunen et al., 2003). During this process, acyl-CoAs are produced as an intermediate and could act as donors for acylation reactions (Simithy et al., 2017). Specifically, the donor crotonyl-CoA, a trans-2-enoyl-CoA, is generated as an intermediate during β-oxidation of butyric or crotonic acid as well as during the processing of longer fatty acid chains.

Histone crotonylation has become intensively studied over the last several years, owing to the fact that this chromatin mark is found on a number of lysine residues across core and linker histones and is associated with regions of active chromatin, including enhancers and transcriptional start sites (Sabari et al., 2015; Tan et al., 2011). Furthermore, histone crotonylation was demonstrated to promote transcription similar to acetylation in an *in vitro* transcription assay and following crotonic acid addition in cells, suggesting an activating role in gene expression (Li et al., 2016; Sabari et al., 2015). Although the “writers” of histone crotonylation are still being elucidated, a variety of lysine acetyltransferases have been shown to possess histone crotonyl-transferase activity (Sabari et al., 2015; Simithy et al., 2017). Evidence also indicates that non-enzymatic mechanisms for histone acylation can occur (Simithy et al., 2017). In contrast, removal of histone acylation is known to be facilitated by a number of deacetylases in yeast and by Sirt3 in mammalian cells (Andrews et al., 2016; Bao et al., 2014). Thus, the balance between histone acetylation and crotonylation may be determined by the relative intracellular pools of the acyl-CoAs.

Recent reports show that YEATS domain-containing proteins (Yaf9, ENL, AF9, Taf14, Sas5) are prominent readers of histone acylations and are found in a number of chromatin and transcriptional regulators from yeast to humans (Andrews et al., 2016; Li et al., 2016; 2014; Shanle et al., 2015; Zhao et al., 2016). While significant progress has been made in understanding their acyl-binding preferences, our understanding of how histone acylation and its readers contribute to chromatin biology is poorly understood.

In this report, we utilized the YMC to investigate the role of histone crotonylation in metabolic stability and its relationship with histone acetylation. We show that both histone crotonylation and acetylation dynamically fluctuate across the YMC yet have distinct peaks at different points in the metabolic cycle. Genetic and chemical modification of crotonylation patterns alters the periodicity of the YMC and disrupts the expression and timing of metabolic genes. Mechanistically, we found that the ability of Taf14 to read H3K9 crotonylation was required for proper YMC progression and for the periodic repression of growth genes as cells transition to the LOC phase. Together, our data demonstrate a key role for Taf14 and histone crotonylation in linking metabolic state to key gene expression programs.

Results

Histone Crotonylation is Dynamically Regulated Across the YMC and Regulates Metabolic Cycling

While histone acetylation has been intensely studied, our understanding of how other forms of histone acylation contribute to chromatin biology remains obscure. In S. cerevisiae, the peroxisomal fatty acid oxidation pathway produces long and medium acyl-CoA forms, such as crotonyl-CoA, during periods of limited energy availability and low oxygen consumption (Hiltunen et al., 2003) (Figure 2.1A). In contrast, acetyl-CoA, the cofactor for histone acetylation, is largely generated during high energy availability and utilized during oxygen consumption (Cai et al.,

2011). Thus, the molecular pathways and cellular circumstances that result in the deposition of histone acetylation and crotonylation are predicted to be different.

To explore the role of histone crotonylation in the regulation of gene expression and metabolic stability, we employed a well-established continuous culture system wherein yeast cells become synchronized at the metabolic level and cycle through periods of high oxygen and low oxygen consumption (HOC and LOC, respectively) when grown under limited glucose conditions (Klevecz et al., 2004; Tu et al., 2005). Consistent with previous studies (Cai et al., 2011), H3K9 acetylation is dynamic across the YMC and peaks during the HOC phase, when levels of acetyl-CoA are abundant (Figure 2.1B). Strikingly, we found that H3K9 crotonylation is also dynamic across the YMC but peaks during the HOC to LOC transition when β-oxidation occurs. In addition, the H3K9 crotonylation signal peaks as the H3K9 acetylation signal decreases during the return to the LOC phase, demonstrating that these histone modifications are temporally segregated within the YMC. Notably, and in comparison, only relatively low levels of H3K9 crotonylation were observed in asynchronous yeast cultures grown in nutrient-rich YPD media (Figure 2.2A), demonstrating the utility of the YMC to investigate crotonylation function. Importantly, our H3K9 acetyl- and crotonyl-specific antibodies were validated by peptide dot blot assays and showed no cross reactivity, although some butyrylation reactivity was noted for the anti-crotonyl antibodies (Figure 2.1B). Additionally, the presence of H3K9cr in these YMC samples were verified by mass spectrometric analysis of isolated histones (data not shown).

The transcription of key enzymes involved in fatty acid oxidation and acyl-CoA metabolism correlate well with the distribution of H3K9 crotonylation observed in our western blot data (Figure 2.1C). In budding yeast, Acs2 is required for the generation of nuclear pools of acetyl-CoA for histone acetylation (Falcón et al., 2010; Takahashi et al., 2006) and as expected, we see an increase in ACS2 transcript levels as histone acetylation levels peak (Figure 2.1C). An increase in the levels of ACS1 transcript coincide with an increase in histone crotonylation arguing that it may have a role in generating the nuclear pool of crotonyl-CoA for histone crotonylation. ACS1 is

the homolog of mammalian ACSS2, which is critical for generation of histone crotonylation in human cells upon addition of exogenous crotonate (Sabari et al., 2015). Deletion of ACS1 has been shown to completely abrogate metabolic cycling arguing for a critical role for histone crotonylation in the YMC (Cai et al., 2011).

The temporal expression of fatty acid oxidation genes, previously reported in high temporal resolution RNA-seq experiments (Kuang et al., 2014), peaks during the HOC to LOC transition (Figure 2.1C, which are equivalent to time points 6-9 and 16-19 in Figure 2.1B). Of the fatty acid oxidation genes upregulated during the LOC phase, POX1 and ECI1 are essential to the generation of crotonyl-CoA: POX1 converts acyl-CoAs to trans-2-enoyl-CoA as the first step of the β-oxidation pathway, and ECI1 is part of the auxiliary oxidation pathway involved in processing unsaturated fatty acids (Figure 2.1A) (Hiltunen et al., 2003). Strikingly, deletion of either POX1 or ECI1 resulted in severe defects to the timing of the YMC, with cycles becoming progressively faster and dampened (Figure 2.1D). Notably, these mutants did not display growth defects on either dextrose- or glycerol-containing medium, indicating that the altered YMC patterns are not a consequence of overall fitness defects but likely due to an inability to correctly regulate and synchronize metabolic states in the chemostat (Figure 2.1E). Significantly, levels of H3K9 crotonylation were also greatly diminished in these mutants (Figure 2.1F), suggesting the inability to generate sufficient crotonyl-CoA. Unlike H3K9 crotonylation, the levels of H3K9 acetylation were high throughout the mutant cycles, comparable to a wild-type sample at the peak of acetylation. We also examined the YMC profiles of other mutants in this pathway and found that deletion of FOX2 (converts trans-2-enoyl-CoA to 3-ketoacyl-CoA) or POT1 (converts 3-ketoacyl-CoA to acetyl-CoA and an acyl-CoA containing n-2 carbons) also exhibits disrupted YMC and reduced H3K9 crotonylation (Figure 2.2C and 2.2D). Together, these data demonstrate an important role for fatty acid oxidation in the YMC, and further, suggests the intriguing possibility that H3K9 crotonylation, which is produced via fatty acid oxidation, may have an important role in regulating the YMC.

Histone Crotonylation and Acetylation are Associated with Highly Expressed Metabolic Genes

The genomic locations of H3K9 crotonylation have not been previously mapped in any organism. Given the significance of Pox1 and Ecl1 for the timely progression of the YMC and for H3K9 crotonylation levels, we next sought to determine where this mark resides across the genome at the peak of H3K9 crotonylation (i.e., during the HOC to LOC transition at time points 3 and 4) (Figure 2.3A). For comparison and as a control, we also performed H3K9 acetylation ChIP-seq at these same two time points. We found that both H3K9 acetylation and crotonylation are enriched at transcriptional start sites (TSSs) and termination sites (TTSs) of RNA polymerase II (RNAPII)-regulated genes genome-wide (Figure 2.3B). The location of H3K9 crotonylation at TSSs is consistent with our previous findings that show H3K9 crotonylation is deposited, in part, by Gcn5 and removed by transcription-linked histone deacetylases similar to H3K9 acetylation (Andrews et al., 2016).

When analyzed individually, there was a positive association of H3K9 acetylation and crotonylation with YMC gene expression during the HOC to LOC transition (Figure 2.3C). Specifically, the highest quartiles of gene expression at timepoints 3 and 4 also displayed the highest occupancy of histone acetylation and crotonylation. Furthermore, changes in gene expression correlate with H3K9 modification levels at the TSSs, while modification at the TTSs were predominantly static, suggesting both modifications are linked to the regulation of gene expression.

Further analysis of our ChIP-seq data set showed that H3K9 crotonylation and acetylation occupy many of the same TSSs during the peak of crotonylation (r = 0.88 at timepoint 3), implicating a possible cooperative relationship between these two acylations. To further examine this relationship, we examined the relative ratio of H3K9 crotonylation to H3K9 acetylation at TSSs during time points 3 and 4 (Figure 2.1B) when both acylations can be detected. This analysis found that genes periodically expressed during the HOC phase (i.e., time points 1 and 2, Figure

2.3A) were among those with the highest H3K9 crotonylation/acetylation ratios during the transition to LOC (timepoints 3 and 4, Figure 2.3A and 2.3D). These included genes that function in ribosome biogenesis and translation (Figures 2.3E and 2.3F), which are pro-growth genes with the highest amplitude of periodic gene expression in the YMC (Tu et al., 2005). These genes have a burst of expression during the HOC that is accompanied with increased H3K9 acetylation and energy production, followed by active repression and H3K9 acetylation loss during the LOC phase when oxygen is no longer consumed (Cai et al., 2011). As such, the high H3K9 crotonylation to acetylation ratios seen on these genes in this study likely represent a combination of decreasing levels H3K9 acetylation concomitate with increasing levels of H3K9 crotonylation.

Collectively, these results demonstrate that H3K9 crotonylation, like H3K9 acetylation, is associated with periodic expression of YMC genes. The high H3K9 crotonylation to acetylation ratios on these genes during the transition from HOC to LOC further implicate a role for these two marks in the precise regulation of energy-demanding, highly expressed HOC genes.

The YEATS Domain of Taf14 is Required for Proper YMC Progression and for the Precise Control of Metabolic Gene Transcription

Given that H3K9 crotonylation is associated with periodic gene expression, we next sought to determine how this mark might function in the YMC. Previous work by our group and others has shown that the YEATS domain of Taf14 is a prominent reader of acylated H3K9 (Andrews et al., 2016; Shanle et al., 2015) with a notable preference for H3K9 crotonylation (Andrews et al., 2016). Consistent with past observations, we confirmed these results quantitatively using isothermal titration calorimetry (ITC), which showed that the YEATS domain of Taf14 has strong preference for H3K9 crotonylation over other acyl-H3K9 forms (K_d of 70 µM versus 171 µM for Kcr versus Kac (Figure 2.4A). These values agree with previously reported ITC values (Li et al., 2016). Interestingly, like bromodomains, the Taf14 YEATS domain binds more tightly to a peptide

that is poly-crotonylated or poly-acetylated compared to singly acylated peptides, however the mechanism by which poly-acylation leads to higher affinity binding remains unclear (Figure 2.4A).

To determine if Taf14 reading of H3K9 crotonylation might impact YMC function, we engineered a genomic point mutation (W81A) in the Taf14 YEATS domain (*taf14*$_{W81A}$) that abolishes its binding to all forms of acylated histones (Shanle et al., 2015). *In vivo* Taf14 is a member of multiple chromatin-modifying complexes and the general transcription apparatus (Schulze et al., 2009) and is known to occupy gene promoters marked with H3K9 and H3K14 acetylation (Liu et al., 2005). ChIP-qPCR analysis revealed that the *taf14*$_{W81A}$ mutant resulted in abrogated binding of Taf14 to the promoters of several cycling genes, indicating an important as well as an undocumented role for H3K9 acylation in the recruitment of Taf14 to genes (Figure 2.4B). ChIP-seq analysis confirmed the enrichment of Taf14 proximal to transcriptional start sites, and to a lesser extent, transcriptional stop sites (Figure 2.4C). Conversely, *taf14*$_{W81A}$ ChIP did not produce sufficient material for sequencing (data not shown), confirming its reduced ability to localize to chromatin.

Consistent with our past report (Andrews et al., 2016), complete deletion of *TAF14* resulted in a slow growth phenotype on glucose-containing (YPD) medium whereas the YEATS domain pocket mutant that disrupts acyl-H3K9 binding did not (Figure 2.4A). Interestingly, growth of the *taf14*Δ strain on non-fermentable glycerol-containing media (YPG) was comparable to the wild-type strain, suggesting that the slow growth phenotype observed in deletions of *TAF14* are due to disrupted glycolysis rather than oxidative phosphorylation.

Strikingly, a complete loss of Taf14 resulted in a dramatically altered YMC profile, with cycles oscillating rapidly through LOC phases when genes associated with glycolysis peak (Tu et al., 2005) (Figure 2.4B). Importantly, the Taf14 YEATS domain mutant also altered the timing and amplitude of the YMC, with cycles occurring slightly slower than that found with our wild-type strain. We also confirmed that the *taf14*$_{W81A}$ strain did not substantially alter H3K9 crotonylation

levels in cycling strains (Figure 2.4C). Thus, the ability of Taf14 to read H3K9 acylation is important for proper regulation of the YMC.

To identify how YMC gene expression would be altered in the absence of Taf14 reading of H3K9 acylation, we performed RNA-seq analysis in wild-type and *taf14*$_{W81A}$ cells across two consecutive YMC cycles (Figure 2.6A). Principal component analysis (PCA) of this experiment revealed that both wild-type and *taf14*$_{W81A}$ samples are generally arranged in a circle, reflecting the cyclical nature of the YMC (Figure 2.6B). Timepoints 1 and 2, which represent the peak of H3K9 acetylation, are clustered close together, indicating a high degree of similarity between the wild-type and *taf14*$_{W81A}$ mutant. However, timepoints 3 and 4, which represent the peak of H3K9 crotonylation during the transition to the LOC quiescent phase (see Figure 2.1B), are farther apart, indicative of transcriptional profiles that have more differences between the wild-type and *taf14*$_{W81A}$ mutant at these times points.

Consistent with the PCA analysis, there were more significantly differentially expressed (SDE) genes, with higher magnitude and significance of difference, during the histone crotonylation peak (timepoints 3 and 4) compared with the histone acetylation peak (timepoints 1 and 2) in the *taf14*$_{W81A}$ mutant (Figure 2.6C). More than twice as many up-regulated SDE genes (n=595) compared to down-regulated genes (n=266) were identified in the *taf14*$_{W81A}$ at the peak of histone crotonylation. Unexpectedly, these up-regulated genes were significantly enriched in pro-growth pathways, such as ribosome biogenesis and translation (Figure 2.6D). As previously mentioned, pro-growth genes are normally highly expressed during the HOC phase when H3K9 crotonylation levels are low and are repressed in the LOC phase when H3K9 crotonylation levels increase (Figure 2.3D-F). In the *taf14*$_{W81A}$ mutant, these genes are still repressed, albeit to a lesser degree during the HOC to LOC transition (Figure 2.6E and Figure 2.7). Conversely, down-regulated genes in the *taf14*$_{W81A}$ mutant exhibit broad expression defects throughout the YMC, suggesting these genes may be less related to the direct function of histone crotonylation (Figure 2.6E).

The data above suggests the possibility that Taf14 association with H3K9 crotonylation directly represses HOC genes; however, loss of Taf14-H3K9 acyl reading might also alter the expression of 'master' metabolic transcriptional regulators that influence the expression of these genes. A variety of transcription factors are known to coordinate the expression of numerous metabolic genes in phase with the YMC (Kuang et al., 2017; Rao and Pellegrini, 2011). We, therefore, examined the expression of 41 master transcription factors and the expression of their target genes in the *taf14*$_{W81A}$ mutant. Of these, Dot6/Tod6-regulated gene expression in the mutant compared to wildtype cells showed a notable increase (Figure 2.7B). In metabolically asynchronous cultures, Dot6/Tod6 are transcriptional repressors of ribosome biogenesis, and are inactivated by TORC1 and PKA-dependent signaling (Huber et al., 2011; Lippman and Broach, 2009). At timepoints when ribosomal gene expression is increased in the *taf14*$_{W81A}$ mutant, Tod6 expression is elevated while Dot6 is reduced (Figure 2.7C). However, the functional output of these transcription factors in the YMC is not clear, as both TORC1-signaling and Dot6/Tod6 expression are normally elevated during the peak of ribosomal gene expression (Gowans et al., 2018). Thus, it is likely that a combination of repressors and activators are responsible for the tight transcriptional regulation of ribosome biogenesis, the coordination of which is disrupted in the *taf14*$_{W81A}$ mutant.

Nevertheless, taken together, these findings demonstrate that disrupting the association of Taf14 with H3K9 acylation primarily impacts HOC gene expression patterns during the transition to LOC. They further provide evidence that Taf14-H3K9 crotonylation interaction is important for the proper repression of HOC genes in the LOC phase when oxygen consumption and energy production are depleted (and when H3K9 crotonylation levels are high).

Elevated Histone Crotonylation Alters the YMC and Reduces Pro-Growth Gene Expression

To further investigate the influence of histone crotonylation on YMC gene expression, we manipulated the levels of H3K9 crotonylation by adding a gradual increase of crotonic acid to the YMC medium, which becomes metabolized into crotonyl-CoA and used for histone crotonylation (Li et al., 2016; Sabari et al., 2015). Increasing crotonic acid levels resulted in a dramatic decrease in the periodic length of the YMC (Figure 2.8A). Conversely, equal molar addition of sodium acetate produced a more gradual decrease in the YMC period. Addition of crotonic acid persistently increased crotonylation on several H3 and H4 lysines, including H3K9, while acetylation levels fluctuated at a reduced amplitude, perhaps as a consequence of altered cycles (Figure 2.8B and Figure 2.9A). Interestingly, addition of crotonic acid to *pox1Δ* mutants also increases H3K9 crotonylation (Figure 2.9B and C), suggesting that crotonyl-CoA can be produced by short chain fatty acyl-CoA synthetase conversion of excess crotonic acid.

qPCR analysis of transcript levels demonstrated that ribosomal gene expression was dramatically down-regulated following addition of crotonic acid that was concomitant with increased histone crotonylation (Figure 2.8C). Conversely, non-cycling genes that were not differentially expressed in the *taf14*$_{W81A}$ mutant were not significantly changed by the addition of crotonic acid (Figure 2.8C). Accordingly, these ribosomal genes have higher histone crotonylation to acetylation ratio during the HOC to LOC transition, compared to genes with peak expression in the LOC phase and non-cycling genes (Figure 2.8D). These results provide further support for the idea that increased crotonylation on genes expressed during the HOC phase reduces expression.

In addition to the influence of Taf14 binding to H3K9 acylations, another way histone crotonylation could reduce expression of HOC genes is through the repulsion of bromodomain-containing transcriptional activators, which have been shown to not tolerate longer acyl lysine forms (Andrews et al., 2016; Li et al., 2016). To examine this possibility, we performed ChIP-

qPCR assays for several bromodomain-containing transcriptional regulators including Bdf1/2 and Snf2 in the YMC before and after crotonic acid addition (Figure 2.10). Surprisingly, we observed increased abundance of these transcription factors on several HOC- and LOC-regulated genes following the addition of crotonic acid. The reasons for this are currently unknown, however it does demonstrate that histone crotonylation does not simply rely on inhibition of bromodomain factor binding to facilitate its transcriptional changes.

Collectively, these data show that disruption of the normal levels of histone crotonylation results in altered metabolic synchronization and the expression of ribosomal genes. Taken together with all of our findings, they suggest an unexpected role for Taf14 association with H3K9 crotonylation in regulating the timely repression of energy-consuming gene expression.

Discussion

Our results demonstrate that the metabolic state of the cell is connected to histone crotonylation and transcriptional regulation. Specifically, we show that histone crotonylation: 1) is dynamically regulated across the YMC; 2) displays a temporally distinct pattern from acetylation; 3) is sensitive to disruption of the fatty acid oxidation pathway; 4) contributes to transcription in a Taf14 YEATS domain-dependent manner; and 5) is linked to the timely control of energy demanding gene expression. These studies also show that short-chain acylations, such as crotonylation, are functionally distinct from acetylation and contributes to the transition from high energy metabolic status (i.e. HOC) to low energy status (i.e. LOC).

Our results show that increased H3K9 crotonylation functions to dampen the expression of pro-growth genes that are normally turned off during the HOC to LOC transition when cellular energy becomes depleted (Figure 2.11). This is consistent with the idea that metabolic changes lead to the generation of new metabolites that then contribute to the regulation of transcription programs required for cell growth and survival in diverse nutrient conditions (Gut and Verdin,

2013). In the case of H3K9 crotonylation, its distinct role in regulating gene expression is evident by its post-acetylation increase during the HOC to LOC phase transition.

Taf14-mediated Repression of Genes with H3K9 Crotonylation

A major surprise of our studies is the unexpected role of H3K9 crotonylation and Taf14 in gene repression rather than activation, which was our initial expectation based on previous publications (Li et al., 2016; Sabari et al., 2015). While the YEATS domain of Taf14 binds H3K9 crotonylation, this domain is capable of also recognizing H3K9 acetylation, albeit to a lesser degree (Andrews et al., 2016). Taf14 is also a component of several transcriptional complexes, including chromatin remodelers, NuA4 acetyltransferase, and the Pol II pre-initiation (PIC) complex (Schulze et al., 2009). It would be reasonable to think that Taf14 might then function in the YMC through reading both acetylation and crotonylation. However, our findings point to the idea that Taf14 preferentially functions through H3K9 crotonylation, as the greatest number of differentially expressed genes observed in the *taf14*$_{W81A}$ mutant occurred precisely during the peak of H3K9 crotonylation rather than the peak of H3K9 acetylation.

The idea that Taf14 functions primarily through H3K9 crotonylation is also supported by a recent study that found Taf14-regulated genes can be properly regulated by a form of Taf14 only capable of binding H3K9 crotonylation (Klein et al., 2018). This leads to an important question: how could the binding of crotonylation over acetylation be so profoundly different? Although the answer to this question is currently unknown, we speculate that the unique structural change found in the Taf14 YEATS domain when bound to H3K9 crotonylation (a π-π-π stacking mechanism involving aromatic residues in the YEATS domain (Andrews et al., 2016) may result in either recruitment of Taf14 directly to one or more of its complexes that are already bound on chromatin to block transcriptional initiation or that recognition of H3K9 crotonylation by Taf14 allosterically inhibits some aspect of the PIC or initiation/re-initiation. In support of the idea that Taf14 may be a transient member of repressive transcriptional complexes, a recent mass

spectrometry analysis of active RNAPII transcription complexes that bind to yeast promoters found that Taf14 was absent from these RNAPII and TFIID-containing complexes (Joo et al., 2017). Thus, future biochemical and structural studies will be required to determine the distinct mechanisms that regulate Taf14 recruitment and function.

Fatty Acid Metabolism Attenuates Energy-consuming Transcription in the YMC

The precise regulation of transcriptional processes in the YMC optimizes energy production and consumption with cell growth and division (Wang et al., 2015). During the HOC phase, energy production in the form ATP and acetyl-coenzyme A (CoA) are increased (Cai et al., 2011; Machné and Murray, 2012), concomitant with energy-consuming pro-growth programs. For example, translation is a pro-growth process important for creating components of new cells completing cell division, yet it also necessitates tremendous energy expenditure. Gene expression programs related to translation and ribosome biogenesis often exhibit more than 40-fold increase in expression in the HOC phase compared to the LOC phase. Ribosome biogenesis alone involves nearly 10% of the genome, and has been proposed to account for approximately 60% of total *S. cerevisiae* transcription (Warner, 1999). Thus, pro-growth transcriptional programs, such as ribosome biogenesis, must be tightly regulated to ensure energy efficiency in the cell.

Our data demonstrate that peroxisomal fatty acid β-oxidation and histone crotonylation increase during the HOC to LOC transition, concomitant with reduction of ATP and acetyl-CoA levels and decreased expression of ribosome biogenesis genes (Cai et al., 2011; Machné and Murray, 2012). Thus, the metabolites of fatty acid β-oxidation, an alternative energy source, can communicate with the transcriptional machinery to signal the depletion of available energy and enact co-coordinated transcriptional responses. Consistent with this idea, as cells prepare to transition from LOC back to HOC, histone crotonylation levels are removed both in wild type (Figure 2.1B) and the *taf14*$_{W81A}$ mutant unable to recognize H3K9 crotonylation (Figure 2.4C).

Although it is currently unknown which deacetylases participate in H3K9 crotonylation removal in the YMC, our previous studies suggest the involvement of Rpd3 given its deletion results in increased H3K9 crotonylation (Andrews et al., 2016).

It should be noted that another cellular pathway for unsaturated crotonyl-CoA production is the conversion of saturated butyryl-CoA. However, the dramatic reduction of periodic histone crotonylation in the YMC upon deletion of β-oxidation pathway components suggests that β-oxidation is the primary metabolic pathway that coordinates the transition from HOC to LOC phases (Figures 2.1F and 2.2C).

Additionally, our results highlight the benefits of utilizing a synchronized system, as we were unable to detect significant levels of histone crotonylation in asynchronous cultures grown in rich media. Recent work has also characterized other histone modifications derived from short-chain fatty acids, namely histone propionylation (Kebede et al., 2017) and butyrylation (Goudarzi et al., 2016), as enriched at the TSS of highly expressed genes. It would, therefore, be interesting to examine temporal changes in these modifications across the YMC.

Broader Implications in Fatty Acid Metabolism

The role of fatty acid metabolism in metabolic stability and transcriptional responses has been somewhat understudied. A currently outstanding question is the nuclear accumulation of intermediary metabolites of fatty acid metabolism, such as crotonyl-CoA. Our preliminary analysis was unable to detect specific peroxisomal proteins, such as Pox1, in the nucleus (data not shown). However, we were able to detect nuclear Acs1 (data not shown), the yeast homologue of mammalian ACSS2 that metabolizes exogenous crotonate (Sabari et al., 2015). Nevertheless, much research is still needed to decipher the connection between histone acylation and diverse metabolic pathways.

Importantly, recent research demonstrates that fatty acid metabolism is critical for human health and may contribute to disease when disrupted (Koh et al., 2016). For example, short-chain

fatty acid metabolism occurs in gut microbiota and influences epigenetic profiles in multiple tissues (Donohoe et al., 2011; Krautkramer et al., 2016), including histone crotonylation in the colon that is dynamically regulated by the cell cycle (Fellows et al., 2018). Disruptions in fatty acid metabolism have also been linked to cancer progression (Nath and Chan, 2016). This suggests that fluctuations in histone crotonylation that are linked to metabolic state are likely a normal function of cell physiology and may contribute to disease when disrupted. We predict that the findings we have made in this report will be found to be conserved in other biological contexts.

Materials and Methods

Yeast Strains and Metabolic Cycling

Saccharomyces cerevisiae strains were constructed in the CEN.PK background using standard genetic techniques (Key Resources Table), and were negative for the petite phenotype caused by mitochondrial dysfunction, as assessed by the ability to grow on glycerol-containing media. The taf14W81A strain was generated scarlessly using the delitto perfetto system and verified by Sanger sequencing (Stuckey and Storici, 2013). Metabolic cycling conditions were performed as described previously (Burnetti et al., 2016; Tu et al., 2005), except starter cultures were grown in glycerol-containing media. Dissolved oxygen percentage shown in YMC plots is relative to starting culture conditions (~100%). Continuous respiration cycles occur following addition of glucose to starved cells. For each experiment, the time (in hours) relative to the start of the experiment is shown. Crotonic acid (TCI C0416) and sodium acetate (EMD SX02651) were prepared in water and added at the concentrations indicated in figures. Growth assays were performed by plating serial dilutions (1:10) of indicated strains on YP media containing either 2% glucose (YPD) or 3% glycerol (YPG) and grown at 30°C.

Western Blotting

Cultures were collected from the YMC, fixed in 20% trichloroacetic acid and snap-frozen in liquid nitrogen. Protein was extracted as described in (Kushnirov, 2000). Standard conditions

were used for SDS-PAGE and Western blotting. Antibodies used in this study were: anti-H3K9 crotonylation (PTM Biolabs PTM-516), anti-H3K4 crotonylation (PTM Biolabs PTM 527), anti-H3K9 acetylation (Millipore 07-352, Millipore 06-942), anti-H3 (Millipore 05-928, Epicypher 13-0001), anti-HA (Bethyl A190-108A and Abcam Ab9110), anti-G6PDH (Sigma A9521-1VL), and anti-Bdf1/2 (Govin lab).

Dot Blotting

Different concentrations of biotinylated histone peptides (0.05-5 µg) were spotted onto a nitrocellulose membrane then probed with the anti-H3K9ac (Millipore, 06–942) at 1:5,000 or H3K9cr (PTM Biolabs, PTM-516; Revmab Biosciences, 31-1225-00) at 1:500 in a 5% nonfat milk solution and detected with an HRP-conjugated anti-rabbit by enhanced chemiluminescence (ECL).

Isothermal Titration Calorimetry (ITC)

Purified wild-type Taf14 (residues 1-132) and a series of 20-mer histone H3 peptides containing different acyl modifications (H3K9-acetyl, -propionyl, -butyryl, -crotonyl, or H3 peptides acetylated or crotonylated at K9, K14, and K18) were extensively dialyzed into a buffer containing 50mM HEPES pH 7.5, 200mM NaCl, and 1mM tris(2-carboxyethyl)phosphine (TCEP). ITC experimenters were carried out at 10 °C using a MicroCal AutoITC-200 microcalorimeter. After an initial delay of 120s, H3 peptide (2 mM) was titrated into Taf14 (70 or 100 µM) over the course of 20 injections using 2 µL per injection. Reference power was set to 8 µcal/s and the stirring speed was 1000 RPM. Control heat of dilution experiments were performed by titrating each H3 peptide (2 mM) into a cell containing buffer only. Each peptide showed negligible heat of mixing (data not shown) therefore each sample titration into Taf14 was not corrected for the minimal background heat. Analysis of data was performed using MicroCal ITC-200 Origin software using a 1:1 binding model. The Kd represents the average of two experiments ± the standard deviation.

RNA-Seq Analysis

RNA was prepared from samples (approximately 5 ODs) using the MasterPure™ Yeast RNA Purification Kit (Epicentre, MPY03100). The sequencing libraries were prepared from 1 µg of RNA/sample using the NEB Ultra Directional kit (E7420) with the mRNA isolation module (E7490) and adaptor sets 1/2 (E7355/E7500). Libraries were normalized using the NEB Library Quant Kit for Illumina (E7630). The quality of the pooled library was checked using the Agilent Bioanalyser 2100 HS DNA assay. The library was sequenced on an Illumina HiSeq 2000 Sequencer (50 bp reads). Minimum of 9 million reads per time-point were aligned using Burrows-Wheeler Aligner (bwa) and analysed using the DESeq2 package (Love et al., 2014). Samples were analysed in duplicate and replicates were combined for final analysis. PCA plots (log-transformed data) and significantly differentially expressed (SDE) genes (adjusted p-value < 0.05 and log2 fold change > 0.6) were generated using the DESeq2 package (Love et al., 2014). Functional annotation analysis was performed on SDE genes using DAVID with default parameters (Huang et al., 2009a; 2009b). Genes expressed in the wild-type YMC were previously identified as “periodic” or “non-periodic” using a periodicity algorithm on RNA-seq compiled at high resolution across the YMC (Kuang et al., 2014).

Chromatin Immunoprecipitation (ChIP)

Antibodies used for ChIP were: anti-H3K9 crotonylation (PTM Biolabs PTM516), anti-H3K9 acetylation (Millipore 06-942), anti-H3 (Millipore 05-928), anti-HA (Bethyl A190-108A and Abcam Ab9110), anti-Bdf1/2 (Govin lab), and anti-Taf14 (Reese lab). Chemostat samples (15 ml of saturated culture) were collected, fixed in 1% formaldehyde for 15 minutes and quenched in 125 mM glycine for 10 minutes. Cells were washed twice in TBS (300 mM NaCl, 40 mM Tris pH 7.5) and snap frozen. Pellets were resuspended in 1 ml of FA buffer (50 mM HEPES pH 7.5, 140 mM NaCl, 1% Triton X-100, 1 mM EDTA, 0.1% Sodium deoxycholate, Roche complete protease inhibitor cocktail (11697498001), split into two 500 µl aliquots and lysed by beat beating for 10 min at 4 ˚C. Aliquot volumes were adjusted to 1 ml with FA buffer and sonicated (30 seconds on,

30 seconds off) for 25 minutes. Samples were pelleted and the supernatants (whole cell lysate) pooled. Lysates (adjusted to 2 mg/ml protein for histones or 5 mg/ml for TAF14, using FA buffer) were precleared using Dynabeads Protein A (10001D, 50 µl beads per 500 µl lysate, 1 hour at 4 ˚C) and 50 µl was saved as input. Antibody was added (2 µl for histones) and samples rotated overnight at 4 ˚C. Dynabeads were washed three times in FA buffer + 0.5% BSA, with the third wash lasting minimum of two hours to preblock beads. Beads were then added (50 µl per 500 µl sample) and samples incubated for 2 hours at 4˚C. Beads were washed as: FA buffer, FA buffer containing 500 mM NaCl, LiCl (10 mM Tris-HCl pH 8.0, 250 mM LiCl, 0.5% NP-40, 0.5% sodium deoxycholate, 1 mM EDTA), 1 ml TE pH 8.0. Beads were resuspended in 100 µl of elution buffer (1% SDS, 0.1 M NaHCO3) and DNA was eluted by incubation at 65˚C for 15 min. Supernatant was collected and the elution step repeated to yield 200 µl of eluate. Crosslinks were reversed by adding 10 µl of NaCl (5 M) to the eluate and incubating at 65˚C overnight. Input samples (50 µl) were treated with 150 µl of elution buffer and 10 µl of NaCl alongside the IP samples. Samples were treated with RNase A (10 µg, 60 min at 37˚C) and proteinase K (20 µg, 60 min at 42 ˚C). DNA was purified using the Zymo ChIP DNA Clean & Concentrator (D5205) and eluted in 30 µl of buffer.

ChIP-Seq

Libraries were prepared from 0.5 ng of eluted DNA using the NEBNext Ultra II DNA Library Prep Kit for Illumina (E7645) and adaptor sets 1/2 (E7355/E7500). The quality of the pooled library was checked using the Agilent Bioanalyser 2100 HS DNA assay. The library was sequenced on an Illumina HiSeq 2000 (101 bp reads). Alignments were performed using Burrows-Wheeler Aligner (bwa) with a minimum of 8 million unique reads obtained per sample. Peaks were called using a custom pipeline to generate uniformly processed reads (Beckwith et al., 2018) and the H3K9 acetylation and crotonylation normalized to H3. Fold change signal over H3 was processed using Deeptools2 computeMatrix function (Ramírez et al., 2016). To generate counts around the

TSS or TTS using the reference-point setting, +/- 200 bp was used for histone marks. To generate profiles across the gene body, the scale-regions setting was used.

RNA Extraction and qPCR

Chemostat samples were collected, pelleted and snap frozen. Pellets were washed in water and resuspended in 400 µl TES buffer (10 mM Tris HCl pH 7.5, 10 mM EDTA, 0.5% SDS). An equal volume of acid phenol added and samples were vortexed for 30 seconds. Samples were then incubated at 65C for 45 minutes with occasional vortexing before being chilled on ice for 5 minutes. Samples were centrifuged (5 min, 4C, 12K RPM) and the upper phase transferred to a fresh tube. Phenol extractions were repeated twice. RNA was precipitated by adding 0.1 volumes of sodium acetate (5M, pH 5.3) and 2.5 volumes of ice-cold ethanol (100%) followed by incubation at -80C for 30 minutes. Samples were centrifuged (5 min, 4C, 12K RPM) and the pellet washed with 70% ice-cold ethanol. Pellets were resuspended in water and the concentration determined. RNA (10 mg) was treated with RQ1 DNase (Promega Corporation Cat# M6101) at 37C for 60 minutes. RNA was purified using RNeasy Mini kit (RNeasy Minikit, Qiagen, Cat# 74104). cDNA was prepared using iScript cDNA synthesis kit (Thermofisher Scientific, 18080051). qPCR was performed using the SYBR green kit (PowerUp SYBRTM Green Mastermix, Biorad, Cat# 170 8880) and the primers in Key Resources Table. Signals were normalized to Actin.

RNA-seq Library Preparation and Sequencing

Yeast strains were grown to saturation in YPD before being diluted to an OD_{600} of 0.2 and grown to an OD_{600} of ~1 at 30°C. Cells were isolated, washed with water, and resuspended in SD media (Cheung et al., 2008). Ten ODs of cells were collected at each time point and RNA was isolated by acid phenol (Ambion/Thermo Fisher Scientific) extraction. Five µg RNA was treated with DNase (Promega) and purified (RNeasy column, QIAGEN). Two and a half µg of the purified RNA was processed with yeast-specific rRNA depletion beads (Illumina). Strand-specific bar-coded sequencing libraries were then prepared (TruSeq Stranded Total RNA Library Preparation

Kit, Illumina). Libraries were pooled and sequenced across two lanes (Hi-Seq 4000, Illumina). Data are representative of three independent biological replicates.

Tables

Table 2.1: List of Yeast Strains, Genotypes, and Primers

Name	Genotype	Reference
CEN.PK122-α	MATα MAL2-8c SUC2	(Shi et al., 2010)
CEN.PK113-7D	MATa MAL2-8c SUC2	(Tu et al., 2005)
taf14$_{W81A}$	CEN.PK122-α	This study
taf14Δ (YJB003)	CEN.PK122-α *taf14::*KanMX	This study
eci1Δ (YJB031)	CEN.PK 113-7D *eci1*::HygMX	This study
pox1Δ (YJB030)	CEN.PK 113-7D *pox1*::HygMX	This study
YAT001	CEN.PK 113-7D *fox2::*NatMX [pFA6a-NATMX4]	This study
YAT003	CEN.PK 113-7D *pot1::*NatMX [pFA6a-NATMX4]	This study

Table 2.2: List of Primers

Name	Primer 1	Primer 2
CLN3	GTGGCTGAGAGTTGAAGTTAGT	CTCAGCGATCAGCGAATACA
MRPL10	CGTGGTTTGAAGGTGGTCAA	GGGACCAGTTACCAGACCAA
MRPL40	GCGTAAAGGGTCAACCAGAC	CTCACTACGGAATCGACCCA
RPS23B	TCTCACGCCAAGGGTATTGT	AAACCGGCTAGCAAGACTTC
RPL33B	GCAGTGACGCTCTGTTGCA	GCCTGGAGACCGCTTCTCTT
RPS30A	CATCCTTGCTGATACGCCAA	TAAGCACGACCCTTAGGCTT
BSD2	GCAGGTTCATCTACTGATGGC	CCCTTCTACGCCAGTTTGTG
CWC27	TGGGCTAAAGAATGCCCTGA	TCCCATCCCAAGAGTCCATC
GPI13	CAACAGGGTCCTTACCGACT	TGGAACAGAGCCATCCATGT
PRE5	TGGCTCCAGATGCTAGAGTT	TCAACAAACCAACACCGTAGG
SWP1	TTTCATGCCGAGCCAAAGAG	ACACCGGTCGGGATGTTATT
YRB2	TGCTGTCAGAGGCTGGTAAA	TTGACGACGGAAAGACCGTA
ACT1	TTCTGGTATGTGTAAAGCCGG	CCATACCGACCATGATACCTTG
POX1 set1	CCTCTGAGAGACCCTTCGAC	TGACGGTGACTGAACCATCT
POX1 set2	CCTCTGAGAGACCCTTCGAC	TGACGGTGACTGAACCATCT
POX1 set3	CCAGCTTGAAAGCCACCAAT	ACCCAGTCGTCATAGCCTTT
POX1 set4	CGTGTACGCCAGATTGATCG	ATCAATACCGTCACGACCCA
ACS1	AGCCTCCGATGCCATTATTC	CTTAGAATAGCCGCCCAGTTTAT

Figure Legends

Figure 2.1. Histone Crotonylation is Regulated by Fatty Acid Metabolism and is Dynamic Across the YMC.

(A) Fatty acid β-oxidation pathways for generating acyl-CoA are shown. Example substrates and products of crotonyl-CoA generation are highlighted in purple.

(B) Western blots showing changes in histone H3K9 crotonylation (cr) and acetylation (ac) across two consecutive YMCs. Histone H3 was used as a loading control. Oxygen consumption is inversely correlated with dissolved oxygen (dO2). Peak acetylation and crotonylation are highlighted in green and purple, respectively.

(C) Heatmap showing expression of genes involved in fatty acid oxidation across the YMC. Bars above illustrate changes in crotonylation, acetylation and oxygen consumption. Gene expression data taken from Kuang et al 2014.

(D) Mutants of fatty acid metabolism have disrupted YMCs. Oxygen consumption is inversely correlated with dissolved oxygen (dO2).

(E) Serial dilutions of wild-type (wt) and indicated mutant strains grown on media containing either dextrose (YPD) or glycerol (YPG).

(F) Westerns of *pox1*Δ (left) and *eci1*Δ (right) YMC samples using the indicated antibodies (cr is crotonylated; ac is acetylated). Wildtype YMC samples from both high (H) and low (L) crotonylation timepoints are included as a comparison on right of blots.

Figure 2.2. Fatty Acid Metabolism Regulates Histone Crotonylation

(A) Western analysis of histone H3K9 crotonylation (cr) in asynchronous (asyn.) and YMC timepoints with High and Low histone crotonylation. Histone H3 was used as a loading control. Intervening lanes on western have been cropped and marked with solid line.

(B) Dot blot of antibody specificity. Different concentrations of the indicated peptides were spotted onto a nitrocellulose membrane and detected with the indicated antibodies.

(C) Mutants of fatty acid metabolism have disrupted YMCs. Oxygen consumption is inversely correlated with dissolved oxygen (dO2).

(D) Westerns of fox2Δ (top) and pot1Δ (bottom) YMC samples using the indicated antibodies (cr is crotonylated; ac is acetylated). Wildtype YMC samples from both high (H) and low (L) crotonylation timepoints are included as a comparison on right of blots.

Figure 2.3. Histone Crotonylation and Acetylation Vary Across the YMC

(A) H3K9 crotonylation and acetylation ChIP (triangles) and RNA-seq (circles) timepoints are indicated on the YMC trace and the peak of crotonylation (as determined by western blot, Figure 2.3B) is highlighted in pink.

(B) H3K9 crotonylation (cr) and acetylation (ac) ChIP signals at timepoints 3 and 4 are shown at +/- 200 bp around transcription start site (TSS) or the transcriptional termination site (TTS) of n = 6008 genes. H3K9cr or H3K9ac ChIP signal is normalized by total H3 ChIP.

(C) At timepoints 3 and 4, mean H3K9 crotonylation (cr) and acetylation (ac) ChIP signals are shown for each quartile of gene expression (FPKM, Fragments Per Kilobase of transcript per Million mapped reads) and shown as different colored lines. H3K9cr or H3K9ac ChIP signal is normalized by total H3 ChIP. Transcription start site is TSS, transcriptional termination site is TTS.

(D) Mean H3K9 crotonylation (cr) to acetylation (ac) ChIP ratios at timepoints 3 and 4 on high oxygen consumption (HOC) or low oxygen consumption (LOC) genes in the YMC. Genes that do not have periodic expression in the YMC are labelled as non-YMC. H3K9cr or H3K9ac ChIP signal is normalized by total H3 ChIP. Transcription start site is TSS, transcriptional termination site is TTS.

(E) DAVID functional enrichment analysis of genes in the top and bottom quartiles of H3K9 crotonylation (cr) to acetylation (ac) ChIP ratios at +/- 200 bp around transcription start site at timepoint 3. Enrichment is shown as -log10 p-value.

(F) Heatmaps of genes shown in (E). n= number of genes in each heatmap. YMC oxygen consumption, H3K9 crotonylation and acetylation patterns are illustrated on top of heatmaps from data in Figure 2.1B.

Figure 2.4. Loss of Acylated Histone Binding by Taf14 Disrupts the YMC

(A) Growth tests of wild-type (wt) and indicated mutant strains grown on media containing either dextrose (YPD) or glycerol (YPG).

(B) YMC profiles for wild-type, *taf14*Δ and $taf14_{W81A}$ point mutant.

(C) Westerns of $taf14_{W81A}$ YMC samples using the indicated antibodies (cr is crotonylated; ac is acetylated). Wildtype YMC samples from both high (H) and low (L) crotonylation or acetylation timepoints are included as a comparison on right of blots. Histone H3 is used as a loading control.

Figure 2.5. Taf14 Prefers H3K9 Crotonylation and is Recruited to Genes in a YEATS Domain-Dependent Manner

(A) Representative isothermal titration calorimetry (ITC) fitting curves comparing the binding of the Taf14 YEATS domain to acylated peptides. Histone H3 peptides containing residues 1-20 baring an acetyl (ac), propionyl (pr), butyryl (bu), or crotonyl (cr) modification at lysine 9 (H3K9) or at lysines 9, 14, and 18 (H3K9,14,18) were titrated into the cell containing the Taf14 YEATS domain. The indicated Kd represents the average of two independent ITC experiments ± the standard deviation.

(B) ChIP qPCR analysis of wild-type Taf14 and taf14W81A at several representative loci. Standard deviation of technical replicates is shown. The oxygen traces of the time points examined are shown on top.

(C) Taf14-ChIP seq signal (normalized to total H3 ChIP-seq) shown at +/- 200 bp around transcription start site (TSS) or the transcriptional termination site (TTS) of n = 6008 genes. Timepoints are shown in Figure 2.2A.

Figure 2.6 RNA-seq Analysis of the taf14W81A Mutant YMC

(A) Samples were collected at the indicated timepoints for RNA-seq analysis. Peak crotonylation, as shown in Figure 2.1B, is highlighted in pink.

(B) Principal component (PC) analysis of RNA-seq samples. Biological replicates are shown for each timepoint and separated by strain.

(C) Volcano plots displaying the differences in gene expression between wild-type and *taf14*$_{W81A}$. log2 fold expression change (x-axis) and significance (-log10 p-value, y-axis) are shown for down-regulated (red) and up-regulated (blue) genes in *taf14*$_{W81A}$. Unchanged genes are shown in black.

(D) DAVID functional annotation enrichment analysis of significantly differentially expressed (SDE) genes at timepoint 3. Enrichment is shown as -log10 p-value.

(E) RNA levels (log2 FPKM) of the genes differentially expressed at timepoint 3 across the YMC.

Figure 2.7. Disruption of Taf14 Binding to Histone Crotonylation Alters YMC Gene Expression

(A) RNA levels (log2 FPKM) shown for indicated periodic genes across the wild-type or taf14W81A mutant YMC as heatmaps scaled by row (left) or mean expression line graphs (right). LOC is low oxygen consumption, HOC is high oxygen consumption N = 1502 HOC genes, 930 HOC to LOC genes, 1381 LOC genes, 2195 non-cycling genes.

(B) Box plots of taf14W81A /wild-type RNA-seq from timepoints 3 and 4, described in Figure 2.2. Shown are genes regulated by the indicated transcription factors, as determined in (Kuang et al, 2017). Control are genes not regulated by indicated transcription factors (n= 356).

(C) Volcano plots displaying the differences in transcription factor expression between wild-type and taf14W81A. log2 fold expression change (x-axis) and significance (-log10 p-value, y-axis) are shown for down-regulated (red) and up-regulated (blue) genes in taf14W81A. Unchanged genes are shown in gray.

Figure 2.8. Increased Histone Crotonylation Alters YMC and Reduces Ribosomal Gene Expression

(A) Wild-type YMC profiles with crotonic acid (left) or sodium acetate (right) supplemented media (1 mM). Coloured lines indicate concentration in the culture based on dilution rate. A rolling average of the cycle lengths is shown below.

(B) Western analysis of wild-type YMC samples before (left) and after (right) crotonic acid addition probed with the indicated antibodies (cr is crotonylated; ac is acetylated). Histone H3 is used as a loading control.

(C) RT-PCR qPCR analysis of wild-type YMC samples before (left) and after (right) crotonic acid addition using primers targeting the indicated gene. HOC is high oxygen consumption. LOC is low oxygen consumption. Standard deviation is shown of technical replicates.

(D) H3K9 crotonylation (cr) and acetylation (ac) ChIP signals at timepoints 3 and 4 are shown at +/- 200 bp around transcription start site (TSS) or the transcriptional termination site (TTS) of n = 6008 genes. H3K9cr or H3K9ac ChIP signal is normalized by total H3 ChIP.

Figure 2.9. Exogenous Addition of Crotonic Acid Increases Histone Crotonylation

(A) Western analysis of wild-type YMC samples before (left) and after (right) crotonic acid (1 mM) addition probed with the indicated antibodies (cr is crotonylated; ac is acetylated).

(B) & **(C)** Western analysis of wild-type and pox1Δ asynchronous cultures supplemented with crotonic acid at the indicated concentrations **(B)** or for the indicated times **(C)** addition probed with the indicated antibodies (cr is crotonylated; ac is acetylated). Samples collected from the peak of crotonylation during the wild-type YMC are included as a comparison.

Figure 2.10. Exogenous Addition of Crotonic Acid Alters Binding of Bromodomain Factors

(A) Top, YMC traces with indicated samples before and after crotonic acid addition. Bottom, western of Bdf1/2 and glucose-6-phosphate dehydrogenase, G6PDH.

(B) ChIP qPCR analysis of Bdf1/2 at indicated promoters during the YMC before and after crotonic acid addition. Standard deviation of technical replicates is shown.

(C) Top, YMC traces with indicated samples before and after crotonic acid addition. Bottom, western of HA-Snf2 and glucose-6-phosphate dehydrogenase, G6PDH. It is currently unclear why Snf2 protein levels are decreased following crotonic acid addition.

(D) ChIP qPCR analysis of HA-Snf2 at indicated promoters during the YMC before and after crotonic acid addition. Standard deviation of technical replicates is shown.

Figure 2.11. Model for Taf14 and Histone Crotonylation Regulation of Metabolic Gene Expression

During HOC in the YMC, an abundance of ATP and acetyl-CoA production and consumption occurs along with elevated histone acetylation. Expression of pro-growth genes is facilitated by transcriptional activators containing bromo-domains (BD) that bind acetylated histones. As cells transition from HOC to LOC, fatty acid β-oxidation is activated and histone crotonylation is increased. The YEATS domain of TAF14 binds crotonylated H3K9 to reduce gene expression as energy sources are depleted. During this transition, cell division also occurs. As cells return to the “quiescent-like” LOC phase, reductive metabolism occurs as crotonylation is removed to further repress pro-growth gene expression.

Figures

Figure 2.1: Histone crotonylation is Regulated by Fatty Acid Metabolism and is Dynamic Across the YMC

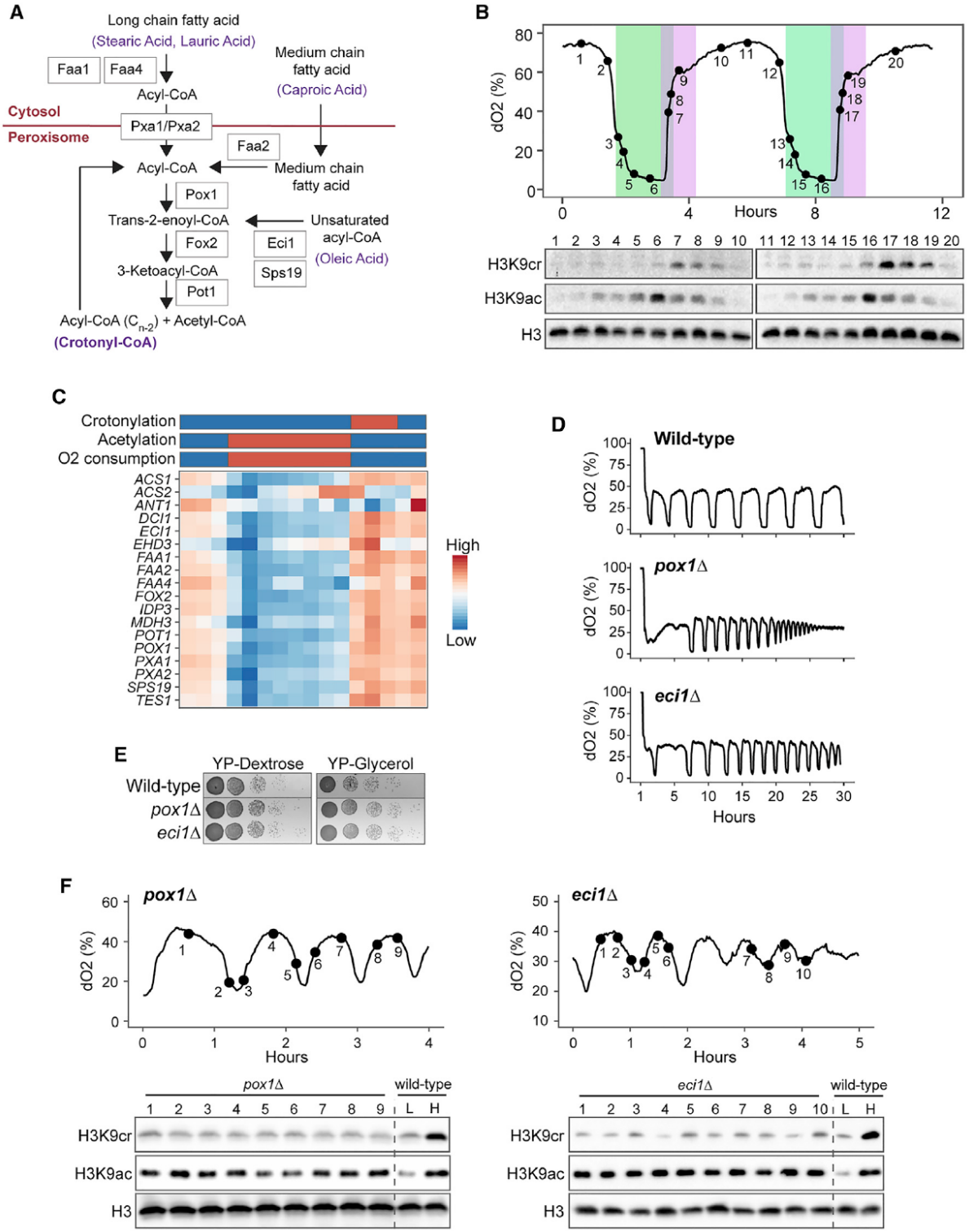

Figure 2.2: Fatty Acid Metabolism Regulates Histone Crotonylation

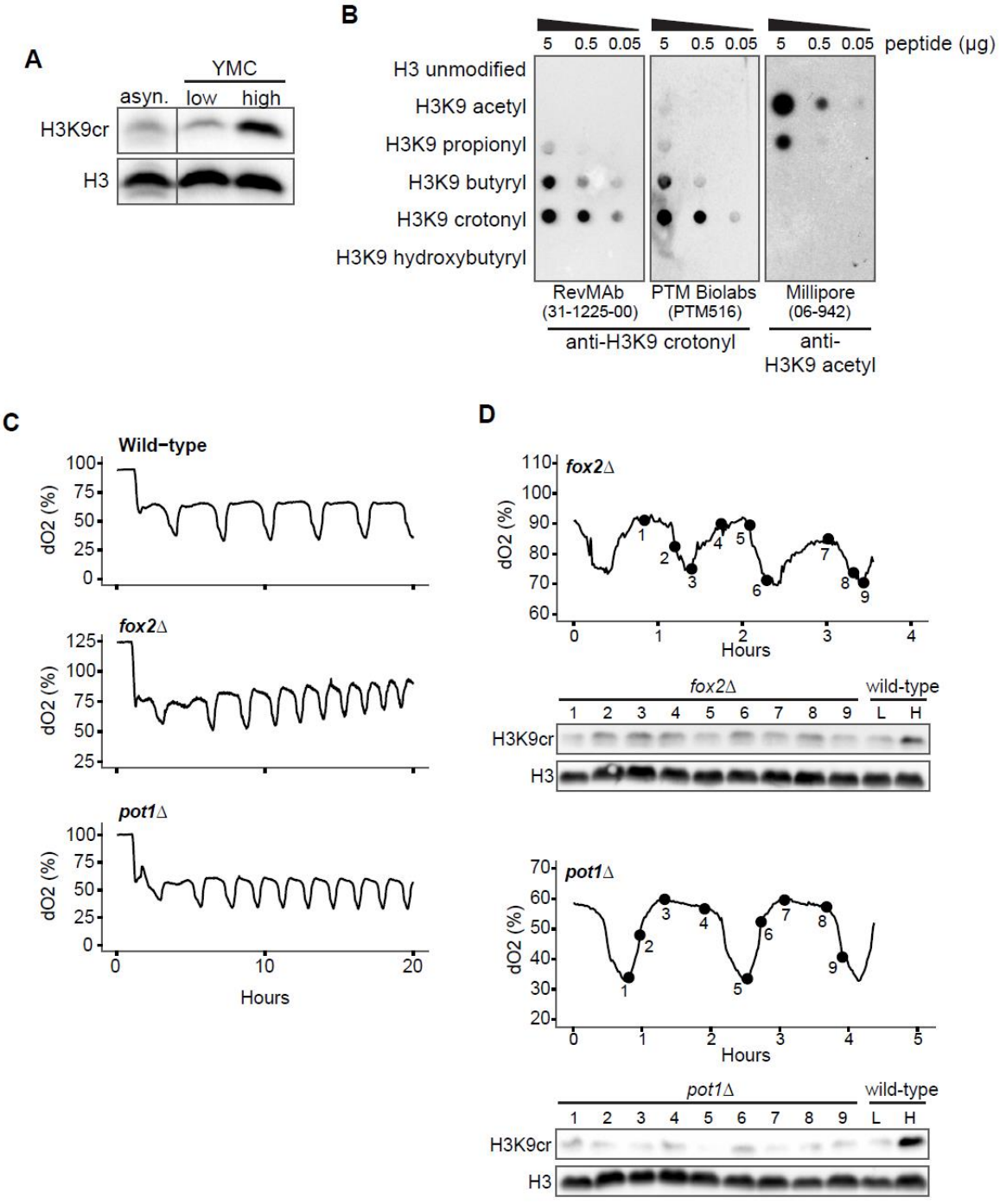

Figure 2.3: Histone Crotonylation and Acetylation Vary Across the YMC

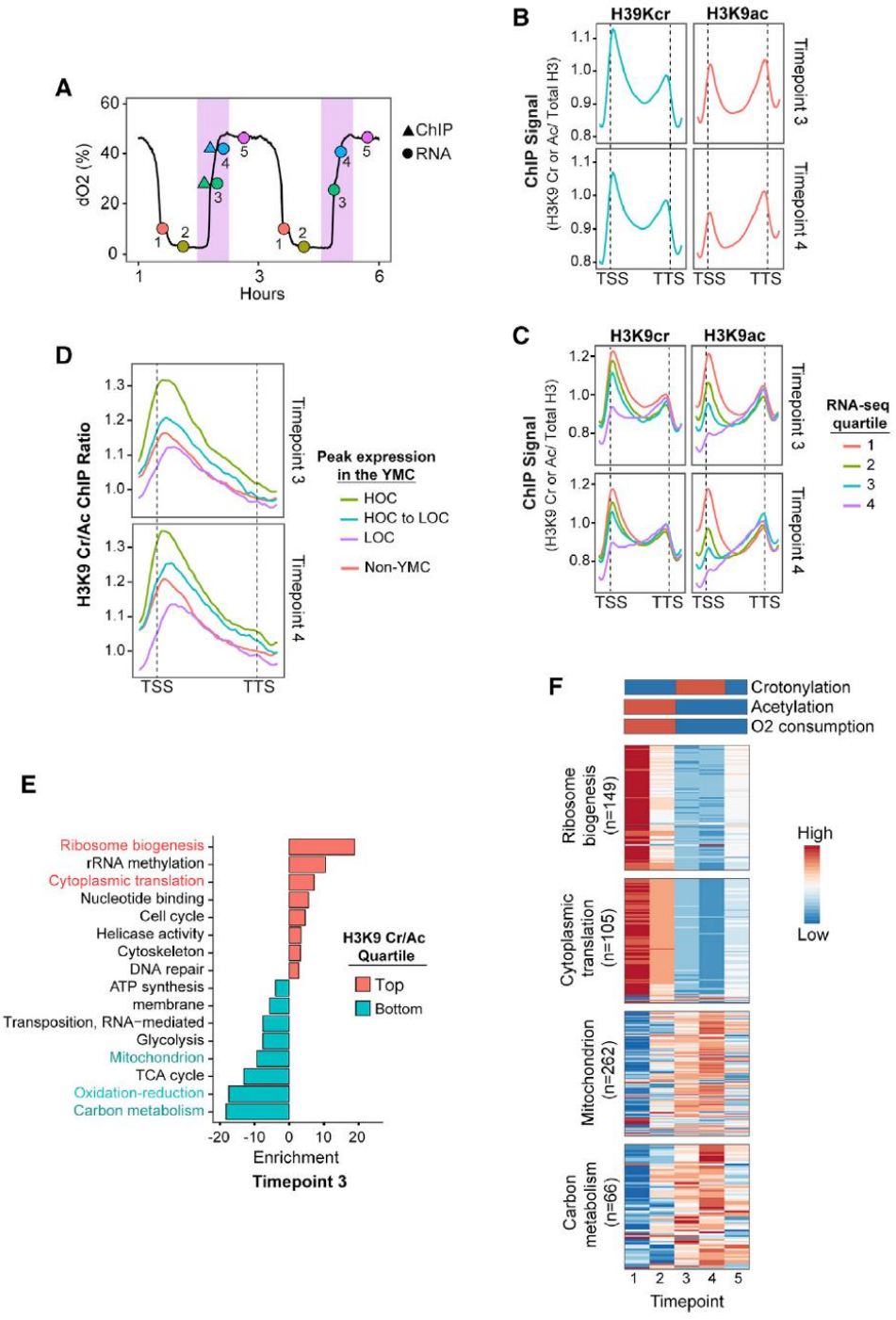

Figure 2.4: Loss of Acylated Histone Binding by Taf14 Disrupts the YMC

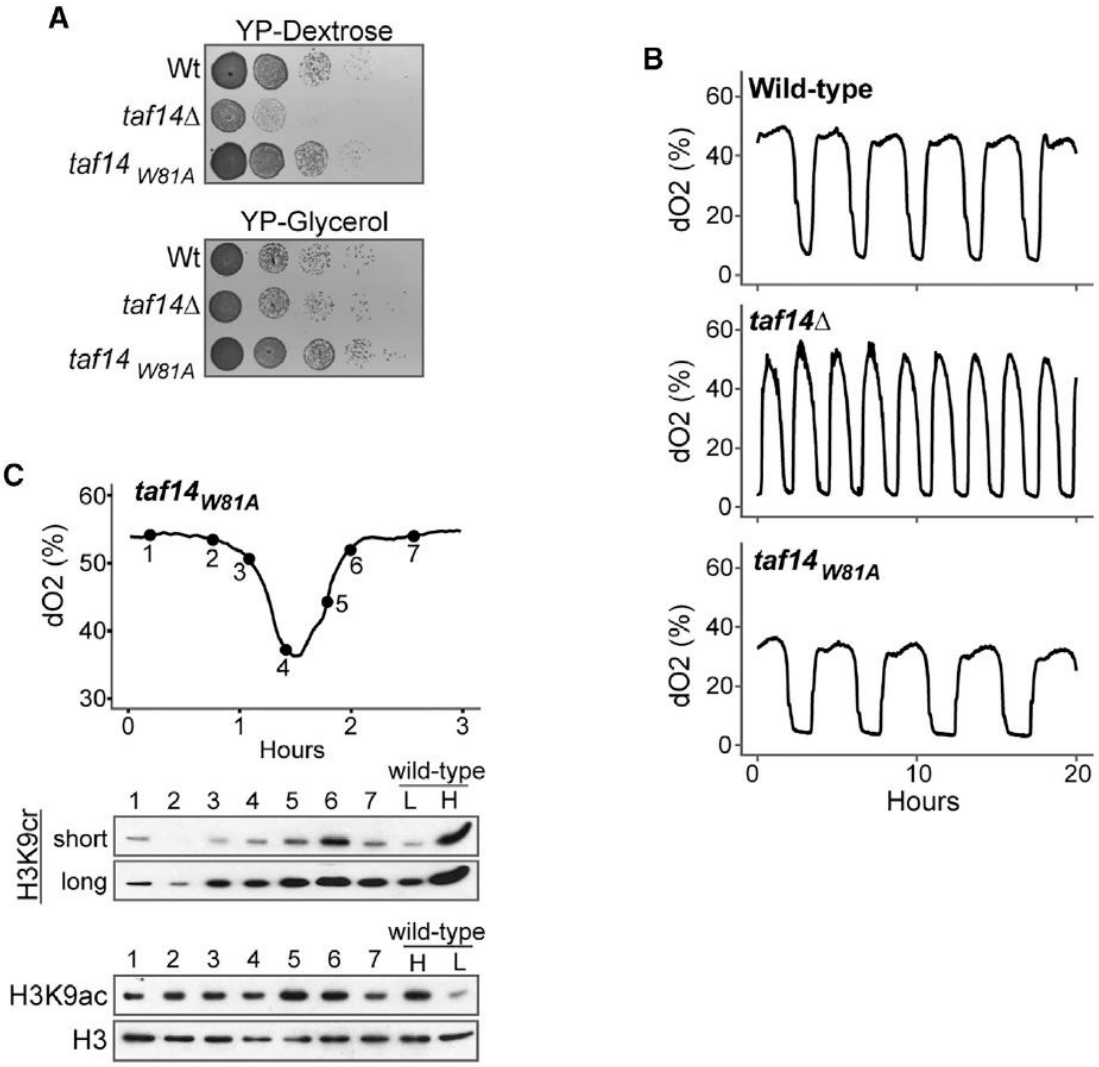

Figure 2.5: Taf14 Prefers H3K9 Crotonylation and is Recruited to Genes in a YEATS Domain-Dependent Manner

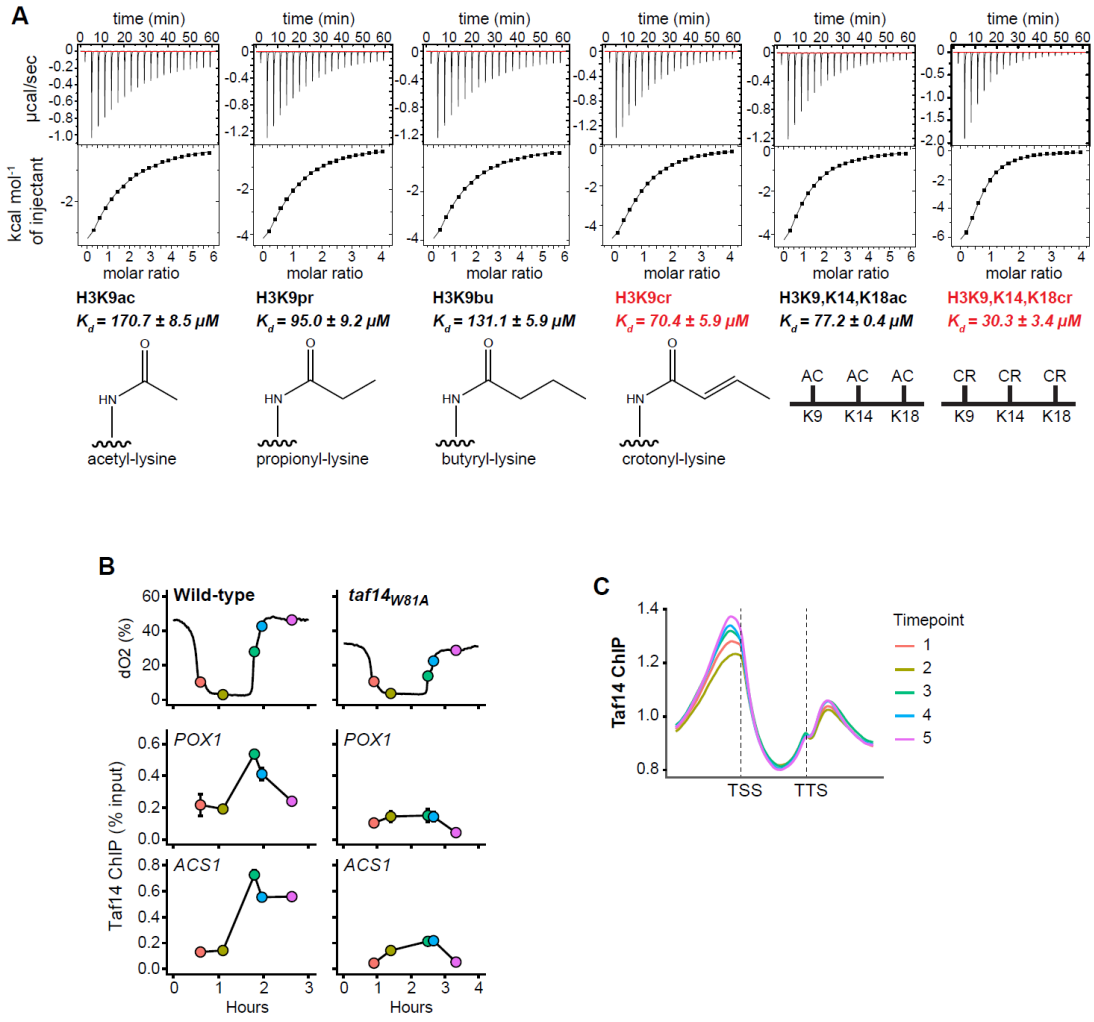

Figure 2.6: RNA-seq Analysis of the taf14W81A Mutant YMC

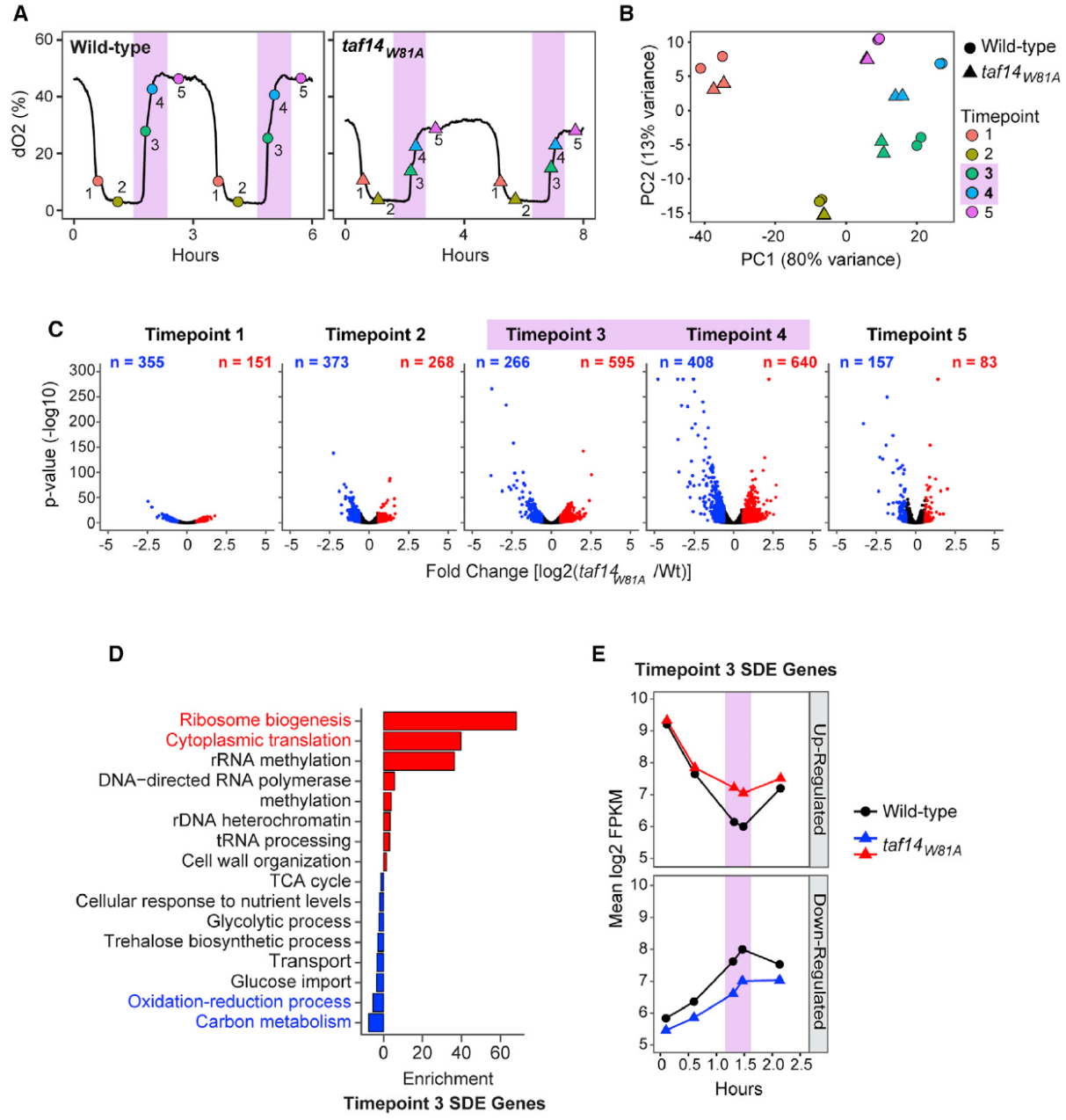

Figure 2.7: Disruption of Taf14 Binding to Histone Crotonylation Alters YMC Gene Expression

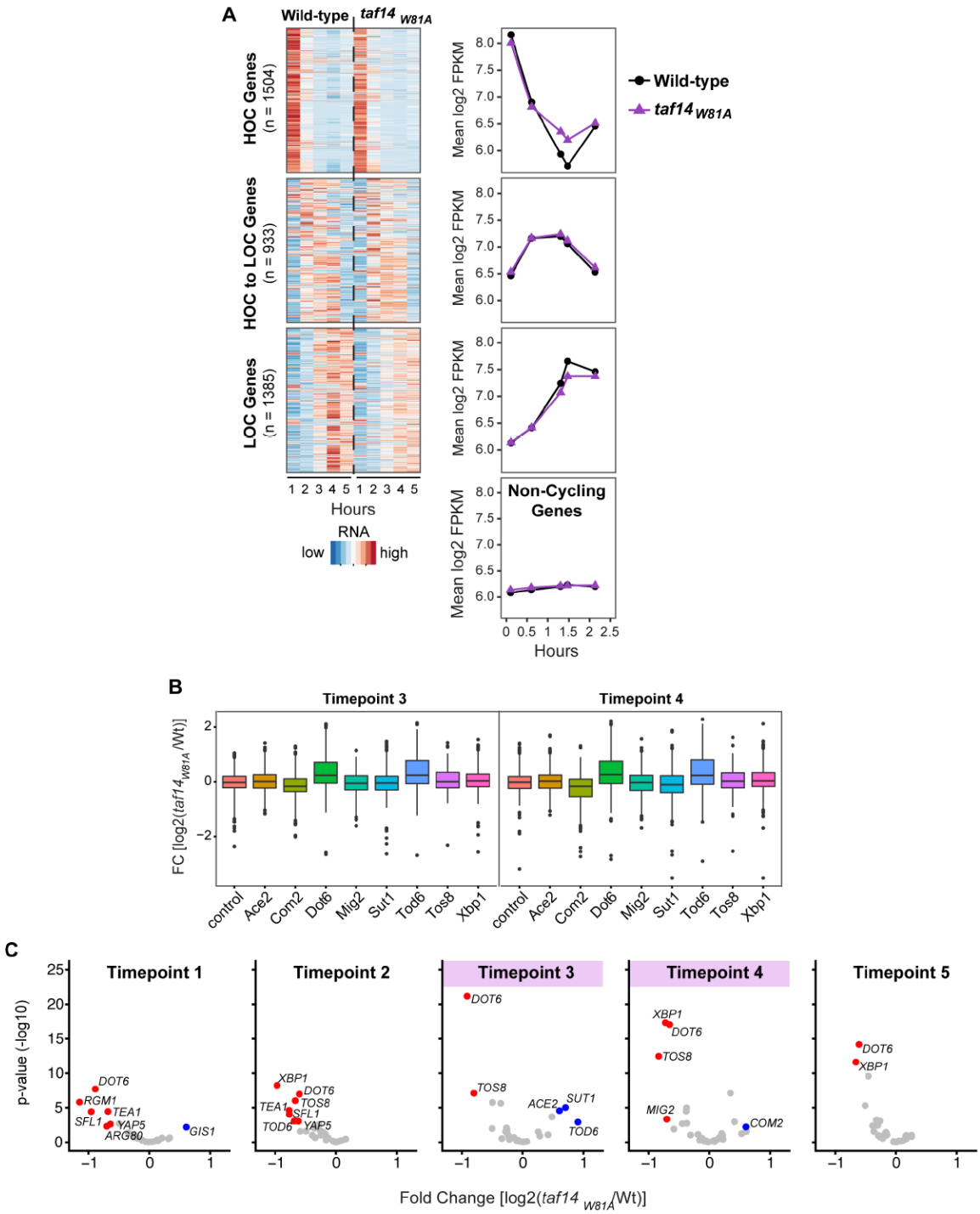

Figure 2.8: Increased Histone Crotonylation Alters YMC and Reduces Ribosomal Gene Expression

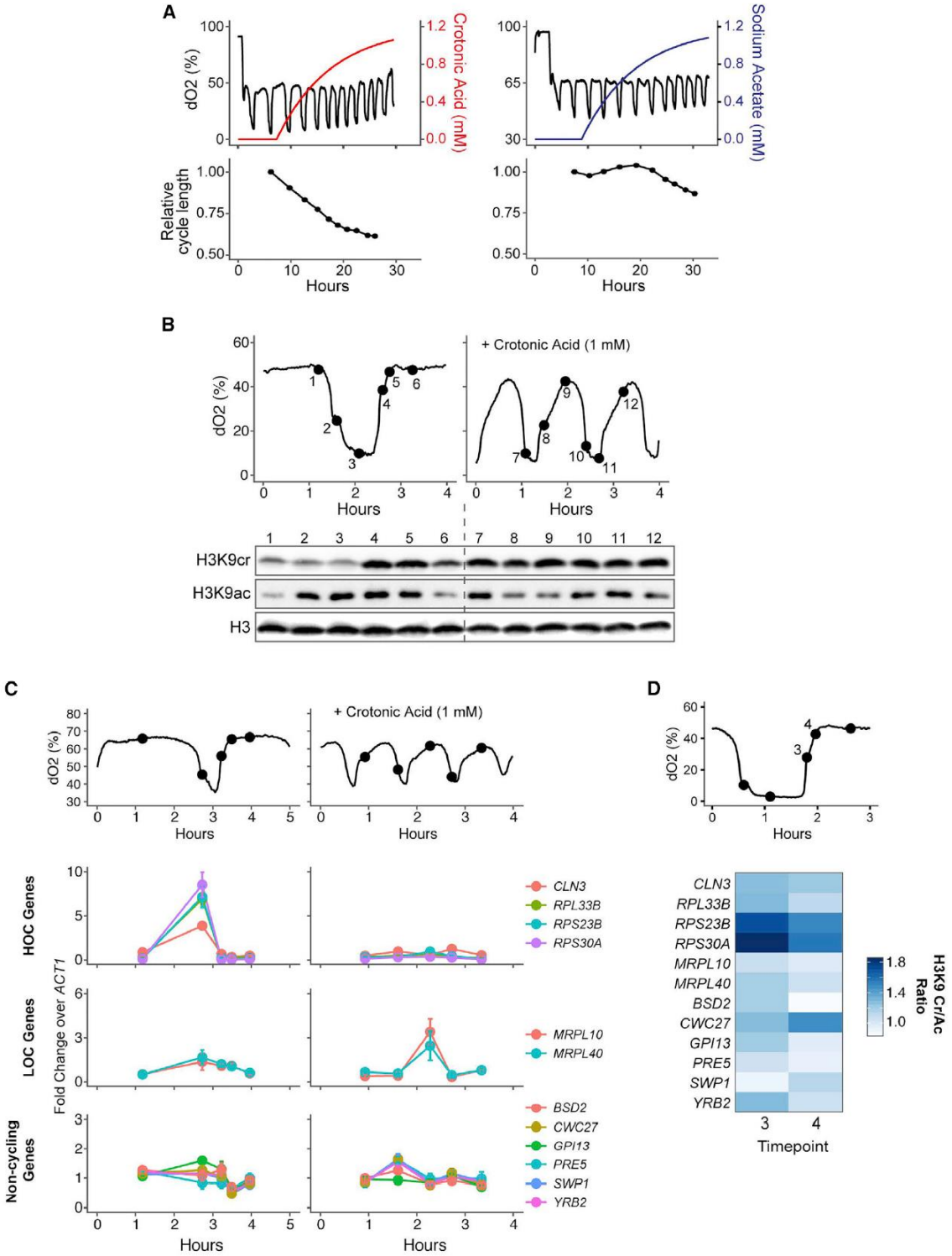

Figure 2.9: Exogenous Addition of Crotonic Acid Increases Histone Crotonylation

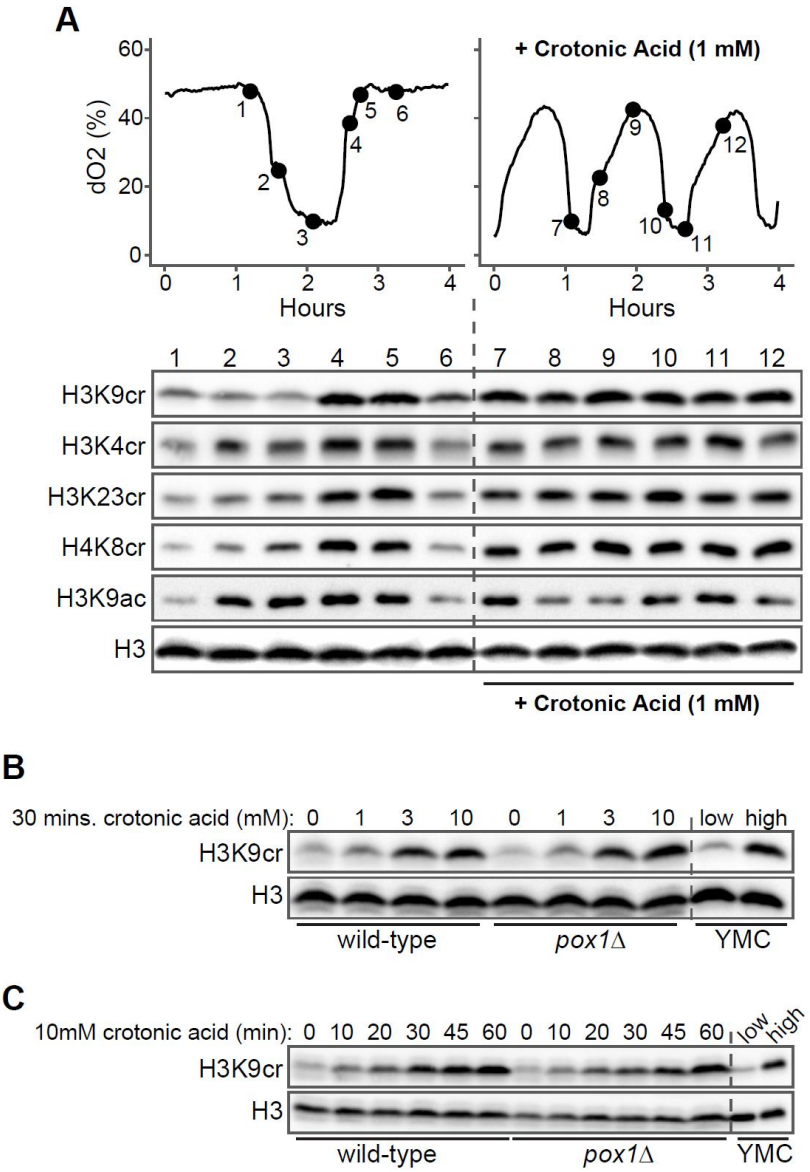

Figure 2.10: Exogenous Addition of Crotonic Acid Alters Binding of Bromodomain Factors

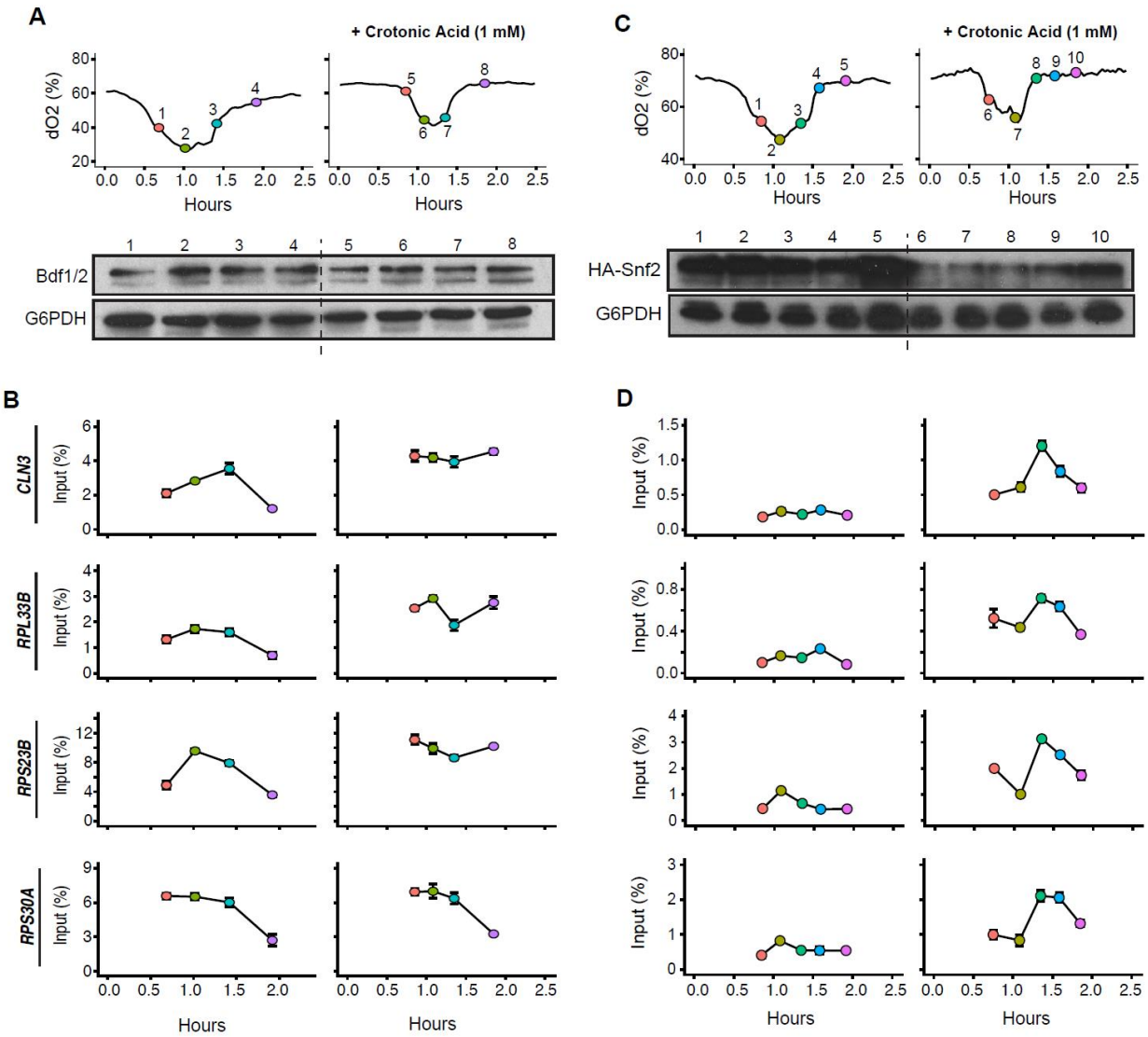

Figure 2.11: Model for Taf14 and Histone Crotonylation Regulation of Metabolic Gene Expression

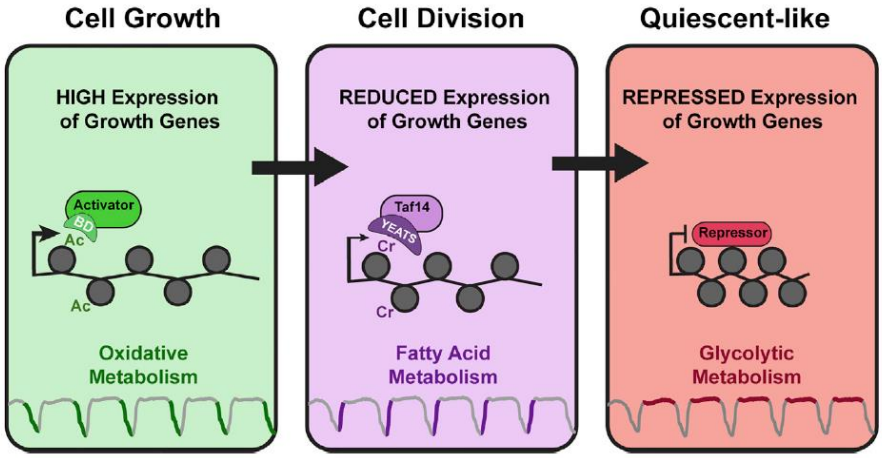

CHAPTER 3 – RECOGNITION OF ACETYLATED HISTONE BY YAF9 REGULATES METABOLIC CYCLING OF TRANSCRIPTION INITIATION AND CHROMATIN REGULATORY FACTORS

Summary

How transcription programs rapidly adjust to changing metabolic and cellular cues remains poorly defined. Here, we reveal a function for the Yaf9 component of the SWR1-C and NuA4 chromatin regulatory complexes in maintaining timely transcription of metabolic genes across the yeast metabolic cycle (YMC). By reading histone acetylation during the oxidative and respiratory phase of the YMC, Yaf9 recruits SWR1-C and NuA4 complexes to deposit H2A.Z and acetylate H4, respectively. Increased H2A.Z and H4 acetylation during the oxidative phase promotes transcriptional initiation and chromatin machinery occupancy while reduces RNA polymerase II levels – a pattern reversed during transition from oxidative to reductive metabolism. Prevention of Yaf9-H3 acetyl reading disrupted this pattern of transcriptional and chromatin regulator recruitment and impaired timely transcription of metabolic genes. These findings reveal that, during the YMC, Yaf9 establishes chromatin and transcription initiation factor signatures that specify unique transcriptional mechanisms in distinct metabolic states.

Introduction

Histone post-translational modifications (PTMs) and histone variants have crucial functions in DNA-templated processes, such as gene transcription, DNA repair and DNA replication (Talbert and Henikoff, 2021; Strahl and Allis, 2000). In large part, distinct epigenetic landscapes are established and maintained by enzymes and/or protein complexes that install, remove, and/or read histone PTMs and histone variants (Henikoff and Smith, 2015, Gardner et

al., 2011). It is not well understood how these chromatin landscapes contribute to the chromatin-based events they regulate.

Although chromatin landscape regulatory mechanisms are yet to be fully explained, recent advances have greatly expanded our understanding of the range of histone modifications and the types of protein domains that read them (Li et al., 2017; Rothbart and Strahl, 2014). For example, the YEATS domain is a newly recognized reader module that associates with histone lysine acetylation and other forms of acylation (e.g., lysine crotonylation) (Li et al., 2017; Zhao et al., 2017; Andrews et al., 2016). Some YEATS domain-containing proteins prefer to bind to histone crotonylation (e.g., Taf14 in yeast and AF9, ENL and YEATS2 in humans), whereas other YEATS proteins such as that found in GAS41 do not greatly distinguish lysine acetylation from crotonylation (Li et al., 2016; Zhao et al., 2016; Zhang et al., 2016; Andrews et al., 2016).

Long-standing evidence points to a positive function for histone acetylation in promoting gene activity (Allfrey et al., 1964; Verdin and Ott, 2015; Barnes et al., 2019); however, the function of histone crotonylation is less well established. Studies with mammalian cells show how p300-mediated crotonylation at H3K18 functions to recruit the AF9 YEATS domain in the super elongation complex to potentiate gene transcription (Sabari et al., 2015). Conversely, studies with budding yeast show that Taf14 binding of histone crotonylation at H3K9 is associated with the timely repression of pro-growth genes during a low energy and reductive metabolic period in which ß-oxidation and longer acyl-CoAs such as crotonyl-CoA are produced (Gowans et al., 2019). These examples highlight the diverse ways histone crotonylation can function, which is likely context- and YEATS domain-dependent.

Yaf9, the founding member of the YEATS domain family (i.e., Yaf9, ENL, AF9, Taf14, and Sas5), is associated within two major catalytically conserved complexes that act on chromatin, namely, the NuA4 acetyltransferase, that targets histones H4, H2A and H2A.Z, and the SWR1-C ATP-dependent chromatin remodeling complex that deposits H2A.Z at gene promoters (Kobor et al., 2004; Mizuguchi et al., 2004; Klein et al., 2018; Zhang et al., 2004) (Figure 3.1A). Yaf9 is

important to the function of both complexes and contributes to the transcriptional regulation and DNA repair activities of NuA4 and SWR1-C (Gerhold et al., 2015; Schulze et al., 2010). The function of the YEATS domain in Yaf9 is less understood, but studies show that it can interact with H3K9ac and H3K27ac and contribute to the H2A.Z deposition function of SWR1-C (Wang et al., 2009; Klein et al., 2018). It is not known whether the YEATS domain of Yaf9 also interacts with histone crotonylation and how exactly this domain regulates the activities of NuA4 and SWR1-C.

The yeast metabolic cycle (YMC) is a powerful system to examine how metabolic changes signal to chromatin and lead to transcriptional changes (Klevecz et al., 2004; Tu et al., 2005; Tu and McKnight, 2007; Mellor, 2016). Under continuous and glucose-limiting growth conditions, yeast becomes metabolically synchronized and oscillates through cycles of oxidative metabolism (i.e., respiration) known as the high-oxygen consumption (HOC) phase followed by periods of reductive metabolism known as the low-oxygen consumption (LOC) phase (Tu and McKnight, 2007; Mellor, 2016). This system closely resembles the nutrient-limiting conditions found in the wild and has direct ties with the circadian rhythm, which itself is underpinned by metabolic processes (Tu and McKnight, 2006). A key feature of cells that oscillate through the HOC phase is high-energy and acetyl-CoA production that fuel the high energy needs of, e.g., ribosome and nucleic acid biosynthesis, pro-growth activities that are initiated with available glucose (Tu et al., 2007). Conversely, the LOC phase is associated with cessation of oxygen consumption and is a period marked by cell division, stress response, ß-oxidation, and autophagy (Tu et al., 2007). The HOC and LOC phases can be further subdivided into additional subphases based on gene expression and GO ontology profiles (oxidative phase (OX), reductive building (RB) phase, and reductive charging (RC) phase (Tu et al. 2005; Mellor, 2016). Significantly, the LOC phase of the YMC is the period in which long-chain fatty acids are metabolized into additional acyl-CoA that include crotonyl-CoA that provide the co-factor for histone crotonylation (Hiltunen et al., 2003; Mellor, 2016; Gowans et al., 2019). We showed that, although histone acetylation is associated

with the HOC phase of the YMC, histone crotonylation occurs in the LOC phase, and, by the action of Taf14, is responsible for the repression of pro-growth genes as cells transition from the HOC into the LOC stages (Gowans et al., 2019). Although we also found that the YEATS domain of Taf14 mediates the timely repression of pro-growth genes, we did not know whether other YEATS domain-containing proteins in yeast also contribute to metabolic gene regulation.

In this report, we describe an important function of Yaf9 in metabolic gene regulation and control of the YMC. We show that Yaf9 is essential for the formation of YMC, and loss of its H3 acetyl-interaction results in defects in the timing of the YMC and proper expression of metabolic genes. Mechanistically, we found that the YEATS domain of Yaf9 contributes to the recruitment of its associated complexes, SWR1-C and NuA4, to enable the deposition of H2A.Z and H4 acetylation during the oxidative phase of the YMC. Recruitment of SWR1-C and NuA4 to genes occurred globally with additional transcriptional initiation and chromatin factors, and this signature was associated with relatively low Pol II levels. Surprisingly, the loss of histone acetylation normally observed during transition into the LOC phase was further associated with globally low levels of SWR1-C and NuA4 and other initiation machinery but high levels of Pol II, a pattern that was largely the reverse of the HOC pattern. We posit that, during metabolic cycling, different energy requirements and nutrient availabilities fuel distinct patterns of chromatin and transcriptional initiation machinery that regulate distinct gene types needed for discrete metabolic states (e.g., HOC vs. LOC).

Results

Yaf9 and its YEATS Domain are Crucial for Proper Progression of the Yeast Metabolic Cycle

Yaf9 is a component of the NuA4 and SWR1-C chromatin regulatory complexes that install H2A and H4 N-terminal tail acetylation and incorporate H2A.Z, respectively (Figures 3.1A). Yaf9 contains an evolutionarily conserved YEATS domain, and, although studies illustrate the ability of

the Yaf9 YEATS domain to bind to histone acetylation, less is known about binding of the YEATS domain to other forms of histone acylation (Figure 3.1B). To further interrogate the histone binding preferences of Yaf9, we purified a GST fusion of full-length Yaf9 (GST-Yaf9) and performed a series of solution-based peptide pull-down assays with histone H3 peptides that contained distinct forms of H3K9 or H3K27 acylation. In agreement with previous findings, the YEATS domain of Yaf9 showed robust interaction with H3 peptides that were acetylated at either H3K9 (H3K9ac) or H3K27 (H3K27ac) (Figure 3.1C) (Klein et al., 2018). Intriguingly, the Yaf9 YEATS domain also interacted with crotonylated H3K9 (H3K9cr), albeit with efficiencies less than binding to H3K9ac. Other forms of histone acylation at H3K9 and H3K27 (i.e., propionylation (pr), butyrylation (bu) and β-hydroxyisobutyrylation (β-hydro)) were tolerated less compared with acetylation or crotonylation. These data reveal that Yaf9 can recognize several major forms of histone acylation that normally partition to distinct phases of the yeast metabolic cycle (YMC) (Gowans et al., 2019).

Studies of the function of a related YEATS-containing protein, Taf14, revealed a critical function for the YEATS domain in metabolic gene regulation and timely progression of the YMC. To assess a possible contribution of Yaf9 and its YEATS domain to metabolic gene regulation and the YMC, we generated yeast strains in the prototrophic CEN.PK background that were either deleted of *YAF9* (***yaf9Δ***) or had a mutation in its YEATS domain that abolished all histone acyl-lysine binding ($yaf9_{W89A}$) (Klein et al., 2018). First, we confirmed that the strains grew on a glycerol-containing medium (YPG plates), which verified that the strains had intact mitochondria for proper metabolic cycling (Figure 3.1D). We also examined the ***yaf9Δ*** and $yaf9_{W89A}$ mutant strains for additional growth phenotypes. As shown in Figure 3.1D, the ***yaf9Δ*** and $yaf9_{W89A}$ strains showed similar growth rates on yeast extract-peptone-dextrose (YPD) medium at 30˚C; only ***yaf9Δ*** cells showed slight temperature sensitivity at 37˚C on YPD plates. We next examined the ***yaf9Δ*** and $yaf9_{W89A}$ mutant strains for growth on media containing a variety of genotoxic agents that report on defects in DNA replication (hydroxyurea (HU)), DNA damage repair (phleomycin and methanesulfonate (MMS)), nutrient signaling (caffeine), and transcription (6-azauracil). These

experiments revealed that the complete absence of Yaf9 caused mild to severe growth defects on all the genotoxic agents tested. However, unlike complete absence of Yaf9, mutations in its YEATS domain that blocked histone interaction caused growth phenotypes only on media containing DNA damaging agents (Figure 3.1D). These studies reinforced the important function of Yaf9 in many DNA-templated processes. The results also revealed a significant function for the Yaf9 YEATS domain in DNA repair.

The phenotypic assays described above, and previous studies of Yaf9, were performed in nutrient-rich conditions that can hide important functions for proteins and domains, such as the YEATS domain, that contribute to metabolic gene regulation. To assess a function of Yaf9 and its YEATS domain in metabolic-associated events, we used a continuous culture system wherein yeast cells were synchronized at the metabolic level and cycled through periods of high-oxygen consumption (HOC) and low-oxygen consumption (LOC) when grown under limiting glucose concentration (Klevecz et al., 2004; Tu et al., 2005). As shown in Figure 3.1E, the wild-type CEN.PK cells exhibited a typical metabolic cycle with an average cycle time of ~4 hours. In stark contrast, the *yaf9Δ* strain failed to cycle under the same conditions, which indicated an essential requirement for Yaf9 in proper progression of the YMC (Figure 3.1F). Intriguingly, the histone-binding mutation of Yaf9 ($yaf9_{W89A}$) resulted in an altered metabolic cycle that was approximately 30 min longer than the matched wild-type strain (Figures 3.1G and 3.1H). These findings indicated an important function for Yaf9 and histone acylation binding in metabolic cycling in a nutrient-limited environment.

H2A.Z and H4 Acetylation Oscillate Across the YMC, and Their Levels are Regulated by Yaf9-H3 Acyl Reading

Because of the altered YMC timing observed for the $yaf9_{W89A}$ mutant strain, we next asked whether the prevention of Yaf9 association with histone acylation might affect the downstream activities of NuA4 and Swr1 that incorporate H4 N-terminal tail acetylation (H4ac) and/or H2A.Z,

respectively. We collected wild-type or *yaf9*$_{W89A}$ mutant cells at multiple time points across the YMC (Figure 3.2A) and interrogated them for global levels of H4ac, H2A.Z, and other histone PTMs known to be regulated across the YMC (e.g., H3K9cr and H4K16ac). Samples were matched carefully so that all comparisons between the wild-type and *yaf9*$_{W89A}$ strains were performed at identical locations during their HOC and LOC phases (depicted as time points 1-9). As shown in Figure 3.2B, the general levels of core histones (H2A, H3, H4) and a control cytosolic protein, glucose-6-phosphate dehydrogenase (G6PDH), did not change across the YMC in either the wild-type or *yaf9*$_{W89A}$ mutant cells. As expected, the occurrence of H3K9ac, H4K16ac and H4ac was highest in the HOC phase (timepoints 2-5) and decreased during the LOC phase of the YMC when H3K9cr levels peak (timepoint 6-9) in wild-type cells. Surprisingly, we also observed that the global incorporation of H2A.Z also cycled across the YMC, with highest levels occurring during the HOC phase. We note that H2A.Z metabolic cycling and genome-wide global shifts in a histone variant such as H2A.Z have not been reported; however, such increases of H2A.Z at the HOC phase would be consistent with the observation of high levels of histone acetylation during the HOC phase that could recruit and/or stimulate Swr1 to increase H2A.Z deposition (Kobor et al., 2004; Zhang et al., 2004). Finally, analysis of the histone and histone PTM patterns from *yaf9*$_{W89A}$ cells revealed that they were largely the same as observed in wild-type cells, albeit the levels of H4ac and H2A.Z appeared to be reduced.

Because of the apparent overall reduction of H4ac and H2A.Z levels in *yaf9*$_{W89A}$ cells, we next performed a side-by-side immunoblot comparison of the wild-type and *yaf9*$_{W89A}$ strains at three time points that represented the peaks of the HOC or LOC phases (Figure 3.2C). As shown in Figure 3.2D, and further quantified in Figures 3.2E and 3.2F, the global levels of H2A.Z and H4ac were significantly reduced in the *yaf9*$_{W89A}$ strain, whereas other histones and RNA polymerase II (Pol II) levels were unaffected. These findings demonstrated that Yaf9-H3 acyl reading was important for proper deposition of H2A.Z and H4ac across the YMC, which implied an important function for the Yaf9 YEATS domain in NuA4 and Swr1 activity.

The YEATS Domain of Yaf9 is Required for Precise Metabolic Gene Transcription

Because the Yaf9 YEATS domain was required for proper YMC timing and for the maintenance of H2A.Z and H4 acetylation levels in chromatin, we next asked how the absence of Yaf9-H3 acyl reading affected metabolic and global gene transcription. We performed RNA-seq for our wild-type and *yaf9*$_{W89A}$ cells across three consecutive YMC cycles (Figures 3.4A and 3.4B). Five time points within each cycle were collected and selected to represent the transition into the HOC phase (time points 1 and 2), the transition into the LOC phase (time points 3 and 4), and transition into the quiescent-like LOC phase (time point 5). Principal component analysis (PCA) of the results showed close correlation between the triplicates across all time points except for a possible outlier in time point 4 (Figure 3.4C). The PCA plot also revealed strong similarity between the wild-type and *yaf9*$_{W89A}$ samples at time points 1, 2, and 5. However, time points 3 (transition into the LOC) showed a more distanced relationship between the wild-type and *yaf9*$_{W89A}$ mutant, which suggested that greater differences in transcriptional regulation occur at time points 3 and 4.

Further examination of the RNA-seq data from the list of significantly differentially expressed (SDE) genes revealed that time point 3 (LOC phase) had the greatest changes in gene expression between the wild-type and *yaf9*$_{W89A}$ mutant cells, with twice as many downregulated genes (n = 1505) and upregulated genes (n = 1467) in the *yaf9*$_{W89A}$ mutant as compared with other time points (Figure 3.4D and 3.4F). Among the top SDE genes in time point 3, we observed upregulation of genes that are involved in oxidative and pro-growth pathways, including ribosome and macromolecule biosynthesis, and downregulation of genes that are involved in reductive pathways, such as oxidation-reduction process and oxidoreductase activity (Figure 3.4E). These findings suggested that, in the *yaf9*$_{W89A}$ mutant, pro-growth/HOC-regulated genes were not properly downregulated during the transition into LOC phase and that the normal expression of LOC genes was attenuated during this phase.

To further understand how the *yaf9*$_{W89A}$ mutation affected HOC and LOC gene expression, we selected from the RNA-seq data a subset of genes found to be dysregulated in time point 3 and measured their expression across the YMC by quantitative reverse transcriptase (RT)-qPCR. As shown in Figure 3.5A, two representative HOC phase genes, *CLN3* and *RPL18B*, showed partially reduced transcription in the *yaf9*$_{W89A}$ mutant compared with wild-type at time points 1 and 2. Consistent with the RNA-seq data of these genes, the mRNA levels of *CLN3* and *RPL18B* observed at time point 2 largely persisted into the LOC phase (time point 3) instead of being downregulated as occurs in wild-type cells (Figure 3.5A). In contrast to the HOC genes, a LOC gene, *MRPL10*, showed decreased transcription in the *yaf9*$_{W89A}$ mutant compared with wild-type cells at most time points across the YMC, and, notably, *MRPL10* was less expressed in the LOC phase consistent with the RNA-seq data (Figures 3.4 and 3.5B). The findings that HOC genes maintained expression in the LOC phase and that LOC genes were not properly expressed were recapitulated for additional HOC genes (*RPS5, RPL4B, RPL8B*), and LOC genes (*PYC1*, *SSC1*, *TDH2*) that were measured by RNA-seq (Figure 3.6). Finally, several non-cycling genes identified from our RNA-seq data were largely unaffected throughout the YMC in *yaf9*$_{W89A}$ mutant cells (Figure 3.6).

The results of RNA-seq and RT-qPCR analyses prompted us to determine whether the transcription defects of a subset of metabolic genes in the *yaf9*$_{W89A}$ mutant occurred more broadly for other metabolically-regulated and noncycling genes. Out of 4121 genes that showed measurable signals, we performed an unsupervised hierarchical clustering that resulted in four clusters based on their transcription profiles across the five time points (Figures 3.5C and 3.5D). Cluster 1 genes (n=82) were exclusively HOC-regulated (96%), whereas clusters 3 (n=833) and 4 (n=104) were almost exclusively LOC-regulated genes (85% and 90%, respectively). The largest group, cluster 2, contained a mixture of HOC-regulated genes (n=1086, 35% of this cluster), LOC genes (n=910, 29% of this cluster), and the rest (n=1030) non-metabolically regulated genes (Table S1). Consistent with our RT-qPCR analyses, HOC-regulated genes in

clusters 1 and 2 showed persistent transcription at time point 3 in the *yaf9*$_{W89A}$ cells. In contrast, all the LOC-regulated genes in clusters 3 and 4 exhibited decreased transcription during the LOC phase, which was more pronounced at time point 3 and consistent with our box plot analyses (Figures 3.4D and 3.5C). The line plots in Figure 3.4D show the average mRNA signals in wild-type or *yaf9*$_{W89A}$ mutant cells for each cluster across the YMC. These findings revealed two important observations about how absence of Yaf9-H3 acyl reading affects metabolic gene expression. First, the normal restriction of pro-growth gene expression to the HOC phase was partially lost because HOC genes maintained their expression in the LOC phase. Second, the normal induction of genes in the LOC phase was attenuated.

Yaf9-H3 Acyl Reading is Required for Proper Deposition of H2A.Z and H4 Acetylation at Genes

To further understand how Yaf9-H3 acyl reading contributes to gene transcription, we preformed chromatin immunoprecipitation (ChIP) assays coupled with quantitative PCR (ChIP-qPCR) on a subset of genes to determine whether the absence of Yaf9-H3 acyl reading affected the occupancies of H2A.Z and/or H4 acetylation. Time points from the YMC used for the ChIP-qPCR assays were the same as those used in the foregoing RNA-seq experiments (Figures 3.4A and 3.4B). For this analysis, we selected *RPL4B* as a representative HOC gene, *SSC1* as a representative LOC gene, and *FBA1* as a control non-cycling gene whose transcription level was largely unaffected in the *yaf9*$_{W89A}$ mutant (Figure 3.7 and 3.8) H2A.Z and H4ac occupancy levels were examined at the -1 nucleosome, +1 nucleosome, and 3' end of these genes (+1 nucleosome results shown in Figure 3.7B; the full data set is presented in Figure 3.8). In agreement with the global changes observed with H2A.Z and H4ac in bulk chromatin (Figure 3.11A), the levels of H2A.Z and H4ac at all genes examined also cycled across the YMC in wild-type cells with levels being highest during the HOC phase (Figure 3.7B). In contrast to wild-type cells, the occupancies

of H2A.Z and H4ac decreased significantly in the *yaf9*$_{W89A}$ mutant at all time points examined (Figures 3.7B and 3.8).

We next measured the occupancy of Pol II at the same genes described above to determine the effect of Yaf9-H3 acyl reading on Pol II occupancy levels. Strikingly, Pol II occupancy oscillated across the YMC at all genes examined in wild-type cells, with Pol II levels being lowest at the HOC phase and highest at the LOC phase (Figures 3.7C, 3.9 and 3.10). To our knowledge, it has not been reported that Pol II levels are influenced by metabolic state and are anticorrelated with H2A.Z and histone acetylation levels over the YMC, although our findings are consistent with reports of antagonism between H2A.Z and Pol II during transcription (Ranjan et al, 2020; Weber et al., 2014; Tramantano et al., 2016)). These findings also agree with other work showing that the nucleosome free regions of genes are in competition between Swr1 and initiation factors for transcription (Ranjan et al., 2013; Yen et al., 2013). Pol II occupancy in the *yaf9*$_{W89A}$ mutant had a cycling pattern similar to Pol II in wild-type cells, albeit with reduced levels at the non-cycling *FBA1* gene during the peak of Pol II levels in the LOC phase.

Histone-binding by Yaf9 is Required for SWR1-C and NuA4 Chromatin Recruitment

The totality of transcription and global H2A.Z/H4ac defects observed in the *yaf9*$_{W89A}$ strain prompted us to ask how Yaf9 H3-acyl binding contributes to the chromatin-based functions defective in *yaf9*$_{W89A}$. We reasoned that Yaf9 H3-acyl binding was either required for proper recruitment of the SWR1C and NuA4 complexes to chromatin or that these complexes were already on chromatin and that Yaf9 H3-acyl binding stimulates their enzymatic activities. To test these possibilities, we performed chromatin association assays across three YMC time points that covered the HOC and LOC phases (time point tp1 = LOC, tp2 = HOC, and tp3 = LOC; the same time points shown in Figure 3.2). Consistent with the immunoblotting analyses of whole cell lysates (Figure 3.2D), the chromatin levels of H2A.Z and H4ac were significantly reduced at all times points in the *yaf9*$_{W89A}$ strain compared with wild-type (Figure 3.11A). However, the soluble

fraction (nucleoplasm and cytoplasm) did not contain any detectable H2A.Z or H4ac (Figure 3.11A). As controls, we probed for H2A and H3 to monitor the chromatin fraction and G6PDH to monitor the soluble fraction. In all time points, and between strains, the levels of histones and G6PDH were unchanged (Figure 3.11B). Intriguingly, the chromatin-bound form of Yaf9 was largely absent in the Yaf9 H3 acyl-blocking mutant and relocated to the soluble fraction (Figure 3.11A). Thus, H3-acyl binding function of Yaf9 is critical for its recruitment to chromatin.

Because Yaf9's association with chromatin was dependent on its H3-acyl reading activity, we next asked whether absence of Yaf9 H3 acyl-reading also influences the chromatin-association of the SWR1 and/or NuA4 complexes that contain Yaf9. Using antibodies that specifically target members of the SWR1 and NuA4 complexes (Swr1 and Eaf1, respectively) (Wu, et al., 2009; Auger, et al., 2008), we examined the levels of these complexes in our chromatin association assays as described in Figure 3.11A. Strikingly, although the total amounts of Swr1 and Eaf1 did not differ significantly across the three YMC time points, their chromatin levels did differ. Specifically, Eaf1 and Swr1 chromatin levels were highest in the HOC phase, tp2, and lowest in the LOC phases, tp1 and tp3 (Figure 3.11C). These association patterns also followed the cyclic patterns observed with histone acetylation across the YMC (Figures 3.2C). In contrast to the wild-type situation, the chromatin levels of Swr1 and Eaf1 in the in $yaf9_{W89A}$ samples were greatly reduced at all time points; instead, they had quantitatively relocated to the soluble fractions (Figure 3.11C). Additionally, the total amount of Eaf1 in $yaf9_{W89A}$ samples was lower compared with wild-type, which explained the lower levels of Eaf1 in the chromatin and soluble fractions of $yaf9_{W89A}$. Figure 3.11E shows the quantified chromatin levels of Yaf9, Eaf1 and Swr1 from these experiments.

Our study of the function of Yaf9's YEATS domain also revealed a surprising observation. Although the Yaf9 YEATS domain was critical to the recruitment of SWR1C and NuA4 under nutrient-limiting conditions, the $yaf9_{W89A}$ mutant, in addition to the complete absence of Yaf9, had no impact on H2A.Z or H4ac levels in the prototrophic strain grown in nutrient-rich (YPD)

conditions (Figures 3.2A and 3.2B). Thus, under optimal growth conditions, Yaf9 was dispensable for the functions of SWR1-C and NuA4; its function was revealed only under more naturally occurring and nutrient-limiting growth conditions, as occurs in the wild.

The requirement of Yaf9's H3 acyl-reading activity for the global recruitment of NuA4 and SWR1-C to chromatin prompted us assess whether other aspects of the transcriptional apparatus were affected during YMC growth of the Yaf9 YEATS domain mutant. To test this possibility, we measured the levels of representative transcription initiation factors including proteins in the TFIID and SAGA complex (Taf3, Taf4, Taf12) and BET family members (Bdf1/Bdf2) that occur in TFIID and in SWR1-C (Figures 3.11C and 3.11D). Intriguingly, all the aforementioned initiation factors were localized to chromatin across all of the time points in the YMC, with their associations being highest in the HOC phase (i.e., time point 2). We also attempted to examine Pol II levels in these assays; however, the chromatin association assay resulted in an unexpected loss of Pol II protein compared to trichloroacetic acid extraction assay during sample processing that precluded its global examination (Figure 3.12). In contrast to the wild-type situation, the absence of Yaf9's H3 acyl-interaction resulted in a global decrease in all of the initiation factors tested. The decrease was most notable for Brd1/Brd2 (see Figure 3.11E for quantification of chromatin levels for several of these initiation factors).

Taken together, these findings emphasize the critical function of Yaf9 and its histone reading activity in the timely recruitment and stability of transcription initiation factors and chromatin modifiers on genes during the YMC. During oxidative metabolism in which glucose levels are high, Yaf9 and its H3 reading contribute to the timely recruitment of the SWR1-C and NuA4 complexes that then establish a chromatin H2A.Z and histone acetylation signature – a signature that then reinforces further recruitment of bromodomain-containing initiation machinery.

Discussion

The YEATS domain has become recognized as a critical regulator of metabolic- and chromatin-based gene transcription events (Schulze et al., 2009; Li et al., 2017; Gowans et al., 2019). Intriguingly, although some YEATS domains prefer histone crotonylation (e.g., Taf14), others, such as the YEATS domain of Yaf9, bind histone acetylation and crotonylation equally (Figure 3.1C). This expanded acyl selectivity may explain why, unlike Taf14, Yaf9 appears to function largely during the respiration (HOC) phase when acetyl-CoA and histone acetylation levels are highest. We also found that, during respiration, Yaf9-H3 acetyl reading mediates recruitment of its associated complexes (SWR1-C and NuA4) to install H2A.Z and H4 acetylation. The high levels of histone acetylation in the HOC phase likely act to further recruit transcriptional initiation and chromatin machinery to genes by the acetylation-driven recruitment of bromodomain-containing factors (e.g., SAGA/TFIID/Bdf1/Bdf2 and likely RSC). Coincident with this acetylation-dependent chromatin signature, Pol II levels were anticorrelated and decreased at genes – a finding that agreed with other reports of an antagonistic relationship between Pol II and H2A.Z, and other chromatin regulators, that compete with Pol II for binding to the nucleosome free regions of genes (Yen et al., 2013; Ranjan et al, 2020; Weber et al., 2014; Tramantano et al., 2016). As yeast cycle out of the HOC phase and into the LOC phase, the pattern of chromatin and initiation factor recruitment is reversed, with Pol II levels becoming higher at genes. Thus, our study unveils an intriguing metabolic cycling of both histone PTMs and factors to genes that is dependent on the functions of Yaf9.

Different Chromatin and Transcription Factor States for Different Metabolic Situations

The distinct chromatin and factor recruitment states that exist at different phases of the YMC is an intriguing finding of this study. Other investigators have reported the cyclic nature of histone acetylation across the YMC on genes and globally on chromatin (Cai et al., 2011; Mellor, 2016); however, our findings extend those observations to the recruitment of transcription and

chromatin machinery that also associate with acetylated histones. Thus, our findings show that distinct chromatin states are established at distinct metabolic states. A puzzling question then is why Pol II occupancy is low during the oxidative phase at a time when histone acetylation and factor recruitment is high, and why is low Pol II occupancy reversed in the reductive phase of the metabolic cycle? Perhaps one explanation for this phenomenon is that the high levels of pre-initiation machinery increased on chromatin during the oxidative phase facilitates rapid re-initiation of Pol II to help achieve the high levels of transcription needed for transcription of ribosomal genes and other pro-growth genes. However, this explanation might be considered at odds with finding of low Pol II levels during this phase (compared with that observed during the reductive phase; see Figures 3.7C and 3.8D). The reduced occupancy of Pol II in the oxidative phase is likely a consequence of having high levels of H2A.Z, which has been shown to antagonizes Pol II (Tramantano et al., 2016; Ranjan et al., 2020). We speculate that lower levels of Pol II occupancy coupled with high levels of H2A.Z provides a controlled step of pausing during each round of transcription to ensure that the polymerase has successfully initiated and entered productive elongation. Additionally, the high H2A.Z levels may ensure proper directionality and/or prevention of inappropriate antisense transcription (Gu et al., 2015; Bagchi et al., 2020). Conversely, and during the LOC phase when histone acetylation on chromatin and initiation factors and H2A.Z levels are reduced, high Pol II levels at this time may enable genes to overcome the lack of abundant pre-initiation machinery that is less abundant due to less histone acetylation. Thus, the cell appears to have evolved ways to overcome major differences that exist with chromatin under vastly different metabolic and cellular conditions to achieve precise and productive transcription (Figure 3.13). Further work is be needed to determine whether this model is correct.

Although our studies suggest that Yaf9 functions primarily during the HOC phase, we note that absence of Yaf9 H3 acetyl-reading still affects recruitment of SWR1-C and NuA4 (and other initiation and chromatin factors) in the LOC phase, albeit normally the levels recruited during this phase are much lower compared to the oxidative phase. We speculate that the ability of Yaf9 to

equally bind H3 acetylation and crotonylation implies that Yaf9's YEATS domain still facilitates some recruitment of SWR1-C and NuA4 during the LOC phase because of the lower levels of histone crotonylation that exist during this period.

Finally, the chromatin and transcription signatures described above that change across the YMC appear to occur globally for all genes transcribed in their respective YMC phases. This condition raises the question as to how cells fine-tune and regulate the transcription of genes in a cyclic manner if the chromatin and transcription signatures described herein also occur on actively transcribed non-cycling genes? We suggest that the chromatin and transcription initiation signatures that are found at distinct YMC phases occur broadly at genes, but do not take into account the actions of additional transcription factors that also contribute to metabolic gene transcription at each phase (both positive and negative regulation). It is likely that the transcription factors deployed at each distinct phase to activate or repress transcription do so in the context of the distinct chromatin contexts that occur in the HOC and LOC phases.

Detailing Yaf9's Function: Context Matters

Unexpectedly, we found that the necessity of Yaf9 was bypassed when yeast was grown in nutrient-rich conditions (i.e., YPD) (Figure 3.3). A complete absence of Yaf9 did not have any effect on histone H4 acetylation level nor H2A.Z incorporation during batch growth in YPD (Figure 3.3A). Also, Yaf9 with the H3 acyl-blocking mutation was still associated with chromatin in YPD conditions. However, in nutrient-limiting conditions, akin to what is observed in the wild, Yaf9 and its histone reading were critical for the activity of NuA4 and SWR1-C complexes required to maintain the normal high levels of chromatin and transcriptional initiation machinery at genes (Figure 3.3B). We surmise that, in a natural setting, Yaf9 provides a key function in facilitating SWR1-C and NuA4 recruitment that could not be achieved without it. In this regard, more nutrient-limiting conditions are like an "all hands-on deck" situation to ensure the timely and appropriate recruitment of needed chromatin and initiation machinery to chromatin. If this correct, it then also

raises an intriguing question: How many other ancillary members of chromatin and transcription complexes have not been fully identified because most studies with yeast were performed in optional growth conditions? Our study makes this point for one member of one complex, but it is important to consider growth conditions and cellular contexts when examining the function of other members of chromatin and transcription machinery.

In conclusion, we have revealed an important function of Yaf9 in maintenance of proper regulation of transcription across the YMC. This function is elicited by the ability of Yaf9 to read histone acetylation and facilitate the recruitment of its associated complexes that establish a chromatin and transcription initiation signature at genes required for timely transcription. Our findings also reveal that distinct mechanisms likely have evolved to regulate transcription during different nutrient and energy states, as shown by the absence of this chromatin and transcription initiation factor signature during times of low histone acetylation and low cellular energy. Because metabolic pathways are often highjacked in cancer, it will be intriguing to determine whether the activities we have observed are conserved and dysregulated in cancer.

Materials and Methods

Yeast Strains and Metabolic Cycling

Saccharomyces cerevisiae strains generated for this study were created in the CEN.PK background. These and other strains used are listed in Table S1. CEN.PK were verified to have mitochondria as indicated by the ability to grow on glycerol-containing media. The yaf9$_{W89A}$ strain was constructed using the delitto perfetto system (Klein et al., 2018). Yeast metabolic cycling conditions were applied as described with minor adjustments (Gowans et al., 2019). Dissolved oxygen percent in media shown in YMC plots is relative to starting culture conditions (~100%). Continuous respiration cycles occur following addition of 0.15% glucose to starved cells. For each experiment, the time (in minutes) is shown relative to the start of the experiment is shown. Spotting assays were performed by plating serial dilutions (1:5) of indicated strains on YP media

containing either 2% glucose (YPD), 3% glycerol (YPG), 80 µg/ml 6-azauracil on synthetic complete minus uracil plates (SC-Ura), 100 mM caffeine, 50 mM methanemethyl sulfonate, or 25 mM phleomycin and grown at 30°C or 37°C.

Immunoblotting

Cultures were collected from the YMC and immediately snap-frozen in liquid nitrogen. Samples for immunoblotting were fixed in 20% trichloroacetic acid after thawing and washing once in water. Protocol of Kushnirov (2000) was used to extract protein from samples. Standard conditions were used for SDS-PAGE and immunoblotting. Antibodies used in this study were the following: anti-H2A.Z (1:10000, Active Motif 39647), anti-H3K9 acetylation (1:2000, Millipore 06-942), anti-H3K9 crotonylation (1:500, PTM Biolabs PTM 527), anti-H4K16 acetylation (1:2000, Millipore 07-329), anti-pan H4 acetylation (1:1000, Active Motif 39925), anti-H2A (1:10000, Active Motif 39235), anti-H3 (1:5000, Epicypher 13-0001), anti-H4 (1:1000, RevMAb 31-1089-00), anti-G6PDH (1:10000, Sigma A9521-1VL), anti-polymerase II (1:1000, Millipore 05-623), anti-Yaf9 (1:5000, Pocono rabbit farm), anti-Eaf1 (1:1000, Côté lab), anti-Swr1 (1:500, Wu lab), anti-Taf4 (1:1000, Weil lab), anti-Taf12 (1:1000, Hahn lab) and anti-Taf14 (1:5000, Reese lab).

RNA-Seq Analysis

RNA was prepared from samples (approximately 10 ODs) using the RNA extraction method. The sequencing libraries were from (Gowans et al., 2019) and the sequencing was performed by Novogene. Triplicates of samples were combined for final analysis. Principal component analysis plots (log-transformed data) and significantly differentially expressed (SDE) genes (adjusted p-value < 0.05 and log2 fold change > 0.6) were generated using the DESeq2 package (Gowans et al., 2019). Gene ontology (GO) term analysis was performed for SDE genes with default parameters to identify enriched genes. The numbers of genes with large and statistically significant fold changes were presented in volcano plots. Line graphs were generated from the four hierarchical cluster lists provided by the analysis from the Novogene company. Heatmaps of the four clusters were generated by Prism.

RNA extraction and qPCR

Yeast samples were collected and snap frozen as described with minor modifications (Gowans et al., 2019). Pellets were washed in water and resuspended in 400 µl TES buffer (10 mM Tris HCl pH 7.5, 10 mM EDTA, 0.5% SDS). An equal volume of acid phenol was added, and samples were vortexed for 30 seconds. Samples were then incubated at 65°C for 45 minutes with occasional vortexing before being chilled on ice for 1 minute. Samples were centrifuged (5 min, 4°C, 12K RPM) and the upper phase was transferred to a fresh tube. Phenol extractions were repeated twice. RNA was precipitated by adding 0.1 volume of sodium acetate (5 M, pH 5.3) and 2.5 volumes of ice-cold ethanol (100%) followed by incubation at -80°C for 1 hour. Samples were centrifuged (5 min, 4°C, 12K RPM), and pellets were washed with 70% ice-cold ethanol. Pellets were resuspended in water, and the concentrations were measured. RNA (10 mg) was treated with RQ1 DNase (Promega Corporation Cat# M6101) at 37°C for 60 minutes. RNA was purified using RNeasy Mini kit (RNeasy Minikit, Qiagen, Cat# 74104). cDNA was prepared using iScript cDNA synthesis kit (Thermofisher Scientific, 18080051). qPCR was performed using the SYBR green kit (PowerUp SYBR™ Green Mastermix, Biorad, Cat# 170 8880), and the primers are listed in Key Resources Table. Actin was used as the standard for signal normalization.

Chromatin Immunoprecipitation (ChIP)

Antibodies used for ChIP were the following: anti-H2A.Z (Active Motif 39647), anti-H3K9 acetylation (Millipore 06-942), anti-polymerase II (Millipore 05-623) and anti-Yaf9 (Pocono rabbit farm). Chemostat samples (40 ml of saturated culture) were collected, fixed in 1% formaldehyde for 15 minutes, and quenched in 125 mM glycine for 10 minutes. Cells were washed twice in TBS (300 mM NaCl, 40 mM Tris pH 7.5) and snap frozen. Pellets were resuspended in 500 ul of FA buffer (50 mM HEPES pH 7.5, 140 mM NaCl, 1% Triton X-100, 1 mM EDTA, 0.1% Sodium deoxycholate, Roche complete protease inhibitor cocktail) and lysed by bead beating for 15 minutes at 4°C. Aliquot volumes were adjusted to 1 ml with FA buffer and sonicated (30 seconds on, 30 seconds off) for 25 minutes. Samples were pelleted (20 min, 4°C, 13K RPM) and the

supernatants (whole cell lysate) pooled. Lysates (adjusted to 2 mg/ml protein for both histones marks, Yaf9, and Pol II, using FA buffer) were precleared using Dynabeads Protein A (10001D, 50 µl beads per 500 µl lysate, 1 hour at 4°C), and 50 µl was saved as input. Antibody was added and samples rotated overnight at 4°C. Dynabeads were washed three times in FA buffer + 0.5% BSA, with the third wash rotated overnight at 4°C to pre-block beads (50 µl per 500 µl sample). Beads were then resuspended in 200 µl FA buffer and added to lysate samples incubated for 2 hours at 4°C. Beads added to lysates were washed as follows: FA buffer, FA buffer containing 500 mM NaCl, LiCl (10 mM Tris-HCl pH 8.0, 250 mM LiCl, 0.5% NP-40, 0.5% sodium deoxycholate, 1 mM EDTA), 1 ml TE pH 8.0. Beads were resuspended in 100 µl of elution buffer (1% SDS, 0.1 M $NaHCO_3$) and DNA was eluted by shaking at 65°C for 15 minutes. Supernatant was collected and the elution step repeated to yield 200 µl of eluate. Crosslinks were reversed by adding 10 µl of NaCl (5 M) to the eluate and incubating at 65°C overnight with shaking. Elution buffer (150 µl) was added to input samples (50 µl) and 10 µl of NaCl alongside the IP samples. Samples were treated with RNase A (10 µg, 60 min at 37°C) and then proteinase K (20 µg, 60 min at 42°C). DNA was purified using the ChIP DNA Clean & Concentrator (Genesee/zymo research, 11-379C/D5205) and eluted in 60 µl of elution buffer.

Chromatin Association Assay

Chemostat samples were collected and pelleted. Pellets were washed in water and chilled SB buffer (1M sorbitol, 20 mM Tris HCl pH 7.4). Pellets were collected (5 min, 4°C, 3K RPM) and resuspended in 1.5 ml PSB buffer (20 mM Tris HCL pH 7.4, 2 mM EDTA, 100 mM NaCl, 10 mM β-ME) for 10 minutes with rotation at ambient temperature. Pellets were collected (5 min, RT, 9K RPM) and washed in 1.5 ml SB buffer (5 min, RT, 9K RPM), then resuspended in 1 ml SB buffer with zymolyase (10 mg/ml in SB). Samples were incubated at room temperature for 1 hour. SB buffer (600 ul) was added to stop the reaction. Spheroplasts were collected (5 min, 4°C, 2K RPM) and washed twice in 1 ml LB buffer (0.4 M sorbitol, 150 mM potassium acetate, 2 mM magnesium acetate, 20 mM PIPES, pH 6.8) with 1 mM PMSF and a protease inhibitor cocktail tablet (Roche,

Cat# 11836170001). Spheroplasts were resuspended in 250 ul LB buffer with 1 mM PMSF, 1 protease inhibitor cocktail and 1% Triton-X, and incubated on ice with occasional mixing for 10 minutes. Samples (125 ul) were transferred to tubes labeled total fraction; the other 125 ul of sample was transferred to tubes labeled chromatin fraction. Lysates in the chromatin fraction tubes were centrifuged 15 min, 4°C, 5K RPM, and supernatants were transferred to tubes labeled soluble fraction. Pellets in the chromatin fraction tubes were washed three times in 1 ml LB buffer with 1 mM PMSF, 1 protease inhibitor cocktail and 1% Triton-X. Pellets were collected after washes (5 min, 4°C, 5K RPM) and supernatants were aspirated. Chromatin fraction sample pellets were resuspended in 125 ul LB buffer.

Tables

Table 3.1: Strains Used in This Study. Related to STAR Methods

Name	Genotype	Reference
CEN.PK122-α	MATα MAL2-8c SUC2	(Pinel et al., 2011)
yaf9W89A	CEN.PK122-α	(Klein et al., 2018)
yaf9Δ	CEN.PK122-α yaf9::KanMX	This study
htz.1Δ		This study
W303-1B	MATa ade2-1 can1-100 his3-11,15 leu2-3,112 trp1-1 ura3-1	(Wallis et al., 1989)
esa1E338Q	W303-1B esa1::K.l.URA3	(Decker et al., 2008)

Table 3.2: Primers Used for RT-qPCR and ChIP-qPCR. Related to STAR Methods

Name	Genotype	Reference
CLN3	GTGGCTGAGAGTTGAAGTTAGT	CTCAGCGATCAGCGAATACA
RPL18B	TCACACTTCCAAGCAACACA	GCACGCAACGATACTAAGACTG
MRPL10	ACTAGCGTAGCTGGTAACGA	GACCACGCCCTGATGTCTTA
ACT1	TTCTGGTATGTGTAAAGCCGG	CCATACCGACCATGATACCTTG
RPL4B -1 nucleosome	GCTAAGAACTGCACTGAAGGC	TGTGGACGGGACATTATTATTGG
RPL4B +1 nucleosome	TCCCGTCCACAAGTTACTGT	GTACCACCACCACCAACTCT
RPL4B 3'	CCTCCAAGGTCGGTTACACT	CAAAGACCTTGGCGTAAGGG
SSC1 -1 nucleosome	GCTTACGGTGCGGTGTATAA	GTCACTCTGGCAAAGGTTGG
SSC1 +1 nucleosome	GTCTAGCTCTTTCCGTATTGCC	TGGGTTCACTACGGCTTGAC
SSC1 3'	TACAAGGTGGCGAAGAGGTT	GCATTGTTGCCGTTGTTGTT
FBA1 -1 nucleosome	GCTTCAATTACGCCCTCACA	CGCAAGGAAGAACAATAACTGAA
FBA1 +1 nucleosome	TCTTAAAGAGAAAGACCGGTGT	AGAGATACCCTTACCAGCGA
FBA1 3'	TGGTTCCGGTTCTACTGTCC	ACCTTCTGGGTTACCGACTG
TDH2 +1 nucleosome	TGCAAAGAAAGAACGTCGAAGT	TGGCGATCTTGTGACCATCA
PYC1 +1 nucleosome	GTCGCAAAGAAAATTCGCCG	GTCAATGGCCAAATAAGCGC
HOM6 +1 nucleosome	ACTAAAGTTGTTAATGTTGCCGT	GTCCTTGGAGATTAAAGAACGCT
TPI1 +1 nucleosome	GAACTTTCTTTGTCGGTGGTAAC	AAGTAGGTAGCTGGAGGACA

Table 3.3: Distribution of Genes in the 4 Hierarchical Clusters Based on Their Transcription Profiles Across the 5 Time Points

	cluster 1 (82)	cluster 2 (3102)	cluster 3 (833)	cluster 4 (104)	total	total/category genes (100%)
HOC genes (1501)	79 (96%)	1086 (35%)	5 (0.6%)	0 (0%)	1170	0.779480346
LOC genes (2309)	0 (0%)	910 (29 %)	704 (85%)	94 (90%)	1708	0.739714162
non-cycling genes (2194)	2 (2.4%)	1030 (33%)	109 (13%)	8 (7.6%)	1149	0.523701003

Figure Legends

Figure 3.1: Yaf9 and its YEATS Domain are Crucial for Proper YMC Progression

(A) Schematic representations of the Yaf9-containing SWR1-C and NuA4 complexes. (B) Schematic representation of Yaf9. (C) Pull-down assays using histone H3 peptides and purified GST-tagged Yaf9 with the indicated acylated or un-acylated peptides (residues 1-15 and 15-34 of the H3 tail). Bar graph underneath represents the quantitation of the pull-downs in which Yaf9 binding to H3K9ac or H3K27ac was normalized to 1.0 for comparison to other acylation interactions. Standard deviation of independent triplicates is shown. (D) Growth of serially diluted wild-type, *yaf9*$_{W89A}$ and *yaf9Δ* strains on media containing various genotoxic agents or glycerol. (E) YMC profile for wild-type *under* 0.15% glucose. (F) YMC profile for *yaf9*$_{W89A}$ *under* 0.15% glucose. (G) YMC profile for *yaf9Δ* under 0.15% glucose. (H) Overlapped YMC profile of wild-type (black line) and *yaf9*$_{W89A}$ (blue line). The *yaf9*$_{W89A}$ strain shows an average elongated YMC of 30 minutes per cycle.

Figure 3.2: H2A.Z and H4 Acetylation Oscillate Across the YMC and Their Levels are Regulated by Yaf9-H3 Acyl Reading

(A) Nine YMC samples from wild-type and *yaf9*$_{W89A}$ strains were collected to cover one complete YMC cycle. The collecting times are indicated on the YMC profiles. A segment of a complete YMC experiment of each strain is shown to demonstrate the collection strategy and the distance between samples. (B) Immunoblots of wild-type and *yaf9*$_{W89A}$ YMC whole cell lysates with the indicated antibodies (ac is acetylation; cr is crotonylation). Histones H2A, H3, H4 and G6PDH are loading controls. (C) Overlapped wild-type (black line) and *yaf9*$_{W89A}$ (blue line) YMC profiles show the collection strategy for comparing three distinct time points between the strains. Time points (tp) 1 and 3 represent LOC phase samples, whereas tp2 represents the HOC phase. (D) Immunoblots of wild-type and *yaf9*$_{W89A}$ YMC whole cell lysates to compare the time points collected in (C). Corresponding time point samples of each strain were loaded next to each other.

Histones H2A and H3 are loading controls. The blots presented are one of three independent experiments. (E) Bar graph showing quantification of H2A.Z levels compared with H2A control within the same time point of both strains. Error bars show standard deviation of three independent experiments ($P < 0.005$). (F) Bar graph showing quantification of H4ac levels compared with H2A control within the same time points for both strains. Error bars show standard deviation of three independent experiments ($P < 0.005$).

Figure 3.3: Yaf9 Necessity Can be Bypassed Under Optimal Growth Conditions

(A) Western analysis of H2A.Z, H4ac and Yaf9 in wild-type, yaf9W89A, yaf9Δ, htz.1Δ (H2A.Z delete) and esa1E338Q (Esa1 catalytic-dead) strains in YPD. G6PGH and H3 and H2A were used as loading controls. (B) Wild-type, yaf9W89A and yaf9Δ YMC samples, as well as samples in batch YPD media, were subjected to chromatin association assays described for Figure 3.11. The time points of the YMC samples were collected as described in Figure 3.2C. H2A and H3 were used as controls for chromatin fractions, G6PDH was used as a control for soluble fractions. Total fractions were used as loading controls

Figure 3.4:The YEATS Domain of Yaf9 is Required for Precise Metabolic Gene Transcription

(A-B) YMC traces corresponding to samples collected from wild-type and *yaf9*$_{W89A}$ strains for RNA-Seq analysis. Biological triplicates of each YMC sample were collected from three consecutive cycles. Time-point 3, which showed the greatest defect in gene expression from the analyses, is highlighted in green background on both YMC traces. (C) Principal component analysis of RNA-seq samples. Biological triplicates are shown for each time point. Each time point is indicated by one color. Wild-type samples are represented by circles and *yaf9*$_{W89A}$ samples are represented by triangles. (D) Box plot of log2 fold change of SDE genes showing highest polar distribution on time point 3. Time-point 3 is highlighted in green background. (E) DAVID functional

annotation enrichment analysis of SDE genes at time-point 3. Enrichment is shown as -log10 p value. (F) Volcano plots showing differences in gene expression between wild-type and *yaf9*$_{W89A}$. Log2 fold expression change (x axis) and -log10 p value significance (y axis) displays upregulated (red) sand downregulated (blue) genes in *yaf9*$_{W89A}$. Unchanged genes are represented in black. Time-point 3 is highlighted in green background.

Figure 3.5: Individual RT-qPCR Experiments Coincide with the RNA-seq Data

(A-B) Transcription patterns of two HOC genes and one LOC gene across YMC are plotted using RNA-seq data for wild-type and *yaf9*$_{W89A}$. RT-qPCR analysis of the same genes in wild-type and *yaf9*$_{W89A}$ YMC samples performed with targeted primers. RT-qPCR transcription patterns are plotted to compare with the RNA-seq graphs. SD shows technical triplicates. Actin was used as the standard for signal normalization. HOC, high oxygen consumption LOC, low oxygen consumption. (C) Unsupervised Hierarchical cluster analysis of RNA-seq gene transcription (n=4121) based on log2(fpkm+1) showing four clusters. The clusters are shown in separate heatmaps. Bars above heatmaps show metabolic phase and time points collected in the phase. (D) Line plots showing the transcription trends of four gene clusters from hierarchical-clustering. There are 4121 SDE genes, and the number of genes in each cluster is indicated. Wild-type transcription trends are represented by red solid lines, and *yaf9*$_{W89A}$ transcription trends are represented by blue solid lines. The transcription trends represented by the solid lines are the median centroids of each cluster. The transcription range of clustered genes is represented by shaded area (red for wild-type and blue for *yaf9*$_{W89A}$).

Figure 3.6: The YEATS Domain of Yaf9 is Required for Precise Metabolic Gene Transcription

Transcription patterns of selected 3 HOC genes and 3 LOC genes across YMC are plotted using RNA-seq data for wild-type and yaf9W89A. 3 non-cycling genes were plotted as controls.

Figure 3.7: Yaf9 H3-acyl Reading is Required for Proper Deposition of H2A.Z and H4 Acetylation at Genes

Schematic representation of the locations of -1 nucleosome, +1 nucleosome and 3' primers on RPL4B, SSC1 and FBA1 genes. Each gene was selected to represent its metabolic gene category. (B-D) ChIP-qPCR analysis of H2A.Z, H4ac and Pol II occupancy on all three loci of selected genes. Standard deviation of technical triplicates is shown. YMC sample collection strategy is consistent with Figures 3.4A and 3.4B.

Figure 3.8: H2A.Z, H4ac and Pol II Occupancy Levels were Examined at the -1 Nucleosome, +1 Nucleosome and 3' End of Various of Genes

Schematic representation of the locations of -1 nucleosome, +1 nucleosome and 3' primers *on RPL4B*, *SSC1* and *FBA1* genes. Each gene was selected to represent its metabolic gene category. (B-D) ChIP-qPCR analysis of H2A.Z, H4ac and Pol II occupancy on all three loci of selected genes. Standard deviation of technical triplicates is shown. YMC sample collection strategy is consistent with Figures 3.4A and 3.4B.

Figure 3.9: Yaf9-H3 Acyl Reading is Required for Proper Deposition of H2A.Z, H4 Acetylation and Pol II at LOC Genes

(A) Schematic representation of the locations of +1 nucleosome primers on two selected LOC genes *TDH2* and *PYC1*. (B) ChIP-qPCR analysis of H2A.Z, H4ac and Pol II occupancy on +1 nucleosome loci of selected LOC genes. Standard deviation of technical triplicates is shown. The Pol II ChIP-qPCR was performed with a rabbit primary antibody gifted from Dr. David Gross. YMC sample collection strategy is consistent with Figures 3.4A and 3.4B.

Figure 3.10: Yaf9-H3 Acyl Reading is Required for Proper Deposition of H2A.Z, H4 Acetylation and Pol II at Non-cycling Genes

(A) Schematic representation of the locations of +1 nucleosome primers on two selected non-cycling genes *HOM6* and *TPI1*. (B) ChIP-qPCR analysis of H2A.Z, H4ac and Pol II occupancy on +1 nucleosome loci of selected non-cycling genes. Standard deviation of technical triplicates is shown. The Pol II ChIP-qPCR was performed with a rabbit primary antibody gifted from Dr. David Gross. YMC sample collection strategy is consistent with Figures 3.4A and 3.4B.

Figure 3.11: Histone-binding by Yaf9 is Required for SWR1-C and NuA4 Chromatin Recruitment

(A-D) Immunoblots of chromatin and soluble fractions from chromatin association assays. Total fractions are used as inputs. Levels of chromatin bound Yaf9, H2A.Z, H4ac, Eaf1, Swr1, Taf3, Taf4, Taf12, and Taf14 in wild-type and *yaf9*$_{W89A}$ YMC samples are shown in the chromatin fraction blots. Histones H2A, H3 and G6PDH are loading controls. YMC sample collection strategy of the three time points is consistent with Figure 3.2C. (E) Bar graphs showing quantitation of chromatin bound Yaf9, H2A.Z, H4ac, Eaf1, Swr1, and Taf12 levels compared with their corresponding total fraction counterparts. Wild-type normalized chromatin-bound protein levels are indicated by red lines, and *yaf9*$_{W89A}$ normalized chromatin-bound protein levels are indicated by blue lines. Error bars show standard deviation of three independent experiments ($P < 0.005$).

Figure 3.12: The Chromatin Association Assay Reduces Ability to Detect Chromatin-Associated Factors

Samples collected from batch YPD media and wild-type YMC samples were subjected to TCA protein extract. Another group of wild-type YMC samples were subjected to chromatin association assays. The 3 time points of the YMC samples were collected as described in Figure 3.2C. The levels of Yaf9, Pol II, Bdf1/Bdf2, Taf12 and Rpb3 in the total fractions were then compared to the

protein samples from the TCA experiments through western analysis. Histone H2A and G6PDH were used as controls.

Figure 3.13: Model for Yaf9-H3 Acyl-binding Regulation of Precise Timing and Level of Metabolic Gene Transcription

These studies define a function for Yaf9 and its YEATS domain in chromatin and metabolic gene regulation. During respiration and oxidative metabolism, in which levels of acetyl-CoA and histone acetylation are high (the high oxygen consumption phase; HOC), we found that Yaf9, by its reading of H3 acetylation, was required for the timely recruitment of SWR1-C and NuA4 that increase H4 acetylation and H2A.Z deposition. This phase is associated with high levels of histone acetylation-driven recruitment of bromodomain factors that include Brd1/Brd2 and other chromatin and pre-initiation machinery (e.g., TFIID). But this phase also results in reduced Pol II levels at genes. In contrast to the HOC phase, and as cells metabolically cycle into the reductive and low oxygen consumption phase (LOC), the production of acyl-CoAs is increased (e.g., histone crotonylation (cr)), and overall histone acetylation levels are dramatically reduced. Absence of histone acetylation results in reduced recruitment of Yaf9 and its associated complexes but allows for increased occupancy of Pol II at genes compared with occupancy in the HOC phase. The function of anti-corelated levels of Pol II and H2A.Z/H4ac across the YMC is not yet understood. Altogether, these findings reveal an unexpected cycling of chromatin and transcriptional initiation machinery at distinct metabolic states that likely underpins how cells precisely regulate transcription programs during nutrient flux.

Figures

Figure 3.1: Yaf9 and its YEATS Domain are Crucial for Proper YMC Progression

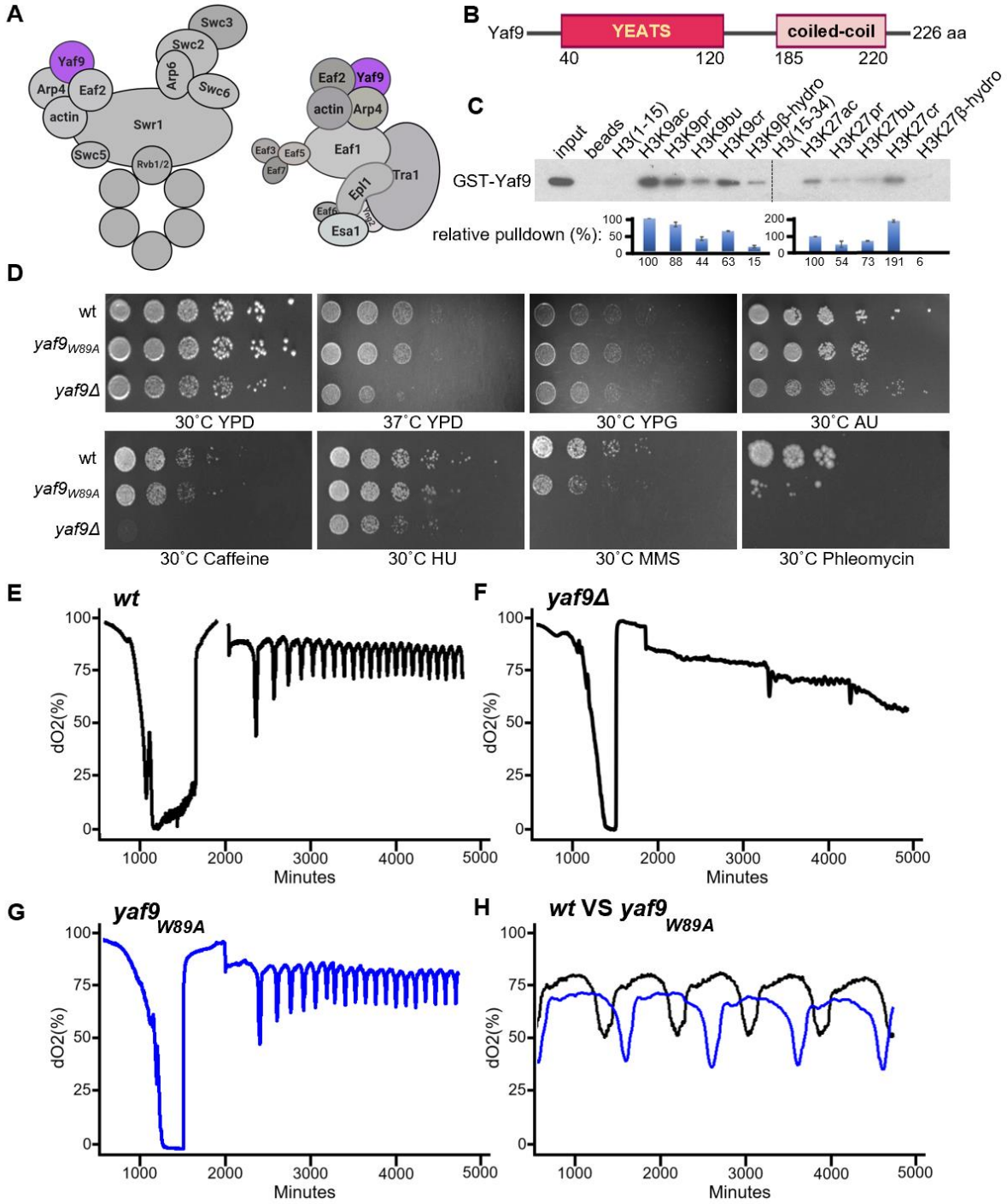

Figure 3.2: H2A.Z and H4 Acetylation Oscillate Across the YMC and Their Levels are Regulated by Yaf9-H3 Acyl Reading

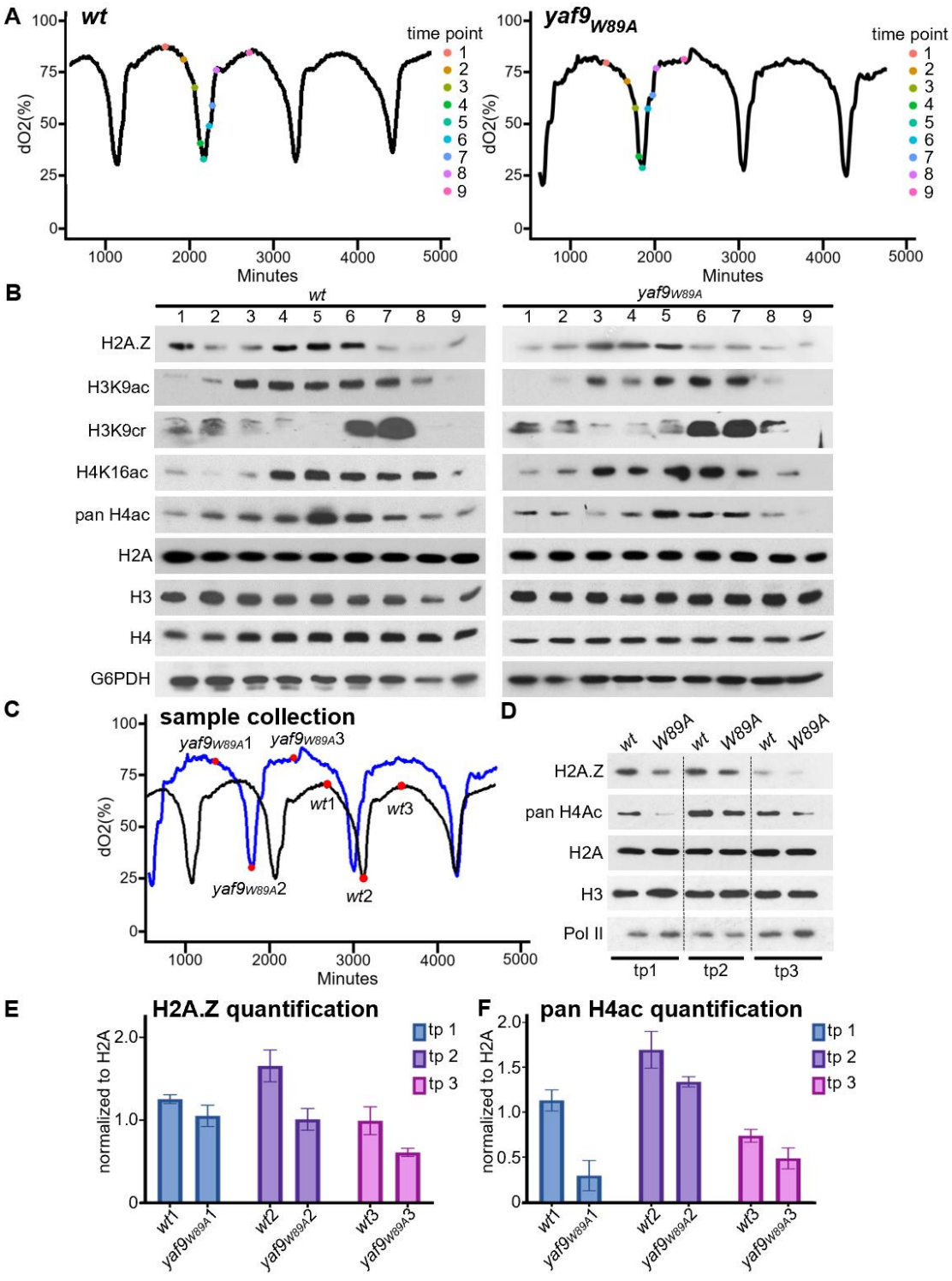

Figure 3.3: Yaf9 Necessity Can be Bypassed Under Optimal Growth Conditions

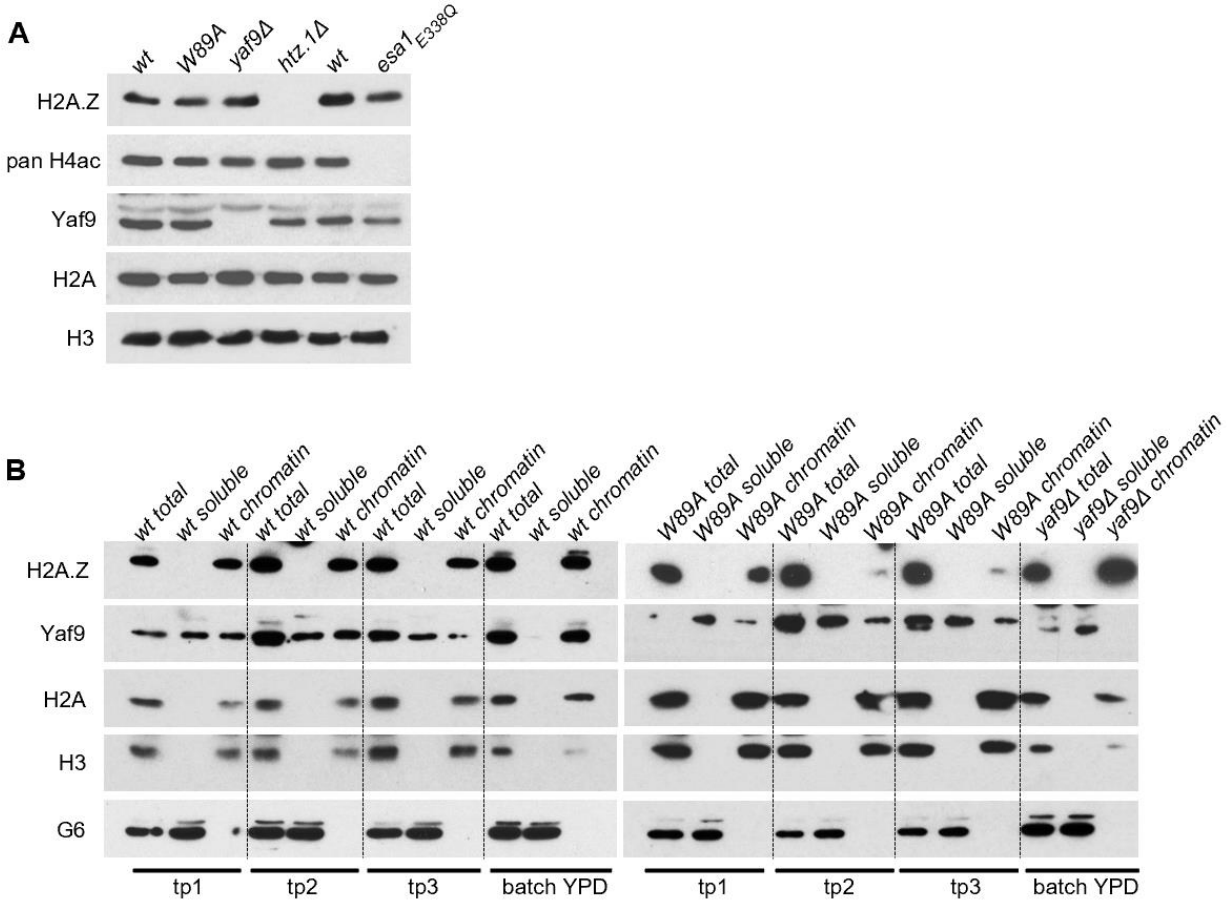

Figure 3.4: The YEATS Domain of Yaf9 is Required for Precise Metabolic Gene Transcription

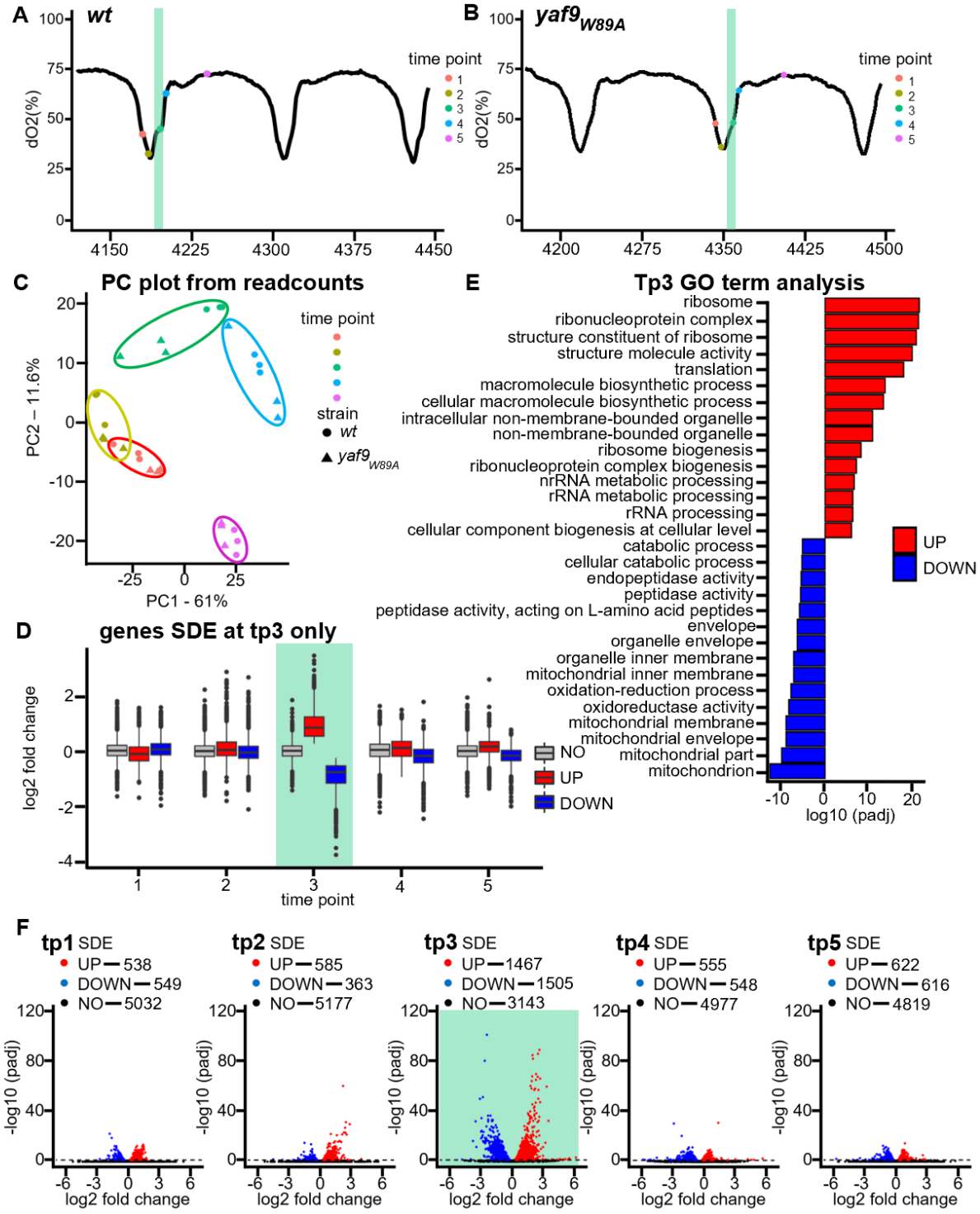

Figure 3.5: Individual RT-qPCR Experiments Coincide with the RNA-seq Data

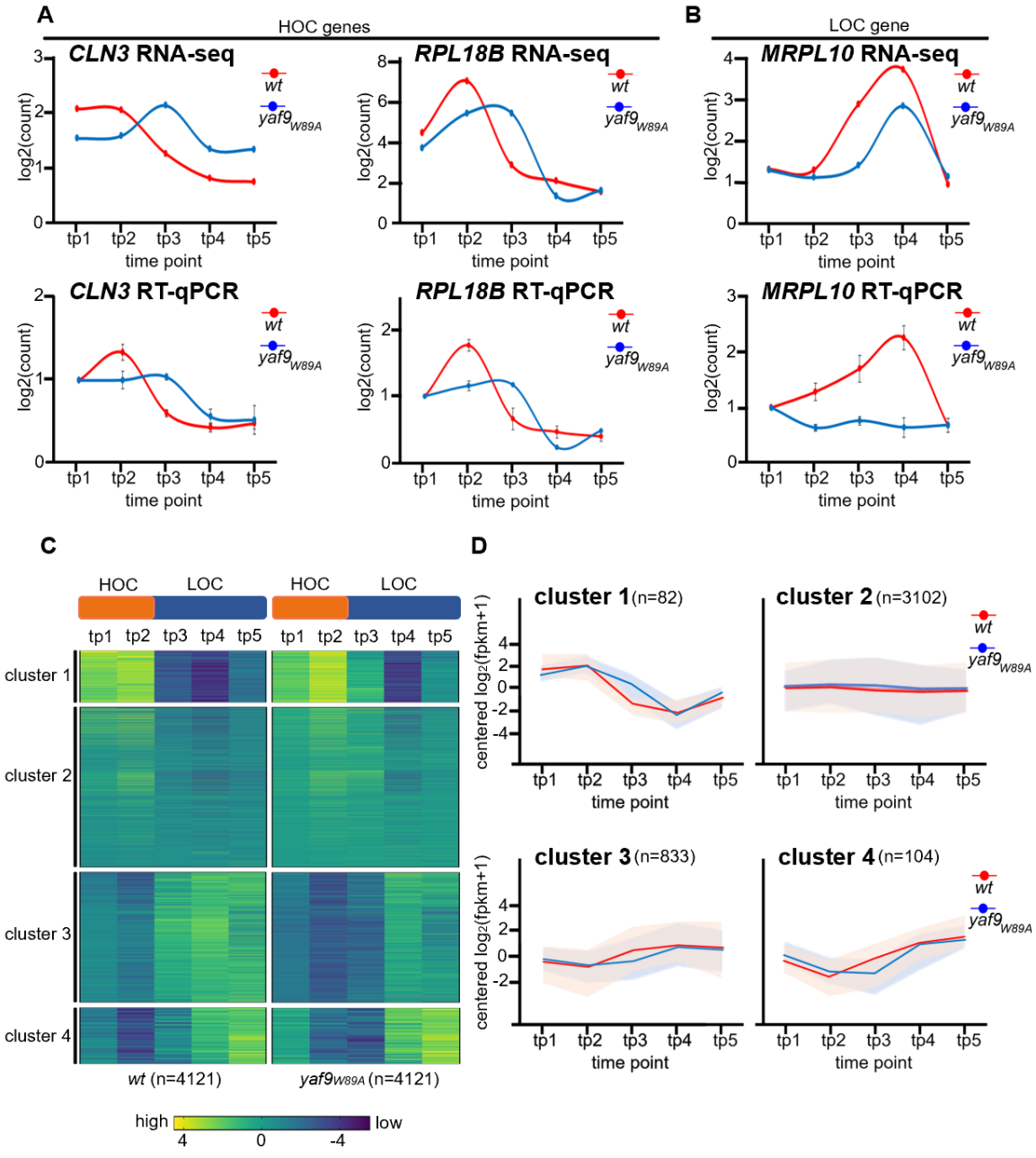

Figure 3.6: The YEATS Domain of Yaf9 is Required for Precise Metabolic Gene Transcription

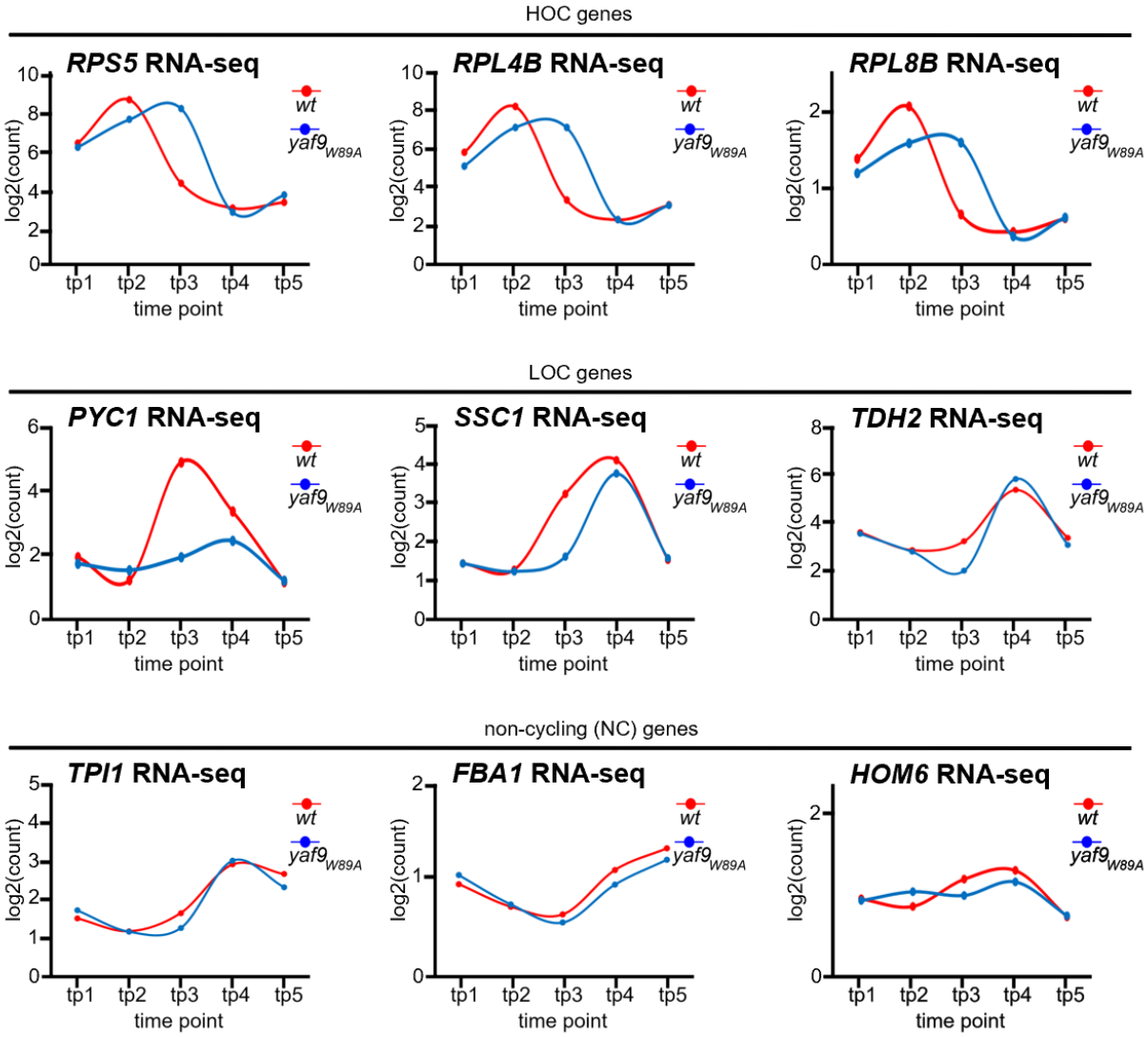

Figure 3.7: Yaf9 H3-acyl Reading is Required for Proper Deposition of H2A.Z and H4 Acetylation at Genes

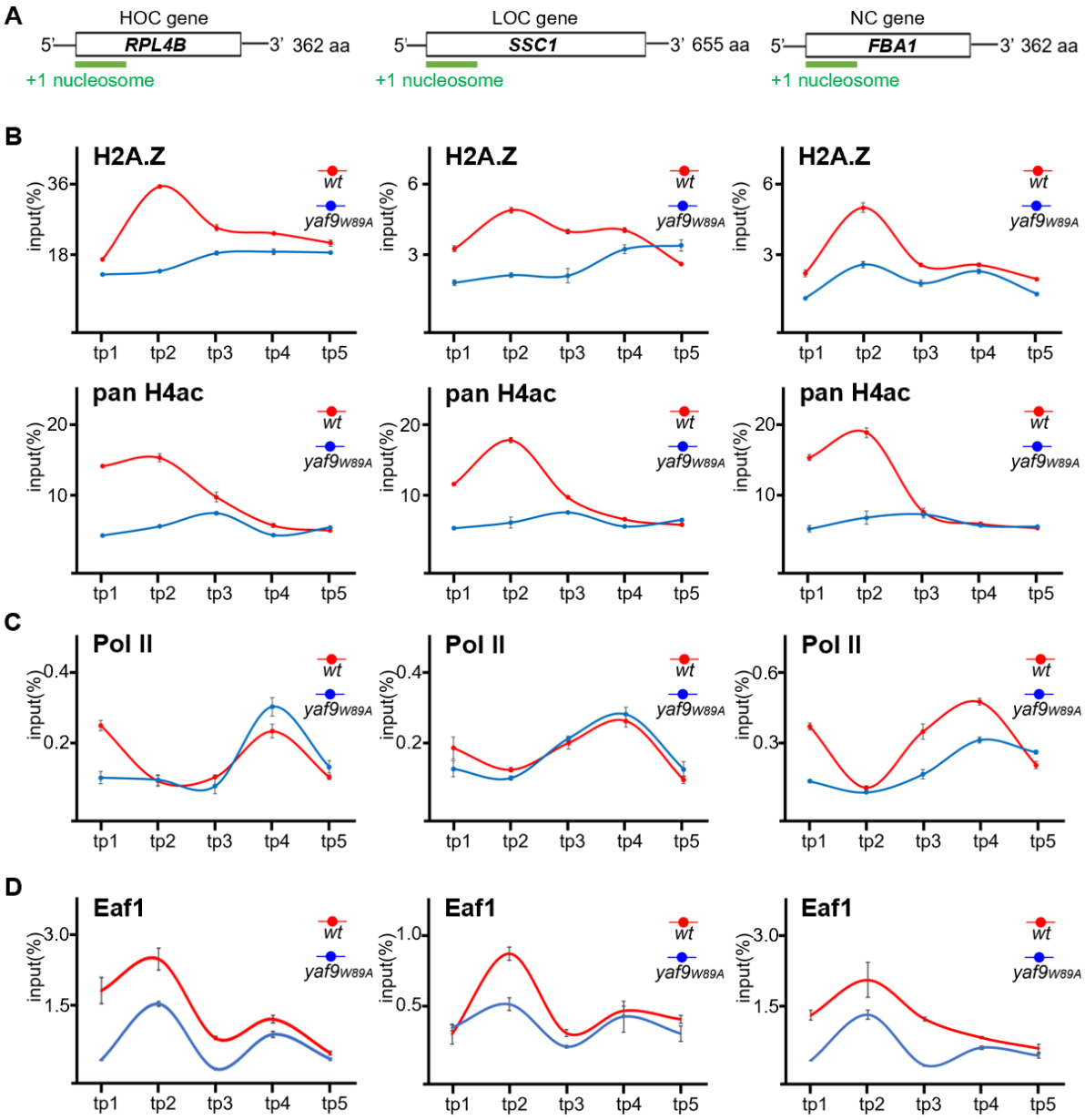

Figure 3.8: H2A.Z, H4ac and Pol II Occupancy Levels were Examined at the -1 Nucleosome, +1 Nucleosome and 3' End of Various of Genes

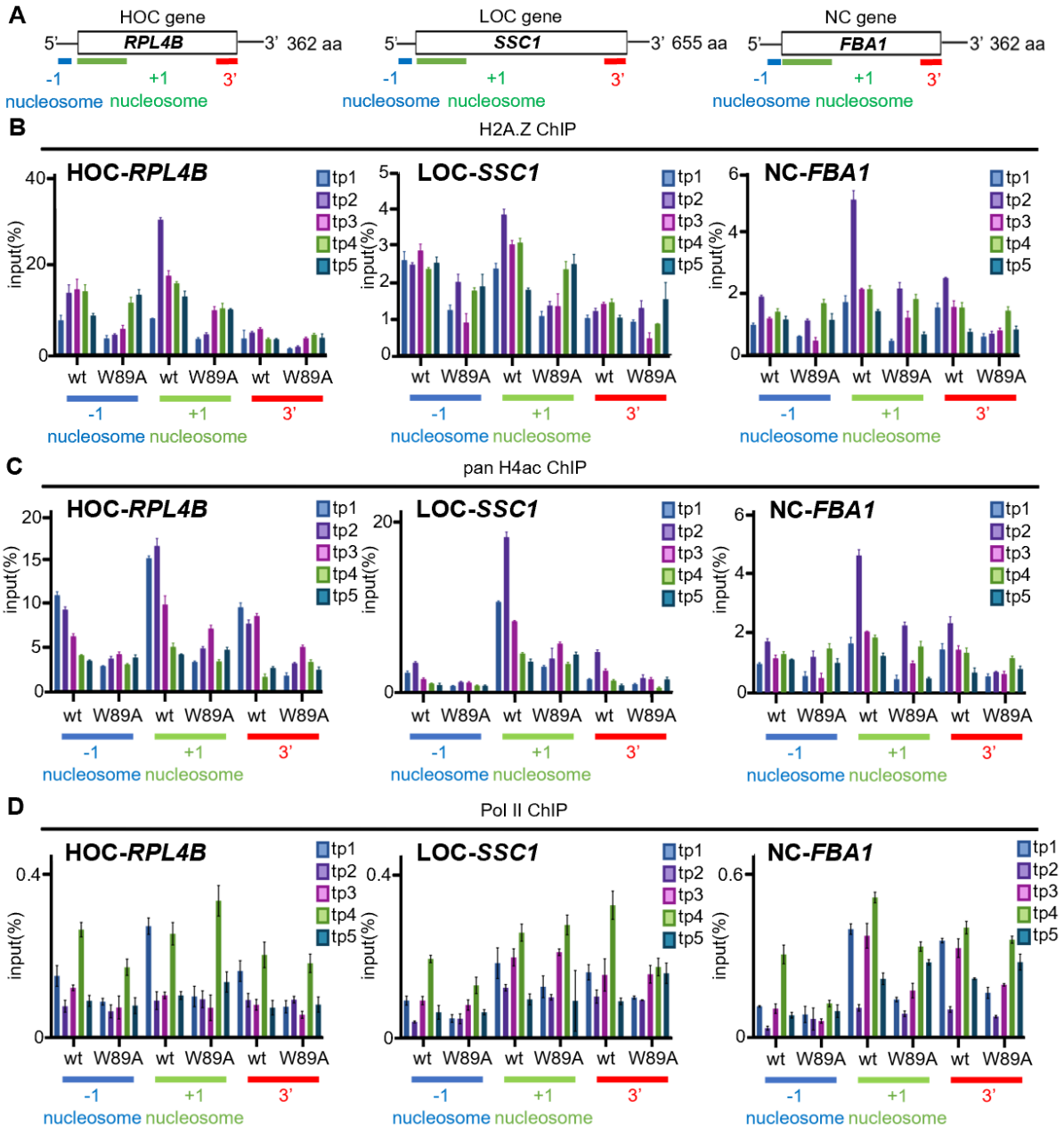

Figure 3.9: Yaf9-H3 Acyl Reading is Required for Proper Deposition of H2A.Z, H4 Acetylation and Pol II at LOC Genes

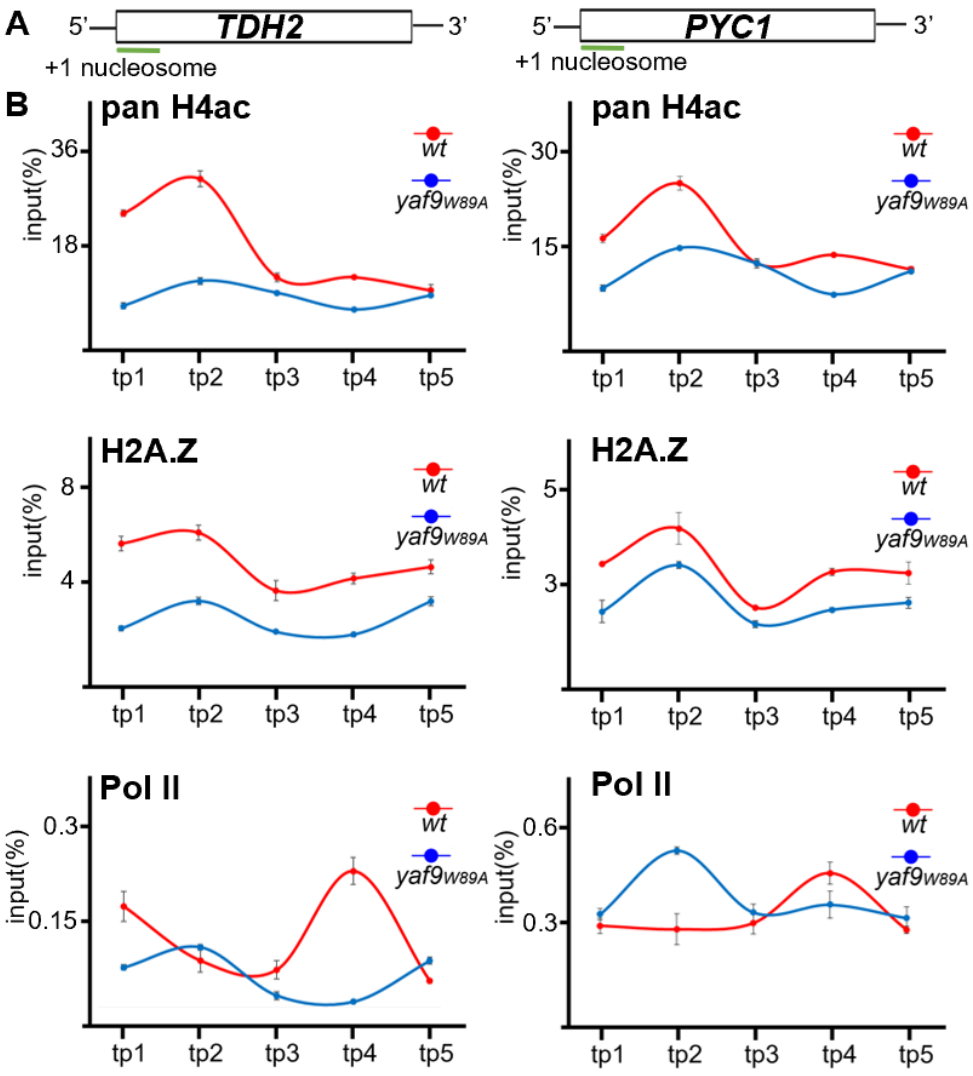

Figure 3.10: Yaf9-H3 Acyl Reading is Required for Proper Deposition of H2A.Z, H4 Acetylation and Pol II at Non-cycling Genes

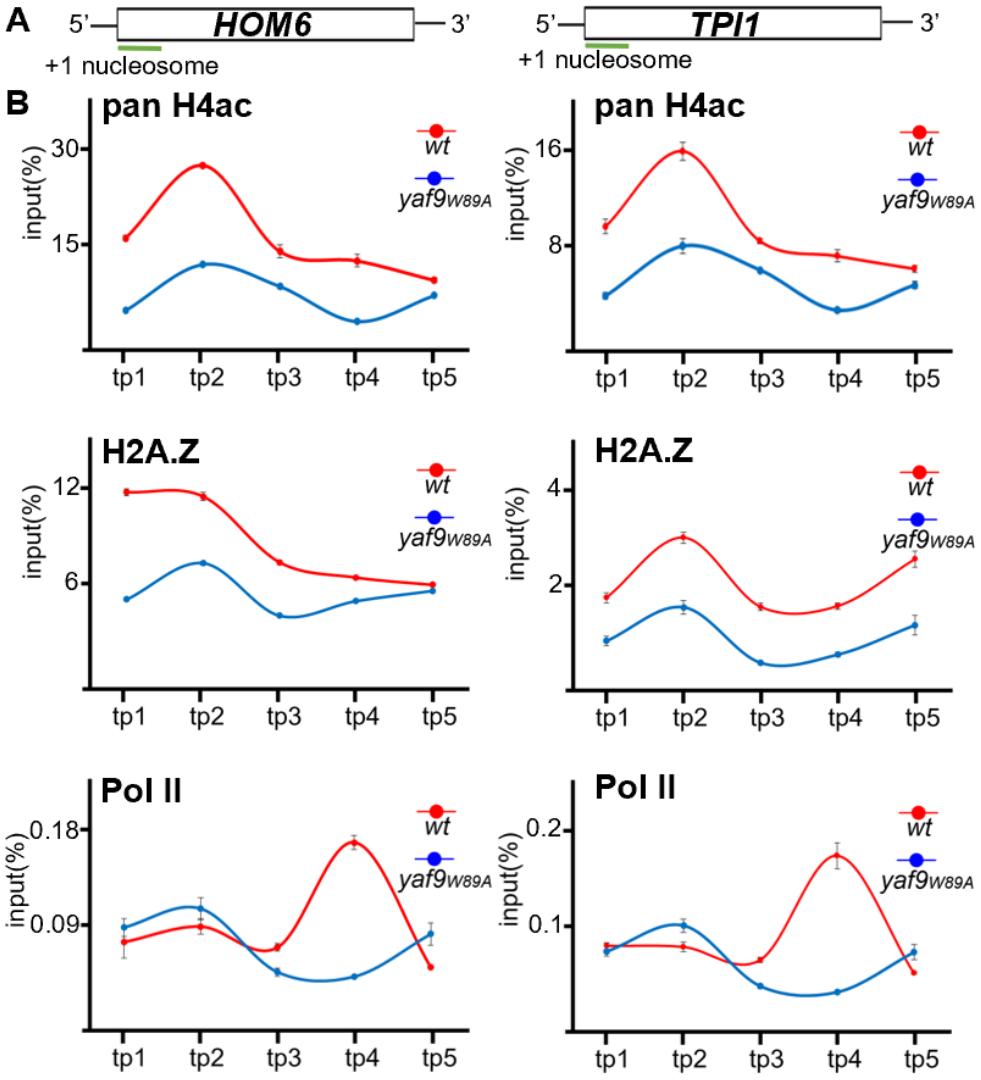

Figure 3.11: Histone-binding by Yaf9 is Required for SWR1-C and NuA4 Chromatin Recruitment

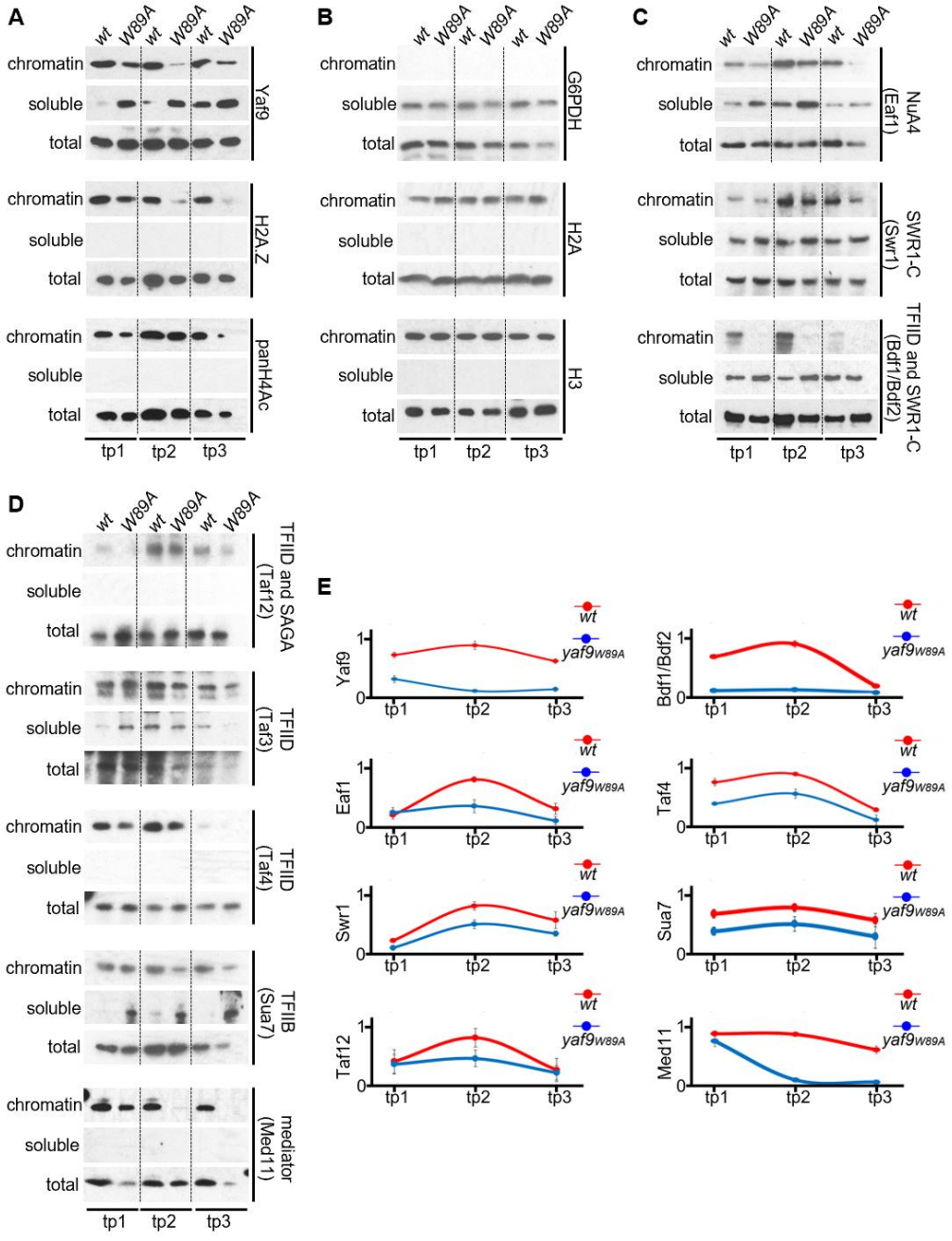

Figure 3.12: The Chromatin Association Assay Reduces Ability to Detect Chromatin-Associated Factors

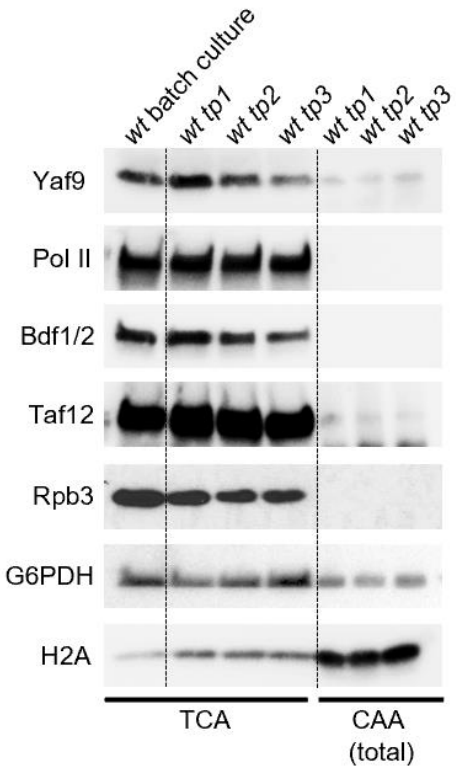

Figure 3.13: Model for Yaf9-H3 Acyl-binding Regulation of Precise Timing and Level of Metabolic Gene Transcription

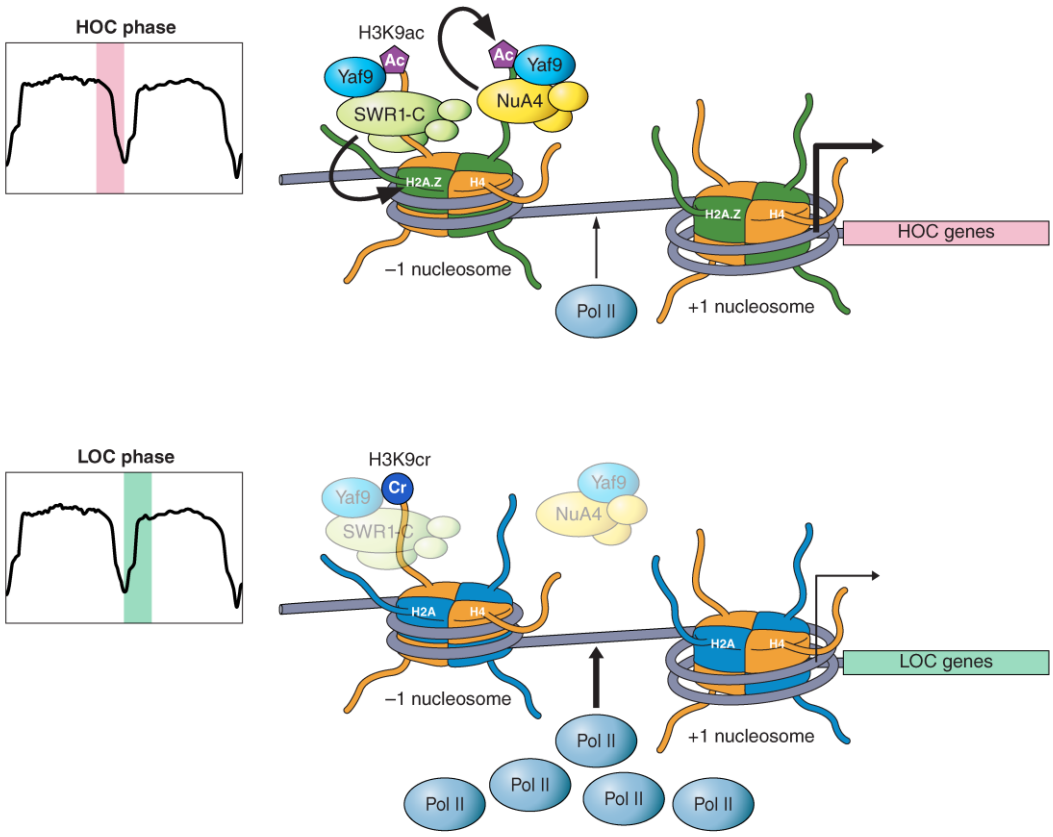

CHAPTER 4 – CONCLUSIONS AND FINAL THOUGHTS

Phenotypical evidence provided by the yeast growth assay has the limitation that the authentic functions and interactions of a protein could be bypassed by optimal growth conditions. This means the acyl-lysine binding inhibited *yaf9*$_{W89A}$ strain might show stronger growth defects if plated on nutrient-limiting plates containing genotoxic agents. The chemostat is the best equipment to simulate wild yeast living environment. The synchronized YMC traces forced by the nutrient-limiting conditions suggest that losing Yaf9 H3-acyl reading function disrupts proper YMC progression. Combining with the surprising result of failed YMC in *yaf9Δ*, the phenotype of a 30 minutes YMC elongation in the pocket mutant strain highlights the importance of the H3-acyl binding on yeast YMC progression under natural living habitat.

By utilizing the chemostat, we were able to discover the cycling patterns of H4ac, H2A.Z, Pol II and other transcription factors (Bdf1/2, TFIID and SAGA members) in synchronized yeast cells. Other than Pol II, the chromatin-bound levels of the rest share an identical cycling pattern, as they gradually increase during the HOC phase until reaching the peak at the end of the HOC phase, then decrease during the LOC phase. As a result, the transcription of genes involved in high oxygen demanding processes is induced. This demonstrates that the high cellular acetyl-CoA level from glycolysis limits the transcription timeframe for necessary and effective expression of HOC genes. In stark contrast, the chromatin bound Pol II levels were found to be cyclic as well, but in an opposite manner. As shown in the ChIP data, chromatin-bound Pol II reaches the peak level during LOC phase, which coincides with the cycling pattern of cellular crotonyl-CoA level. This suggests that the high cellular crotonyl-CoA from beta-oxidation pathways signals the end of HOC phase and the beginning of induced transcription of genes involved in reductive processes. Therefore, my work reveals a new regulatory system in yeast that compartmentalizes the

transcription of metabolic-driven genes according to metabolic state. Yaf9's role in this regulatory system is discovered from the delayed HOC gene transcription and decreased LOC gene transcription in *yaf9*$_{W89A}$ strain. Our evidence shows that the YEATS domain pocket mutant, unable to bind acylation, causes Yaf9 to relocate into the soluble fraction, resulting in unsuccessful recruitment of NuA4 and SWR1-C complexes. Less chromatin bound NuA4 and SWR1-C complexes lead to decreased H4ac and H2A.Z levels, which subsequently affects the recruitment of transcription factors (Bdf1/2, TFIID and SAGA members). This series of events argues that Yaf9 is the conductor of the regulatory system through its H3-acyl binding ability. As our model illustrates, under nutrient-limiting conditions, Yaf9 predominantly binds to increased H3K9ac in the HOC phase. NuA4 and SWR1-C are recruited by Yaf9, resulting in increased chromatin-bound H4ac, H2A.Z and transcription factors. Due to the antagonist relation between Pol II and H2A.Z, less Pol II is recruited. However, the amount of chromatin bound Pol II is enough to ensure HOC gene up-regulation. On the other hand, Yaf9 isn't able to securely bind with H3K9cr in the LOC phase. NuA4 and SWR1-C complexes are released from chromatin, resulting in decreased chromatin bound H4ac, H2A.Z and transcription factors. In the end, H3K9cr becomes the factor that promotes the release of chromatin bound H2A.Z, and thereby collaborates with high level Pol II to overcome the lack of transcription factors to ensure LOC gene up-regulation. We propose that in wild-living yeast, Ya9 operates as a regulator to manage the transcription of HOC and LOC genes, accordingly, reinforcing the important role of Yaf9 H3-acyl binding in connecting cell metabolic state and gene transcription.

During the journey of studying Yaf9's role in metabolic-driven transcription, we discovered a surprising characteristic of Yaf9, that is, the necessity of Yaf9 could be bypassed if yeast is provided with optimal nutrient condition. The first piece of data supporting this theory was the chromatin bound Yaf9 level compared between batch culture samples and YMC samples. We found that all Yaf9 binds to chromatin in batch culture samples, while Yaf9 relocates into the soluble fraction in YMC samples. This could be caused by limited acetyl-CoA in the YMC samples

due to low glucose, but also suggests that wild yeast requires the proper amount of chromatin bound Yaf9 to sense the equilibrium between histone acetylation and crotonylation. Optimal nutrient condition provides constant high level of H3K9ac which prevents Yaf9 from leaving chromatin and releasing NuA4 and SWR1-C. Therefore, nutrient-limiting conditions require Yaf9 to fulfill both roles of the 2-way regulatory system. Another set of evidence is comparing the global H4ac and H2A.Z levels between batch culture samples of *yaf9Δ* strain and YMC samples of $yaf9_{W89A}$ strain. Deleting Yaf9 does not affect the global levels of H4ac and H2A.Z in yeast living in optimal nutrient condition. However, under nutrient-limiting conditions, $yaf9_{W89A}$ causes significant decrease of global H4ac and H2A.Z levels. This suggests that Yaf9's regulation on the downstream products of NuA4 and SWR1-C complexes can be bypassed with optimal nutrient condition. Together, our data demonstrate that the transcriptional regulatory functions of Yaf9 are reveled under naturally occurring conditions, highlighting the importance of utilizing nutrient-limiting conditions simulated by the chemostat to study the authentic functions and interactions of protein subjects.

In summary, my work uncovers three major findings: 1) Yaf9 H3-acyl reading is essential for proper YMC progression. 2) The 2-way regulatory system conducted by Yaf9, including the recruitment of NuA4, SWR1-C and transcription factors (Bdf1/2, TFIID and SAGA) in HOC phase and the substitution of Pol II in LOC phase, is how metabolic state influences gene transcription. 3) yeast metabolism and the proteins involved in metabolic pathways need to be studied in nutrient-limiting conditions simulated with a chemostat to avoid information bypasses from optimal nutrient environment.

Final Thoughts

The project on the ability of Yaf9 to read acylations connects yeast metabolic state to gene transcription was started two years ago. With the work coming full circle, there still are questions left unanswered due to limited time. This is my opportunity to raise some of the questions and propose feasible solutions for future students to continue the work.

First of all, it is important to utilize the *Yaf9Δ* strain to further specify the threshold of the glucose concentration of the chemostat nutrient-limiting media. All the YMC experiments mentioned in my work were performed within 0.1-0.2% glucose concentration. Under such condition, we learned that *Yaf9Δ* strain fails to perform YMC. But an important observation is that the YMC oscillation reappears after increasing the glucose input flow rate, suggesting that higher glucose concentration could rescue the phenotype caused by deleting Yaf9. Since the functions of Yaf9 only become essential under nutrient-limiting condition but could be bypassed in optimal nutrient media. One possible explanation is that the low glucose concentration applied in the YMC experiments had reached a threshold that made the deletion of Yaf9 intolerable. Increasing the glucose concentration above the threshold could overcome the loss of Yaf9 functions. Therefore, *Yaf9Δ* strain is the suitable tool to identify the glucose threshold that defines the importance of Yaf9 functions. The reappearing of *Yaf9Δ* YMC also provides chances to collect yeast samples for downstream experiments that were applied in previous chapters. It would be informative to observe the cycling patterns of histone acylations and H2A.Z in *Yaf9Δ* YMC samples.

Second, even though we concluded that Yaf9 is essential for the proper recruitment of NuA4 and SWR1-C complexes, the necessity of YEATS domain in bringing in all the subunits remains a mystery. We learned that the shared anchoring module of NuA4 and SWR1-C consists of Arp4/Act1/Yaf9/Swc4. Yaf9 and Swc4 interact with each other though their C-termini and form a dimer. The rest of the module binds to the dimer which starts the recruitments of the complexes. It would be interesting to add the Yaf9 YEATS domain onto Swc4 and determine if the partial dimerization is still efficient enough to recruit Arp4 and Act1, and subsequently NuA4 and SWR1-

C complexes. As a comparison to the complete deletion of Yaf9, whether the YEATS-Swc4 strain can establish stable YMC oscillation under low glucose concentration is a subject that can help us to understand the role of the YEATS domain in maintaining proper YMC when the nutrient threshold is surpassed. Another idea to further study the specificity of Yaf9's YEATS domain is to switch the domain with Taf14's YEATS domain. Since Taf14 is shown to preferably bind Kcr while Yaf9 has higher affinity for Kac, switching their YEATS domains will reverse the binding preference. The model we built in Chapter 3 could be challenged if Yaf9 does not leave chromatin during the LOC phase due to its binding to Kcr. A possible outcome is that the transcription of HOC genes during the oxidative phase does not drastically change. Because the 3-fold higher level of acetyl-CoA than crotonyl-CoA in the cytoplasm bypasses the Kcr preference of mutated Yaf9. However, the transcription of LOC genes could be negatively influenced. Unable to leave chromatin, Kcr-bound Yaf9 keeps both NuA4 and SWR1-C complexes who subsequently maintain high levels of H4ac and H2A.Z. The antagonistic relation between H2A.Z and Pol II prevents the later from binding to chromatin, which leads to down-regulated LOC gene transcription. On the other hand, Taf14-Kcr induced HOC gene down-regulation during the reductive phase is likely disrupted if the YEATS domain binds to Kac with a higher affinity. It will also be interesting to observe the YMC of the YEATS domain-switched strains. These hypotheses aim to discover more details of YEATS domain proteins.

REFERENCES

Allfrey, V. G., Faulkner, R., & Mirsky, A. E. (1964). Acetylation and methylation of histones and their possible role in the regulation of RNA synthesis. Proceedings of the National Academy of Sciences of the United States of America, 51(5), 786–794.

Altaf, M., Auger, A., Monnet-Saksouk, J., Brodeur, J., Piquet, S., Cramet, M., Bouchard, N., Lacoste, N., Utley, R. T., Gaudreau, L., & Côté, J. (2010). NuA4-dependent acetylation of nucleosomal histones H4 and H2A directly stimulates incorporation of H2A.Z by the SWR1 complex. The Journal of biological chemistry, 285(21), 15966–15977.

Andrews, F. H., Shinsky, S. A., Shanle, E. K., Bridgers, J. B., Gest, A., Tsun, I. K., Krajewski, K., Shi, X., Strahl, B. D., & Kutateladze, T. G. (2016). The Taf14 YEATS domain is a reader of histone crotonylation. Nature chemical biology, 12(6), 396–398.

Andrews, F. H., Strahl, B. D., & Kutateladze, T. G. (2016). Insights into newly discovered marks and readers of epigenetic information. Nature chemical biology, 12(9), 662–668.

Auger, A., Galarneau, L., Altaf, M., Nourani, A., Doyon, Y., Utley, R. T., Cronier, D., Allard, S., & Côté, J. (2008). Eaf1 is the platform for NuA4 molecular assembly that evolutionarily links chromatin acetylation to ATP-dependent exchange of histone H2A variants. Molecular and cellular biology, 28(7), 2257–2270.

Babiarz, J. E., Halley, J. E., & Rine, J. (2006). Telomeric heterochromatin boundaries require NuA4-dependent acetylation of histone variant H2A.Z in Saccharomyces cerevisiae. Genes & development, 20(6), 700–710.

Bagchi, D. N., Battenhouse, A. M., Park, D., & Iyer, V. R. (2020). The histone variant H2A.Z in yeast is almost exclusively incorporated into the +1 nucleosome in the direction of transcription. Nucleic acids research, 48(1), 157–170.

Bao, X., Wang, Y., Li, X., Li, X.-M., Liu, Z., Yang, T., Wong, C.F., Zhang, J., Hao, Q., and Li, X.D. (2014). Identification of “erasers” for lysine crotonylated histone marks using a chemical proteomics approach. eLife 3, e02999.

Barnes, C. E., English, D. M., & Cowley, S. M. (2019). Acetylation & Co: an expanding repertoire of histone acylations regulates chromatin and transcription. Essays in biochemistry, 63(1), 97–107.

Beckwith, S.L., Schwartz, E.K., Garcia-Nieto, P.E., King, D.A., Gowans, G.J., Wong, K.M., Eckley, T.L., Paraschuk, A.P., Peltan, E.L., Lee, L.R., et al. (2018). The INO80 chromatin remodeler sustains metabolic stability by promoting TOR signaling and regulating histone acetylation. PLoS Genet 14, e1007216.

Bittner, C. B., Zeisig, D. T., Zeisig, B. B., & Slany, R. K. (2004). Direct physical and functional interaction of the NuA4 complex components Yaf9p and Swc4p. Eukaryotic cell, 3(4), 976–983.

Bloch, K., & Borek, E. (1946). Biological acetylation of natural amino acids. The Journal of biological chemistry, 164, 483.

Bohley, P., and K.-U. Fröhlich. (1997). A prize-winning discovery of 1896: Buchner provides evidence of cell-free fermentation, in New Beer in an Old Bottle: Eduard Buchner and the

Growth of Biochemical Knowledge, edited by A. Cornish-Bowden. Universitat de València, Valencia, Spain. pp. 51–60.

Bönisch, C., & Hake, S. B. (2012). Histone H2A variants in nucleosomes and chromatin: more or less stable? Nucleic acids research, 40(21), 10719–10741.

Bowers, E. M., Yan, G., Mukherjee, C., Orry, A., Wang, L., Holbert, M. A., Crump, N. T., Hazzalin, C. A., Liszczak, G., Yuan, H., Larocca, C., Saldanha, S. A., Abagyan, R., Sun, Y., Meyers, D. J., Marmorstein, R., Mahadevan, L. C., Alani, R. M., & Cole, P. A. (2010). Virtual ligand screening of the p300/CBP histone acetyltransferase: identification of a selective small molecule inhibitor. Chemistry & biology, 17(5), 471–482.

Brownell, J. E., Zhou, J., Ranalli, T., Kobayashi, R., Edmondson, D. G., Roth, S. Y., & Allis, C. D. (1996). Tetrahymena histone acetyltransferase A: a homolog to yeast Gcn5p linking histone acetylation to gene activation. Cell, 84(6), 843–851.

Burnetti, A.J., Aydin, M., and Buchler, N.E. (2016). Cell cycle Start is coupled to entry into the yeast metabolic cycle across diverse strains and growth rates. Mol Biol Cell 27, 64–74.

Cai, L., Sutter, B. M., Li, B., & Tu, B. P. (2011). Acetyl-CoA induces cell growth and proliferation by promoting the acetylation of histones at growth genes. Molecular cell, 42(4), 426–437.

Cheng, X., & Côté, J. (2014). A new companion of elongating RNA Polymerase II: TINTIN, an independent sub-module of NuA4/TIP60 for nucleosome transactions. Transcription, 5(5), e995571.

Cosgrove, M. S., Boeke, J. D., & Wolberger, C. (2004). Regulated nucleosome mobility and the histone code. Nature structural & molecular biology, 11(11), 1037–1043.

Crespo, M., Damont, A., Blanco, M., Lastrucci, E., Kennani, S. E., Ialy-Radio, C., Khattabi, L. E., Terrier, S., Louwagie, M., Kieffer-Jaquinod, S., Hesse, A. M., Bruley, C., Chantalat, S., Govin, J., Fenaille, F., Battail, C., Cocquet, J., & Pflieger, D. (2020). Multi-omic analysis of gametogenesis reveals a novel signature at the promoters and distal enhancers of active genes. Nucleic acids research, 48(8), 4115–4138.

Crick F. H. (1958). On protein synthesis. Symposia of the Society for Experimental Biology, 12, 138–163.

De Castro, M. (2016). Johann Gregor Mendel : paragon of experimental science. Mol. Genet. Genomic Med. 3–8

Dhalluin, C., Carlson, J. E., Zeng, L., He, C., Aggarwal, A. K., & Zhou, M. M. (1999). Structure and ligand of a histone acetyltransferase bromodomain. Nature, 399(6735), 491–496.

Donohoe, D.R., Garge, N., Zhang, X., Sun, W., O'Connell, T.M., Bunger, M.K., and Bultman, S.J. (2011). The microbiome and butyrate regulate energy metabolism and autophagy in the mammalian colon. Cell Metabolism 13, 517–526.

Dreveny, I., Deeves, S. E., Fulton, J., Yue, B., Messmer, M., Bhattacharya, A., Collins, H. M., & Heery, D. M. (2014). The double PHD finger domain of MOZ/MYST3 induces α-helical structure of the histone H3 tail to facilitate acetylation and methylation sampling and modification. Nucleic acids research, 42(2), 822–835.

Falcón, A.A., Chen, S., Wood, M.S., and Aris, J.P. (2010). Acetyl-coenzyme A synthetase 2 is a nuclear protein required for replicative longevity in Saccharomyces cerevisiae. Mol. Cell. Biochem. 333, 99–108.

Fellows, R., Denizot, J., Stellato, C., Cuomo, A., Jain, P., Stoyanova, E., Balázsi, S., Hajnády, Z., Liebert, A., Kazakevych, J., et al. (2018). Microbiota derived short chain fatty acids promote histone crotonylation in the colon through histone deacetylases. Nature Communications 9, 105.

Filippakopoulos, P., Qi, J., Picaud, S., Shen, Y., Smith, W. B., Fedorov, O., Morse, E. M., Keates, T., Hickman, T. T., Felletar, I., Philpott, M., Munro, S., McKeown, M. R., Wang, Y., Christie, A. L., West, N., Cameron, M. J., Schwartz, B., Heightman, T. D., La Thangue, N., … Bradner, J. E. (2010). Selective inhibition of BET bromodomains. Nature, 468(7327), 1067–1073.

Fischer, E. H., Graves, D. J., Crittenden, E. R., & Krebs, E. G. (1959). Structure of the site phosphorylated in the phosphorylase b to a reaction. The Journal of biological chemistry, 234(7), 1698–1704.

Flynn, E. M., Huang, O. W., Poy, F., Oppikofer, M., Bellon, S. F., Tang, Y., & Cochran, A. G. (2015). A Subset of Human Bromodomains Recognizes Butyryllysine and Crotonyllysine Histone Peptide Modifications. Structure (London, England : 1993), 23(10), 1801–1814.

Friis, R. M., Wu, B. P., Reinke, S. N., Hockman, D. J., Sykes, B. D., & Schultz, M. C. (2009). A glycolytic burst drives glucose induction of global histone acetylation by picNuA4 and SAGA. Nucleic acids research, 37(12), 3969–3980.

Gallant-Behm, C. L., Ramsey, M. R., Bensard, C. L., Nojek, I., Tran, J., Liu, M., Ellisen, L. W., & Espinosa, J. M. (2012). ΔNp63α represses anti-proliferative genes via H2A.Z deposition. Genes & development, 26(20), 2325–2336.

Gardner, K. E., Allis, C. D., & Strahl, B. D. (2011). Operating on chromatin, a colorful language where context matters. Journal of molecular biology, 409(1), 36–46.

Gayon, J. (2016). From Mendel to epigenetics: History of genetics. C. R. Biol. 339, 225–230.

Giaimo, B. D., Ferrante, F., Herchenröther, A., Hake, S. B., & Borggrefe, T. (2019). The histone variant H2A.Z in gene regulation. Epigenetics & chromatin, 12(1), 37.

Giaimo, B. D., Ferrante, F., Vallejo, D. M., Hein, K., Gutierrez-Perez, I., Nist, A., Stiewe, T., Mittler, G., Herold, S., Zimmermann, T., Bartkuhn, M., Schwarz, P., Oswald, F., Dominguez, M., & Borggrefe, T. (2018). Histone variant H2A.Z deposition and acetylation directs the canonical Notch signaling response. Nucleic acids research, 46(16), 8197–8215.

Goffeau, A., Barrell, B. G., Bussey, H., Davis, R. W., Dujon, B., Feldmann, H., Galibert, F., Hoheisel, J. D., Jacq, C., Johnston, M., Louis, E. J., Mewes, H. W., Murakami, Y., Philippsen, P., Tettelin, H., & Oliver, S. G. (1996). Life with 6000 genes. Science (New York, N.Y.), 274(5287), 546–567.

Goudarzi, A., Zhang, D., Huang, H., Barral, S., Kwon, O.K., Qi, S., Tang, Z., Buchou, T., Vitte, A.-L., He, T., et al. (2016). Dynamic Competing Histone H4 K5K8 Acetylation and Butyrylation Are Hallmarks of Highly Active Gene Promoters. Mol Cell 62, 169–180.

Gowans, G. J., Bridgers, J. B., Zhang, J., Dronamraju, R., Burnetti, A., King, D. A., Thiengmany, A. V., Shinsky, S. A., Bhanu, N. V., Garcia, B. A., Buchler, N. E., Strahl, B. D., & Morrison, A. J. (2019). Recognition of Histone Crotonylation by Taf14 Links Metabolic State to Gene Expression. Molecular cell, 76(6), 909–921.e3.

Gowans, G.J., Schep, A.N., Wong, K.M., King, D.A., Greenleaf, W.J., and Morrison, A.J. (2018). INO80 Chromatin Remodeling Coordinates Metabolic Homeostasis with Cell Division. Cell Reports 22, 611–623.

Grant, P. A., Duggan, L., Côté, J., Roberts, S. M., Brownell, J. E., Candau, R., Ohba, R., Owen-Hughes, T., Allis, C. D., Winston, F., Berger, S. L., & Workman, J. L. (1997). Yeast Gcn5 functions in two multisubunit complexes to acetylate nucleosomal histones: characterization of an Ada complex and the SAGA (Spt/Ada) complex. Genes & development, 11(13), 1640–1650.

Grant, P. A., Schieltz, D., Pray-Grant, M. G., Yates, J. R., 3rd, & Workman, J. L. (1998). The ATM-related cofactor Tra1 is a component of the purified SAGA complex. Molecular cell, 2(6), 863–867.

Gu, M., Naiyachit, Y., Wood, T. J., & Millar, C. B. (2015). H2A.Z marks antisense promoters and has positive effects on antisense transcript levels in budding yeast. BMC genomics, 16(1), 99.

Gut, P., and Verdin, E. (2013). The nexus of chromatin regulation and intermediary metabolism. Nature 502, 489–498.

Harris, M. E., Böhni, R., Schneiderman, M. H., Ramamurthy, L., Schümperli, D., & Marzluff, W. F. (1991). Regulation of histone mRNA in the unperturbed cell cycle: evidence suggesting control at two posttranscriptional steps. Molecular and cellular biology, 11(5), 2416–2424.

Hebbes, T. R., Thorne, A. W., & Crane-Robinson, C. (1988). A direct link between core histone acetylation and transcriptionally active chromatin. The EMBO journal, 7(5), 1395–1402.

Henikoff, S., & Smith, M. M. (2015). Histone variants and epigenetics. Cold Spring Harbor perspectives in biology, 7(1), a019364.

Hiltunen, J.K., Mursula, A.M., Rottensteiner, H., Wierenga, R.K., Kastaniotis, A.J., and Gurvitz, A. (2003). The biochemistry of peroxisomal β-oxidation in the yeast Saccharomyces cerevisiae. FEMS Microbiology Reviews 27, 35–64.

Hong, J., Feng, H., Wang, F., Ranjan, A., Chen, J., Jiang, J., Ghirlando, R., Xiao, T. S., Wu, C., & Bai, Y. (2014). The catalytic subunit of the SWR1 remodeler is a histone chaperone for the H2A.Z-H2B dimer. Molecular cell, 53(3), 498–505.

Huang, D.W., Sherman, B.T., and Lempicki, R.A. (2009a). Bioinformatics enrichment tools: paths toward the comprehensive functional analysis of large gene lists. Nucleic Acids Research 37, 1–13.

Huang, D.W., Sherman, B.T., and Lempicki, R.A. (2009b). Systematic and integrative analysis of large gene lists using DAVID bioinformatics resources. Nat Protoc 4, 44–57.

Huber, A., French, S.L., Tekotte, H., Yerlikaya, S., Stahl, M., Perepelkina, M.P., Tyers, M., Rougemont, J., Beyer, A.L., and Loewith, R. (2011). Sch9 regulates ribosome biogenesis via Stb3, Dot6 and Tod6 and the histone deacetylase complex RPD3L. Embo J 30, 3052–3064.

Ikura, T., Ogryzko, V. V., Grigoriev, M., Groisman, R., Wang, J., Horikoshi, M., Scully, R., Qin, J., & Nakatani, Y. (2000). Involvement of the TIP60 histone acetylase complex in DNA repair and apoptosis. Cell, 102(4), 463–473.

Jiang, G., Li, C., Lu, M., Lu, K., & Li, H. (2021). Protein lysine crotonylation: past, present, perspective. Cell death & disease, 12(7), 703.

Jiang, G., Nguyen, D., Archin, N. M., Yukl, S. A., Méndez-Lagares, G., Tang, Y., Elsheikh, M. M., Thompson, G. R., 3rd, Hartigan-O'Connor, D. J., Margolis, D. M., Wong, J. K., & Dandekar, S. (2018). HIV latency is reversed by ACSS2-driven histone crotonylation. The Journal of clinical investigation, 128(3), 1190–1198.

Joo, Y.J., Ficarro, S.B., Soares, L.M., Chun, Y., Marto, J.A., and Buratowski, S. (2017). Downstream promoter interactions of TFIID TAFs facilitate transcription reinitiation. Genes Dev 31, 2162–2174.

Kebede, A.F., Nieborak, A., Shahidian, L.Z., Le Gras, S., Richter, F., Gómez, D.A., Baltissen, M.P., Meszaros, G., de Fatima Magliarelli, H., Taudt, A., et al. (2017). Histone propionylation is a mark of active chromatin. Nat. Struct. Mol. Biol. 159, nsmb.3490.

Keogh, M. C., Mennella, T. A., Sawa, C., Berthelet, S., Krogan, N. J., Wolek, A., Podolny, V., Carpenter, L. R., Greenblatt, J. F., Baetz, K., & Buratowski, S. (2006). The Saccharomyces cerevisiae histone H2A variant Htz1 is acetylated by NuA4. Genes & development, 20(6), 660–665.

Klein, B. J., Vann, K. R., Andrews, F. H., Wang, W. W., Zhang, J., Zhang, Y., Beloglazkina, A. A., Mi, W., Li, Y., Li, H., Shi, X., Kutateladze, A. G., Strahl, B. D., Liu, W. R., & Kutateladze, T. G. (2018). Structural insights into the π-π-π stacking mechanism and DNA-binding activity of the YEATS domain. Nature communications, 9(1), 4574.

Klemm, S. L., Shipony, Z., & Greenleaf, W. J. (2019). Chromatin accessibility and the regulatory epigenome. Nature reviews. Genetics, 20(4), 207–220.

Klevecz, R. R., Bolen, J., Forrest, G., & Murray, D. B. (2004). A genomewide oscillation in transcription gates DNA replication and cell cycle. Proceedings of the National Academy of Sciences of the United States of America, 101(5), 1200–1205.

Kobor, M. S., Venkatasubrahmanyam, S., Meneghini, M. D., Gin, J. W., Jennings, J. L., Link, A. J., Madhani, H. D., & Rine, J. (2004). A protein complex containing the conserved Swi2/Snf2-related ATPase Swr1p deposits histone variant H2A.Z into euchromatin. PLoS biology, 2(5), E131.

Koh, A., Vadder, F.D., Kovatcheva-Datchary, P., and Bäckhed, F. (2016). From Dietary Fiber to Host Physiology: Short-Chain Fatty Acids as Key Bacterial Metabolites. Cell 165, 1332–1345.

Kornberg, R. D., & Lorch, Y. (1999). Twenty-five years of the nucleosome, fundamental particle of the eukaryote chromosome. Cell, 98(3), 285–294.

Krautkramer, K.A., Kreznar, J.H., Romano, K.A., Vivas, E.I., Barrett-Wilt, G.A., Rabaglia, M.E., Keller, M.P., Attie, A.D., Rey, F.E., and Denu, J.M. (2016). Diet-Microbiota Interactions Mediate Global Epigenetic Programming in Multiple Host Tissues. Mol Cell 64, 982–992.

Krogan, N. J., Baetz, K., Keogh, M. C., Datta, N., Sawa, C., Kwok, T. C., Thompson, N. J., Davey, M. G., Pootoolal, J., Hughes, T. R., Emili, A., Buratowski, S., Hieter, P., & Greenblatt, J. F. (2004). Regulation of chromosome stability by the histone H2A variant Htz1, the Swr1 chromatin remodeling complex, and the histone acetyltransferase NuA4. Proceedings of the National Academy of Sciences of the United States of America, 101(37), 13513–13518.

Ku, M., Jaffe, J. D., Koche, R. P., Rheinbay, E., Endoh, M., Koseki, H., Carr, S. A., & Bernstein, B. E. (2012). H2A.Z landscapes and dual modifications in pluripotent and multipotent stem cells underlie complex genome regulatory functions. Genome biology, 13(10), R85.

Kuang, Z., Cai, L., Zhang, X., Ji, H., Tu, B.P., and Boeke, J.D. (2014). High-temporal-resolution view of transcription and chromatin states across distinct metabolic states in budding yeast. Nat. Struct. Mol. Biol. 21, 854–863.

Kuang, Z., Pinglay, S., Ji, H., and Boeke, J.D. (2017). Msn2/4 regulate expression of glycolytic enzymes and control transition from quiescence to growth. eLife 6, e29938.

Kushnirov, V.V. (2000). Rapid and reliable protein extraction from yeast. Yeast 16, 857–860.

Lai, W., & Pugh, B. F. (2017). Understanding nucleosome dynamics and their links to gene expression and DNA replication. Nature reviews. Molecular cell biology, 18(9), 548–562.

Le Masson, I., Yu, D. Y., Jensen, K., Chevalier, A., Courbeyrette, R., Boulard, Y., Smith, M. M., & Mann, C. (2003). Yaf9, a novel NuA4 histone acetyltransferase subunit, is required for the cellular response to spindle stress in yeast. Molecular and cellular biology, 23(17), 6086–6102.

Li, B., Pattenden, S. G., Lee, D., Gutiérrez, J., Chen, J., Seidel, C., Gerton, J., & Workman, J. L. (2005). Preferential occupancy of histone variant H2AZ at inactive promoters influences local histone modifications and chromatin remodeling. Proceedings of the National Academy of Sciences of the United States of America, 102(51), 18385–18390.

Li, Y., Sabari, B. R., Panchenko, T., Wen, H., Zhao, D., Guan, H., Wan, L., Huang, H., Tang, Z., Zhao, Y., Roeder, R. G., Shi, X., Allis, C. D., & Li, H. (2016). Molecular Coupling of Histone Crotonylation and Active Transcription by AF9 YEATS Domain. Molecular cell, 62(2), 181–193.

Li, Y., Sabari, B.R., Panchenko, T., Wen, H., Zhao, D., Guan, H., Wan, L., Huang, H., Tang, Z., Zhao, Y., et al. (2016). Molecular Coupling of Histone Crotonylation and Active Transcription by AF9 YEATS Domain. Mol Cell 62, 181–193.

Li, Y., Wen, H., Xi, Y., Tanaka, K., Wang, H., Peng, D., Ren, Y., Jin, Q., Dent, S. Y., Li, W., Li, H., & Shi, X. (2014). AF9 YEATS domain links histone acetylation to DOT1L-mediated H3K79 methylation. Cell, 159(3), 558–571.

Li, Y., Wen, H., Xi, Y., Tanaka, K., Wang, H., Peng, D., Ren, Y., Jin, Q., Dent, S.Y.R., Li, W., et al. (2014). AF9 YEATS Domain Links Histone Acetylation to DOT1L-Mediated H3K79 Methylation. Cell 159, 558–571.

Li, Y., Zhao, D., Chen, Z., & Li, H. (2017). YEATS domain: Linking histone crotonylation to gene regulation. Transcription, 8(1), 9–14.

Lipmann F. (1954). Development of the acetylation problem, a personal account. Science (New York, N.Y.), 120(3126), 855–865.

Lipmann, F., & Kaplan, N. O. (1947). Coenzyme for acetylation, a pantothenic acid derivative. The Journal of biological chemistry, 167(3), 869.

Lippman, S.I., and Broach, J.R. (2009). Protein kinase A and TORC1 activate genes for ribosomal biogenesis by inactivating repressors encoded by Dot6 and its homolog Tod6. Proc Natl Acad Sci USA 106, 19928–19933.

Liu, C.L., Kaplan, T., Kim, M., Buratowski, S., Schreiber, S.L., Friedman, N., and Rando, O.J. (2005). Single-nucleosome mapping of histone modifications in S. cerevisiae. PLoS Biol 3, e328.

Love, M.I., Huber, W., and Anders, S. (2014). Moderated estimation of fold change and dispersion for RNA-seq data with DESeq2. Genome Biol 15, 550.

Lu, P. Y., Lévesque, N., & Kobor, M. S. (2009). NuA4 and SWR1-C: two chromatin-modifying complexes with overlapping functions and components. Biochemistry and cell biology = Biochimie et biologie cellulaire, 87(5), 799–815.

Luger, K., Mäder, A. W., Richmond, R. K., Sargent, D. F., & Richmond, T. J. (1997). Crystal structure of the nucleosome core particle at 2.8 A resolution. *Nature*, *389*(6648), 251–260.

Lv, Y., Bu, C., Meng, J., Ward, C., Volpe, G., Hu, J., Jiang, M., Guo, L., Chen, J., Esteban, M. A., Bao, X., & Cheng, Z. (2021). Global Profiling of the Lysine Crotonylome in Different Pluripotent States. Genomics, proteomics & bioinformatics, S1672-0229(21)00073-5. Advance online publication.

Machné, R., and Murray, D.B. (2012). The yin and yang of yeast transcription: elements of a global feedback system between metabolism and chromatin. PLoS ONE 7, e37906.

Madsen, A. S., & Olsen, C. A. (2012). Profiling of substrates for zinc-dependent lysine deacylase enzymes: HDAC3 exhibits decrotonylase activity in vitro. Angewandte Chemie (International ed. in English), 51(36), 9083–9087.

Malik, H. S., & Henikoff, S. (2003). Phylogenomics of the nucleosome. Nature structural biology, 10(11), 882–891.

Marmorstein, R., & Zhou, M. M. (2014). Writers and readers of histone acetylation: structure, mechanism, and inhibition. Cold Spring Harbor perspectives in biology, 6(7), a018762.

Mellor J. (2016). The molecular basis of metabolic cycles and their relationship to circadian rhythms. Nature structural & molecular biology, 23(12), 1035–1044.

Mellor, J. (2016). The molecular basis of metabolic cycles and their relationship to circadian rhythms. Nat. Struct. Mol. Biol. 23, 1035–1044.

Mendel, G. (1901). Experiments in Hybrdisation.pdf. J. R. Hortic. Soc.

Mitchell, L., Lambert, J. P., Gerdes, M., Al-Madhoun, A. S., Skerjanc, I. S., Figeys, D., & Baetz, K. (2008). Functional dissection of the NuA4 histone acetyltransferase reveals its role as a genetic hub and that Eaf1 is essential for complex integrity. Molecular and cellular biology, 28(7), 2244–2256.

Mizuguchi, G., Shen, X., Landry, J., Wu, W. H., Sen, S., & Wu, C. (2004). ATP-driven exchange of histone H2AZ variant catalyzed by SWR1 chromatin remodeling complex. Science (New York, N.Y.), 303(5656), 343–348.

Narkaj, K., Stefanelli, G., Wahdan, M., Azam, A. B., Ramzan, F., Steininger, C., Jr, Walters, B. J., & Zovkic, I. B. (2018). Blocking H2A.Z Incorporation via Tip60 Inhibition Promotes Systems Consolidation of Fear Memory in Mice. eNeuro, 5(5), ENEURO.0378-18.2018.

Narlikar, G. J., Sundaramoorthy, R., & Owen-Hughes, T. (2013). Mechanisms and functions of ATP-dependent chromatin-remodeling enzymes. Cell, 154(3), 490–503.

Nath, A., and Chan, C. (2016). Genetic alterations in fatty acid transport and metabolism genes are associated with metastatic progression and poor prognosis of human cancers. Sci Rep 6, 18669.

Nishibuchi, I., Suzuki, H., Kinomura, A., Sun, J., Liu, N. A., Horikoshi, Y., Shima, H., Kusakabe, M., Harata, M., Fukagawa, T., Ikura, T., Ishida, T., Nagata, Y., & Tashiro, S. (2014). Reorganization of damaged chromatin by the exchange of histone variant H2A.Z-2. International journal of radiation oncology, biology, physics, 89(4), 736–744.

Peixoto, L., & Abel, T. (2013). The role of histone acetylation in memory formation and cognitive impairments. Neuropsychopharmacology: official publication of the American College of Neuropsychopharmacology, 38(1), 62–76.

Phillips D. M. (1963). The presence of acetyl groups of histones. The Biochemical journal, 87(2), 258–263.

Pokholok, D. K., Harbison, C. T., Levine, S., Cole, M., Hannett, N. M., Lee, T. I., Bell, G. W., Walker, K., Rolfe, P. A., Herbolsheimer, E., Zeitlinger, J., Lewitter, F., Gifford, D. K., & Young, R. A. (2005). Genome-wide map of nucleosome acetylation and methylation in yeast. Cell, 122(4), 517–527.

Raisner, R. M., Hartley, P. D., Meneghini, M. D., Bao, M. Z., Liu, C. L., Schreiber, S. L., Rando, O. J., & Madhani, H. D. (2005). Histone variant H2A.Z marks the 5' ends of both active and inactive genes in euchromatin. Cell, 123(2), 233–248.

Ramírez, F., Ryan, D.P., Grüning, B., Bhardwaj, V., Kilpert, F., Richter, A.S., Heyne, S., Dündar, F., and Manke, T. (2016). deepTools2: a next generation web server for deep-sequencing data analysis. Nucleic Acids Research 44, W160–W165.

Ranjan, A., Mizuguchi, G., FitzGerald, P. C., Wei, D., Wang, F., Huang, Y., Luk, E., Woodcock, C. L., & Wu, C. (2013). Nucleosome-free region dominates histone acetylation in targeting SWR1 to promoters for H2A.Z replacement. Cell, 154(6), 1232–1245.

Ranjan, A., Nguyen, V. Q., Liu, S., Wisniewski, J., Kim, J. M., Tang, X., Mizuguchi, G., Elalaoui, E., Nickels, T. J., Jou, V., English, B. P., Zheng, Q., Luk, E., Lavis, L. D., Lionnet, T., & Wu, C. (2020). Live-cell single particle imaging reveals the role of RNA polymerase II in histone H2A.Z eviction. eLife, 9, e55667.

Rao, A.R., and Pellegrini, M. (2011). Regulation of the yeast metabolic cycle by transcription factors with periodic activities. BMC Syst Biol 5, 160.

Rhee, H. S., Bataille, A. R., Zhang, L., & Pugh, B. F. (2014). Subnucleosomal structures and nucleosome asymmetry across a genome. Cell, 159(6), 1377–1388.

Richmond, T. J., & Davey, C. A. (2003). The structure of DNA in the nucleosome core. Nature, 423(6936), 145–150.

Richmond, T. J., Rechsteiner, T., & Luger, K. (1993). Studies of nucleosome structure. Cold Spring Harbor symposia on quantitative biology, 58, 265–272.

Richon, V. M., Emiliani, S., Verdin, E., Webb, Y., Breslow, R., Rifkind, R. A., & Marks, P. A. (1998). A class of hybrid polar inducers of transformed cell differentiation inhibits histone deacetylases. Proceedings of the National Academy of Sciences of the United States of America, 95(6), 3003–3007.

Rossetto, D., Cramet, M., Wang, A. Y., Steunou, A. L., Lacoste, N., Schulze, J. M., Côté, V., Monnet-Saksouk, J., Piquet, S., Nourani, A., Kobor, M. S., & Côté, J. (2014). Eaf5/7/3 form a functionally independent NuA4 submodule linked to RNA polymerase II-coupled nucleosome recycling. The EMBO journal, 33(12), 1397–1415.

Rothbart, S. B., & Strahl, B. D. (2014). Interpreting the language of histone and DNA modifications. Biochimica et biophysica acta, 1839(8), 627–643.

Sabari, B. R., Tang, Z., Huang, H., Yong-Gonzalez, V., Molina, H., Kong, H. E., Dai, L., Shimada, M., Cross, J. R., Zhao, Y., Roeder, R. G., & Allis, C. D. (2015). Intracellular crotonyl-CoA stimulates transcription through p300-catalyzed histone crotonylation. Molecular cell, 58(2), 203–215.

Sabari, B. R., Zhang, D., Allis, C. D., & Zhao, Y. (2017). Metabolic regulation of gene expression through histone acylations. Nature reviews. Molecular cell biology, 18(2), 90–101.

Schulze, J. M., Wang, A. Y., & Kobor, M. S. (2009). YEATS domain proteins: a diverse family with many links to chromatin modification and transcription. Biochemistry and cell biology = Biochimie et biologie cellulaire, 87(1), 65–75.a

Schulze, J. M., Wang, A. Y., & Kobor, M. S. (2010). Reading chromatin: insights from yeast into YEATS domain structure and function. Epigenetics, 5(7), 573–577.

Seto, E., & Yoshida, M. (2014). Erasers of histone acetylation: the histone deacetylase enzymes. Cold Spring Harbor perspectives in biology, 6(4), a018713.

Shanle, E.K., Andrews, F.H., Meriesh, H., McDaniel, S.L., Dronamraju, R., DiFiore, J.V., Jha, D., Wozniak, G.G., Bridgers, J.B., Kerschner, J.L., et al. (2015). Association of Taf14 with acetylated histone H3 directs gene transcription and the DNA damage response. Genes Dev 29, 1795–1800.

Simithy, J., Sidoli, S., Yuan, Z.-F., Coradin, M., Bhanu, N.V., Marchione, D.M., Klein, B.J., Bazilevsky, G.A., McCullough, C.E., Magin, R.S., et al. (2017). Characterization of histone acylations links chromatin modifications with metabolism. Nature Communications 8, 1141.

Strahl, B. D., & Allis, C. D. (2000). The language of covalent histone modifications. Nature, 403(6765), 41–45.

Stratton, M. S., & McKinsey, T. A. (2015). Acetyl-lysine erasers and readers in the control of pulmonary hypertension and right ventricular hypertrophy. Biochemistry and cell biology = Biochimie et biologie cellulaire, 93(2), 149–157.

Stuckey, S., and Storici, F. (2013). Chapter Eight - Gene Knockouts, in vivo Site-Directed Mutagenesis and Other Modifications Using the Delitto Perfetto System in Saccharomyces cerevisiae. In Laboratory Methods in Enzymology: Cell, Lipid and Carbohydrate, J. Lorsch, ed. (Academic Press), pp. 103–131.

Suganuma, T., and Workman, J.L. (2018). Chromatin and Metabolism. Annu. Rev. Biochem. 87, 27–49.

Szerlong, H., Hinata, K., Viswanathan, R., Erdjument-Bromage, H., Tempst, P., & Cairns, B. R. (2008). The HSA domain binds nuclear actin-related proteins to regulate chromatin-remodeling ATPases. Nature structural & molecular biology, 15(5), 469–476.

Takahashi, H., McCaffery, J.M., Irizarry, R.A., and Boeke, J.D. (2006). Nucleocytosolic acetyl-coenzyme a synthetase is required for histone acetylation and global transcription. Mol Cell 23, 207–217.

Talbert, P. B., & Henikoff, S. (2021). Histone variants at a glance. Journal of cell science, 134(6), jcs244749.

Tan, M., Luo, H., Lee, S., Jin, F., Yang, J. S., Montellier, E., Buchou, T., Cheng, Z., Rousseaux, S., Rajagopal, N., Lu, Z., Ye, Z., Zhu, Q., Wysocka, J., Ye, Y., Khochbin, S., Ren, B., & Zhao, Y. (2011). Identification of 67 histone marks and histone lysine crotonylation as a new type of histone modification. Cell, 146(6), 1016–1028.

Tang, X., Chen, X. F., Sun, X., Xu, P., Zhao, X., Tong, Y., Wang, X. M., Yang, K., Zhu, Y. T., Hao, D. L., Zhang, Z. Q., Liu, D. P., & Chen, H. Z. (2021). Short-Chain Enoyl-CoA Hydratase Mediates Histone Crotonylation and Contributes to Cardiac Homeostasis. Circulation, 143(10), 1066–1069.

Taunton, J., Hassig, C. A., & Schreiber, S. L. (1996). A mammalian histone deacetylase related to the yeast transcriptional regulator Rpd3p. Science (New York, N.Y.), 272(5260), 408–411.

Teves, S. S., Weber, C. M., & Henikoff, S. (2014). Transcribing through the nucleosome. Trends in biochemical sciences, 39(12), 577–586.

Thoma, F., Koller, T., & Klug, A. (1979). Involvement of histone H1 in the organization of the nucleosome and of the salt-dependent superstructures of chromatin. The Journal of cell biology, 83(2 Pt 1), 403–427.

Tramantano, M., Sun, L., Au, C., Labuz, D., Liu, Z., Chou, M., Shen, C., & Luk, E. (2016). Constitutive turnover of histone H2A.Z at yeast promoters requires the preinitiation complex. eLife, 5, e14243.

Tu, B. P., & McKnight, S. L. (2006). Metabolic cycles as an underlying basis of biological oscillations. Nature reviews. Molecular cell biology, 7(9), 696–701.

Tu, B. P., Kudlicki, A., Rowicka, M., & McKnight, S. L. (2005). Logic of the yeast metabolic cycle: temporal compartmentalization of cellular processes. Science (New York, N.Y.), 310(5751), 1152–1158.

Tu, B. P., Mohler, R. E., Liu, J. C., Dombek, K. M., Young, E. T., Synovec, R. E., & McKnight, S. L. (2007). Cyclic changes in metabolic state during the life of a yeast cell. Proceedings of the National Academy of Sciences of the United States of America, 104(43), 16886–16891.

Turner, B. M., Birley, A. J., & Lavender, J. (1992). Histone H4 isoforms acetylated at specific lysine residues define individual chromosomes and chromatin domains in Drosophila polytene nuclei. Cell, 69(2), 375–384.

Valdés-Mora, F., Song, J. Z., Statham, A. L., Strbenac, D., Robinson, M. D., Nair, S. S., Patterson, K. I., Tremethick, D. J., Stirzaker, C., & Clark, S. J. (2012). Acetylation of H2A.Z is a key epigenetic modification associated with gene deregulation and epigenetic remodeling in cancer. Genome research, 22(2), 307–321.

Vardabasso, C., Gaspar-Maia, A., Hasson, D., Pünzeler, S., Valle-Garcia, D., Straub, T., Keilhauer, E. C., Strub, T., Dong, J., Panda, T., Chung, C. Y., Yao, J. L., Singh, R., Segura, M. F., Fontanals-Cirera, B., Verma, A., Mann, M., Hernando, E., Hake, S. B., & Bernstein, E. (2015). Histone Variant H2A.Z.2 Mediates Proliferation and Drug Sensitivity of Malignant Melanoma. Molecular cell, 59(1), 75–88.

Verdin, E., & Ott, M. (2015). 50 years of protein acetylation: from gene regulation to epigenetics, metabolism and beyond. Nature reviews. Molecular cell biology, 16(4), 258–264.

Wan, J., Liu, H., & Ming, L. (2019). Lysine crotonylation is involved in hepatocellular carcinoma progression. Biomedicine & pharmacotherapy = Biomedecine & pharmacotherapie, 111, 976–982.

Wang, A. Y., Schulze, J. M., Skordalakes, E., Gin, J. W., Berger, J. M., Rine, J., & Kobor, M. S. (2009). Asf1-like structure of the conserved Yaf9 YEATS domain and role in H2A.Z deposition and acetylation. Proceedings of the National Academy of Sciences of the United States of America, 106(51), 21573–21578.

Wang, G.-Z., Hickey, S.L., Shi, L., Huang, H.-C., Nakashe, P., Koike, N., Tu, B.P., Takahashi, J.S., and Konopka, G. (2015). Cycling Transcriptional Networks Optimize Energy Utilization on a Genome Scale. Cell Reports 13, 1868–1880.

Wang, X., Ahmad, S., Zhang, Z., Côté, J., & Cai, G. (2018). Architecture of the Saccharomyces cerevisiae NuA4/TIP60 complex. Nature communications, 9(1), 1147.

Warner, J.R. (1999). The economics of ribosome biosynthesis in yeast. Trends in Biochemical Sciences 24, 437–440.

Watson, J. D., & Crick, F. H. (1953). Molecular structure of nucleic acids; a structure for deoxyribose nucleic acid. Nature, 171(4356), 737–738.

Weber, C. M., & Henikoff, S. (2014). Histone variants: dynamic punctuation in transcription. Genes & development, 28(7), 672–682.

Weber, C. M., Ramachandran, S., & Henikoff, S. (2014). Nucleosomes are context-specific, H2A.Z-modulated barriers to RNA polymerase. Molecular cell, 53(5), 819–830.

Wei, W., Liu, X., Chen, J., Gao, S., Lu, L., Zhang, H., Ding, G., Wang, Z., Chen, Z., Shi, T., Li, J., Yu, J., & Wong, J. (2017). Class I histone deacetylases are major histone decrotonylases:

evidence for critical and broad function of histone crotonylation in transcription. Cell research, 27(7), 898–915.

Wei, W., Mao, A., Tang, B., Zeng, Q., Gao, S., Liu, X., Lu, L., Li, W., Du, J. X., Li, J., Wong, J., & Liao, L. (2017). Large-Scale Identification of Protein Crotonylation Reveals Its Role in Multiple Cellular Functions. Journal of proteome research, 16(4), 1743–1752.

West, M. H., & Bonner, W. M. (1980). Histone 2A, a heteromorphous family of eight protein species. Biochemistry, 19(14), 3238–3245.

Willhoft, O., Ghoneim, M., Lin, C. L., Chua, E., Wilkinson, M., Chaban, Y., Ayala, R., McCormack, E. A., Ocloo, L., Rueda, D. S., & Wigley, D. B. (2018). Structure and dynamics of the yeast SWR1-nucleosome complex. Science (New York, N.Y.), 362(6411), eaat7716.

Winston, F., & Allis, C. D. (1999). The bromodomain: a chromatin-targeting module?. Nature structural biology, 6(7), 601–604.

Wolffe, A. P., & Guschin, D. (2000). Review: chromatin structural features and targets that regulate transcription. Journal of structural biology, 129(2-3), 102–122.

Wu, W. H., Wu, C. H., Ladurner, A., Mizuguchi, G., Wei, D., Xiao, H., Luk, E., Ranjan, A., & Wu, C. (2009). N terminus of Swr1 binds to histone H2AZ and provides a platform for subunit assembly in the chromatin remodeling complex. The Journal of biological chemistry, 284(10), 6200–6207.

Xiong, X., Panchenko, T., Yang, S., Zhao, S., Yan, P., Zhang, W., Xie, W., Li, Y., Zhao, Y., Allis, C. D., & Li, H. (2016). Selective recognition of histone crotonylation by double PHD fingers of MOZ and DPF2. Nature chemical biology, 12(12), 1111–1118.

Yen, K., Vinayachandran, V., & Pugh, B. F. (2013). SWR-C and INO80 chromatin remodelers recognize nucleosome-free regions near +1 nucleosomes. Cell, 154(6), 1246–1256.

Zhang, H., Richardson, D. O., Roberts, D. N., Utley, R., Erdjument-Bromage, H., Tempst, P., Côté, J., & Cairns, B. R. (2004). The Yaf9 component of the SWR1 and NuA4 complexes is required for proper gene expression, histone H4 acetylation, and Htz1 replacement near telomeres. Molecular and cellular biology, 24(21), 9424–9436.

Zhang, Q., Zeng, L., Zhao, C., Ju, Y., Konuma, T., & Zhou, M. M. (2016). Structural Insights into Histone Crotonyl-Lysine Recognition by the AF9 YEATS Domain. Structure (London, England : 1993), 24(9), 1606–1612.

Zhao, D., Guan, H., Zhao, S., Mi, W., Wen, H., Li, Y., Zhao, Y., Allis, C.D., Shi, X., and Li, H. (2016). YEATS2 is a selective histone crotonylation reader. Cell Res. 26, 629–632.

Zhao, S., Zhang, X., & Li, H. (2018). Beyond histone acetylation-writing and erasing histone acylations. Current opinion in structural biology, 53, 169–177.

Zhao, Y., and Garcia, B.A. (2015). Comprehensive Catalog of Currently Documented Histone Modifications. Cold Spring Harb Perspect Biol 7, a025064.

Zhou, B. O., Wang, S. S., Xu, L. X., Meng, F. L., Xuan, Y. J., Duan, Y. M., Wang, J. Y., Hu, H., Dong, X., Ding, J., & Zhou, J. Q. (2010). SWR1 complex poises heterochromatin boundaries for antisilencing activity propagation. Molecular and cellular biology, 30(10), 2391–2400.

Zhou, C. Y., Johnson, S. L., Gamarra, N. I., & Narlikar, G. J. (2016). Mechanisms of ATP-Dependent Chromatin Remodeling Motors. Annual review of biophysics, 45, 153–181.

Zovkic, I. B., Paulukaitis, B. S., Day, J. J., Etikala, D. M., & Sweatt, J. D. (2014). Histone H2A.Z subunit exchange controls consolidation of recent and remote memory. Nature, 515(7528), 582–586.